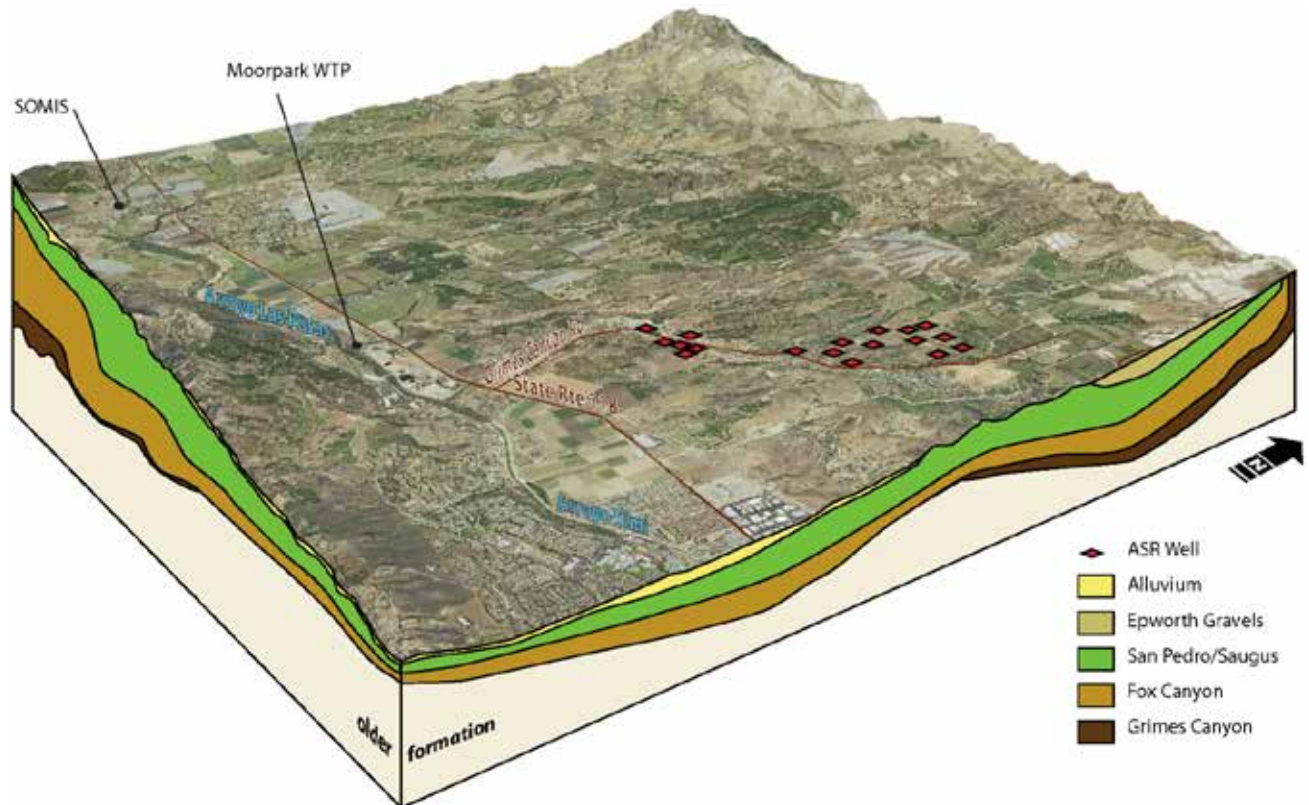


GROUNDWATER FLOW MODEL OF THE EAST AND SOUTH LAS POSAS SUB-BASINS – PRELIMINARY DRAFT REPORT



Prepared for:

Calleguas Municipal Water District
21000 Olsen Road
Thousand Oaks, CA 91360

Prepared by:



3868 W. Carson St, Suite 318
Torrance, California 90503

Jan 17, 2018

TABLE OF CONTENTS

LIST OF TABLES	iii
ACRONYMS AND ABBREVIATIONS.....	iv
PREFACE.....	1
1.0 INTRODUCTION.....	2
2.0 PRIOR MODELING WORK.....	2
3.0 HYDROGEOLOGIC CONCEPTUAL MODEL	3
3.1 Geologic Setting.....	4
3.2 Extent and Boundaries	5
3.2.1 Basin Boundaries.....	5
3.2.2 Boundary for Hydrogeologic Conceptual Model	6
3.3 Stratigraphy and Hydrogeology.....	6
3.3.1 Shallow Aquifer.....	7
3.3.2 The Epworth Gravels Aquifer	8
3.3.3 Upper San Pedro/Saugus Formation	8
3.3.4 Clay Marker Bed	8
3.3.5 Fox Canyon Aquifer.....	8
3.3.6 Upper Portion of the Upper Santa Barbara.....	9
3.3.7 Grimes Canyon Aquifer	9
4.0 HYDROGEOLOGIC STRUCTURE AND PROPERTIES	12
4.1 Updates to Geologic Structure.....	12
4.1.1 Data Sources	12
4.1.2 Geologic Analysis	12
4.1.3 Geologic Surfaces and Isopachs.....	13
4.2 Initial Hydraulic Properties.....	16
4.2.1 Hydraulic Conductivity	16
4.2.2 Storage Properties.....	18
5.0 GROUNDWATER OCCURRENCE AND MOVEMENT.....	20
5.1 Primary Groundwater Recharge Mechanisms	20
5.2 Primary Groundwater Discharge Mechanisms	20
5.3 Historical Groundwater Elevations.....	20
5.3.1 Change in Elevations with Time	21
5.3.2 Variation of Elevations with Depth.....	25
5.4 Groundwater Levels and Flow Direction.....	25
5.4.1 Spatial Trends in Groundwater Elevations.....	25
5.4.2 Estimate of Travel Times	26
6.0 CONCEPTUAL WATER BUDGET.....	28
6.1 Period of Record	28
6.2 Water Budget Components.....	29
6.2.1 Recharge from Precipitation.....	33
6.2.2 Focused Recharge from Arroyo Las Posas/Simi.....	34

6.2.3	Recharge at Moorpark Wastewater Treatment Plant Percolation Ponds	37
6.2.4	Recharge from Return Flows.....	38
6.2.5	Well Production.....	41
6.2.6	Evapotranspiration Losses.....	42
6.2.7	Injection and Extraction at ASR wells and In-Lieu Deliveries	44
6.2.8	Underflow	44
6.2.9	Change in Storage.....	45
6.2.10	Water Budget Limitations	45
7.0	MODEL DESIGN.....	47
7.1	Code and Processor.....	47
7.2	Model Layers and Grid	48
7.3	Simulation Period and Stress Periods	49
7.4	Flow Model Design.....	50
7.4.1	No-Flow, Specified Head, and General Head Boundaries	50
7.4.2	Arroyo Las Posas/Simi Streamflows.....	51
7.4.3	Groundwater Injections and Extractions	54
7.4.4	Areal Recharge and Return Flows.....	56
7.4.5	Evapotranspiration from Phreatophytes	57
7.4.6	Hydraulic Properties.....	57
8.0	MODEL CALIBRATION.....	58
8.1	Calibration Approach.....	58
8.1.1	Calibration Targets	59
8.1.2	Quantitative Calibration Measures	60
8.1.3	Qualitative and Semi-Quantitative Calibration Measures	61
8.2	Calibration of Boundary Conditions.....	62
8.2.1	Recharge	62
8.2.2	Streamflow Parameters.....	63
8.3	Initial Conditions	66
8.4	Hydraulic Properties	66
8.4.1	Hydraulic Conductivities.....	66
8.4.2	Hydraulic Flow Barriers (Faults).....	73
8.4.3	Storage Properties.....	74
8.5	Model Calibration Results	75
8.5.1	Hydraulic Heads	75
8.5.2	Calibration Statistics.....	78
8.5.3	Streamflow	79
8.5.4	Calibrated Water Budget	81
8.5.5	Particle Tracks.....	87
8.6	Model Uncertainty	87
9.0	SENSITIVITY ANALYSIS.....	90
10.0	PREDICTIVE SCENARIOS.....	90
11.0	SUMMARY AND CONCLUSIONS	90
12.0	DATA GAPS AND FUTURE WORK	91

LIST OF TABLES

Table 3-1	Regional Geology and Stratigraphic Column from CH2M (2017, Figure 6).....	11
Table 4-1	Stratigraphic Column from CH2M (2017, Figure 6) and Hydrostratigraphic Column for Groundwater Flow Model.....	14
Table 4-2	Initial Assignment of Hydraulic Conductivity to Groundwater Flow Model.....	18
Table 6-1	Period of Record for Daily Streamflow Gages Considered in the Water Budget Analysis.....	28
Table 6-2	Water Budget Inflows in Acre-Feet Per Year.....	31
Table 6-3	Water Budget Outflows and Change in Storage in Acre-Feet Per Year.....	32
Table 6-4	Basis for Septic System Return Flow Rates.....	41
Table 6-5	Open Channel and Vegetated Areas in the River Channel of Arroyo Las Posas from Huber (2006).....	44
Table 7-1	Model Layers and Active Cells.....	49
Table 8-1	Calibrated Riverbed Conductivity in SFR Package.....	65
Table 8-2	Calibration Residual Statistics.....	78
Table 8-3	Groundwater Budget (AFY) for the Model.....	84

ACRONYMS AND ABBREVIATIONS

ac-ft/ac	acre-feet per acre
AF	acre-feet
amsl	above mean sea level
ASR	aquifer storage and recovery
AFY	acre-feet per year
bgs	below ground surface
BCM	Basin Characterization Model
CIMIS	California Irrigation Management Information System
CMWD	Calleguas Municipal Water District
cfs	cubic feet per second
CH2M	CH2M Hill, Incorporated
DEM	digital elevation model
DWR	California Department of Water Resources
ELPMA	East Las Posas Management Area
ET	Evapotranspiration
ET _o	annual average reference ET
FCA	Fox Canyon Aquifer
FCGMA	Fox Canyon Groundwater Management Agency
ft	foot/feet
ft/day	feet per day
ft ³ /day	cubic feet per day
GCA	Grimes Canyon Aquifer
GHB	general-head boundary
gpcd	gallons per capita per day
GSA	Groundwater Sustainability Agency
GSP	Groundwater Sustainability Plan
HFB	Horizontal Flow Barrier
in/yr	inches per year
INTERA	INTERA Incorporated
LAS	Lower Aquifer System
LPUG	Los Posas Users Group
LPVB	Las Posas Valley Basin

m	meter
M&I	municipal and industrial
MAE	mean absolute error
ME	mean error
Metropolitan	Metropolitan Water District of Southern California
mg/L	milligrams per Liter
mgd	million gallons per day
mm/day	millimeters per day
PRISM	Parameter-elevation Regressions on Independent Slopes Model
RMSE	root mean square error
SFR2	MODFLOW streamflow routing package
SSURGO	Soil Survey Geographic
SVWQCP	Simi Valley Water Quality Control Plant
SWRCB	State Water Resources Control Board
TDS	total dissolved solids
UAS	Upper Aquifer System
UPW	Upstream-Weighting
USGS	United States Geological Survey
UWCD	United Water Conservation District
VCPWA	Ventura County Public Works Agency
VCWPD	Ventura County Watershed Protection Department
VCWWD	Ventura County Water Work District
WLPMA	West Las Posas Management Area
WWTP	Wastewater Treatment Plant

PREFACE

This preliminary draft report describes work completed to date in developing a numerical groundwater flow model for the Las Posas Valley Basin (LPVB) east and south sub-basins by Calleguas Municipal Water District (Calleguas). This document is a draft and is provided for information only. The information contained herein is subject to change. Because this document is in draft form, it should not be relied upon. A final report will be published in the future.

Calleguas is developing the numerical flow model to support LPVB groundwater management and to support developing and refining operational plans for Calleguas' Las Posas Basin Aquifer Storage and Recovery (ASR) Project. Calleguas has reserved a budget for modeling runs to support Fox Canyon Groundwater Management Authority's (FCGMA) development of a Groundwater Sustainability Plan (GSP) for the LPVB.

Calleguas desires to work collaboratively with the FCGMA Technical Advisory Group to finalize this phase of the numerical model development, complete requested model runs for the LPVB GSP, and finalize this report. This preliminary draft report provides background information to facilitate a peer review of the numerical flow model by the FCGMA Technical Advisory Group.

1.0 INTRODUCTION

INTERA Incorporated (INTERA) was retained by the Calleguas Municipal Water District (CMWD) to develop a numerical groundwater model of the East Las Posas Management Area (ELPMA), which includes the locally-recognized east and south sub-basins of the Las Posas Valley Basin (LPVB). Groundwater in the ELPMA is found in a multiple-aquifer system characterized by intense faulting and folding, which is known to exert structural controls on groundwater flow and movement. The ELPMA is known to receive recharge from surface water flows in Arroyo Las Posas/Simi that runs east to west along the southern edge of the basin. Flows in the Arroyo have become perennial as a result of discharges from wastewater treatment plants and dewatering wells within and upstream of the ELPMA. Hence, understanding and modeling the surface-water/groundwater interaction along the Arroyo is an important component of the numerical model development. CMWD also owns and operates the Las Posas Basin Aquifer Storage and Recovery (ASR) Project, consisting of eighteen high capacity ASR wells and associated facilities located in the ELPMA that are used to inject and recover potable water purchased from Metropolitan Water District of Southern California (Metropolitan). Basin response to injection/extractions at the ASR well fields and the evaluation of storage capacity of the ASR well field are key considerations for this modeling project.

This report provides details on INTERA's efforts to conceptualize, construct, and calibrate a robust numerical modeling tool that can accurately simulate groundwater responses to ASR operations while also capturing the surface-water/groundwater dynamics that drive recharge from the Arroyo to the groundwater system.

Ultimately, the groundwater model is meant to support long-term groundwater management of the ELPMA as well as help with the development and refinement of operational plans for Calleguas' Las Posas Basin ASR Project. Groundwater users within the ELPMA fall under the purview of the Sustainable Groundwater Management Act, with the Fox Canyon Groundwater Management Agency (FCGMA) as the Groundwater Sustainability Agency (GSA). The LPVB is designated a "high priority basin" and must be managed under a Groundwater Sustainability Plan (GSP) by January 31, 2022. The model may be used to support groundwater management planning by the FCGMA and its stakeholders. The model may also complement other modeling activities in the basin – for example, the groundwater model of the West Las Posas Management Area (WLPMA) and Pleasant Valley Basin being developed by United Water Conservation District (UWCD).

2.0 PRIOR MODELING WORK

Two prior groundwater models covering the LPVB were completed by CH2MHILL (1993) and Hanson et al. (2003). The CH2MHILL (1993) groundwater flow model of the LPVB was developed to study the potential for conjunctive use. The model considered the potential of storing

imported surface water in aquifers in the LPVB and subsequent extraction via wells for later use to assist in meeting peak demands, emergencies, or drought conditions. The model consisted of three model layers, covering approximately 40 square miles, representing the Fox Canyon Aquifer (FCA), the Grimes Canyon Aquifer (GCA), and the aquitard between those aquifers. Estimates of the groundwater flow budget, estimates of hydraulic properties, and historical groundwater levels were used to calibrate the model for the simulation period of January 1977 through December 1990.

The Hanson et al. (2003) groundwater flow model covered the Santa Clara-Calleguas basin over about 310 square miles in Ventura County. The model was developed to better define the geohydrologic framework of the regional groundwater flow system and to help analyze the major problems affecting water-resources management of a typical coastal aquifer system (Hanson et al., 2003). Vertically, the model consisted of two layers, representing the lower- and upper-aquifer systems. The lower-aquifer system, composed of complexly faulted and folded unconsolidated deposits of the Pliocene and Pleistocene epochs, included the FCA and GCA. The upper-aquifer system included the Shallow Aquifer and the Oxnard aquifer, which is unsaturated throughout most of the LPVB. The model was calibrated to historical surface water and groundwater flow for the period 1891–1993.

In addition to the two basin-wide models, Bachman (2016) simulated groundwater flow and particle tracking in a portion of the ELPMA to examine anticipated changes to the groundwater flow system based on the proposed Moorpark Desalter project. The model domain included the footprint of the Shallow Aquifer and portions of ELPMA. For calibration, the MODFLOW model consisted of three layers representing the Shallow Aquifer, the Upper San Pedro, and the FCA. For particle tracking, the Shallow Aquifer was subdivided vertically into four model layers. The model included a steady-state simulation representing 1976 to 1977, a transient simulation representing 1976 to 2000, and various scenarios that represented the possible operational scenarios of the proposed Moorpark Desalter from 1979 to 2008 with quarterly stress periods. The groundwater flow model was calibrated to measured streamflow, measured groundwater elevations, and the location of gaining and losing reaches and percolation rates from Engle (2012, 2013).

3.0 HYDROGEOLOGIC CONCEPTUAL MODEL

The hydrogeologic conceptual model presented in this study is based on the hydrogeologic conceptual model developed by CH2M (2017), which describes the geologic setting, stratigraphy, and hydrogeology. The basin extent and boundaries inherited from CH2M (2017), were refined to include only the ELPMA (**Figure 3-1**), and the boundaries were extended east about a mile and half to Big Mountain to coincide with the groundwater flow model domain. Refinements to the

CH2M (2017) hydrogeologic conceptual model were made during development of the numerical model. The refinements are described in Section 4.0 of the report.

3.1 Geologic Setting

The LPVB is divided into two management areas based on geologic controls on groundwater flow. The WLPMA is coincident with the west sub-basin of the LPVB (**Figure 3-1**). The ELPMA is comprised of the locally-recognized east and south sub-basins of LPVB (**Figure 3-1**). The ELPMA is the focus of this study.

The LPVB is located within the Transverse Ranges Geologic Province, a long narrow east-west trending province, which is composed of numerous east-west trending mountain ranges separated by valleys. This orientation is distinctive and is the basis for the name of the geologic province, as basins and ranges are more commonly oriented in a north-south direction as seen in Coast Range, the Sierra Nevada, and the Basin and Range Province, which includes southeastern California and other parts of the western United States. Since early Miocene time, the Transverse Ranges block has rotated 80-110 degrees from its original orientation (Kamerling and Luyendyk, 1985). The east-west orientation of mountain ranges and basins is a result of a complex sequence of tectonic events closely linked to the evolving convergence of the Pacific and North American Plates due to the Big Bend in the San Andreas Fault Zone. As a result, the Transverse Ranges Geologic Province is being squeezed together with a maximum compression oriented in a north-south direction, which is perpendicular to the east-west trending mountains, valleys, and folding and faulting. It is one of the most rapidly uplifting areas on Earth (Harden, 2003).

The LPVB is an east-west trending valley between the South and Oak Ridge mountains to the north and the Camarillo and Las Posas hills, which are major anticlinal uplifts, to the south (**Figure 3-1**). The LPVB can be characterized as a synclinal area plunging westward that includes several minor *en echelon* (closely spaced parallel or subparallel) synclines and anticlines (CH2M, 2017). Due to folding, the FCA and GCA are buried deeply in the central portion of the basin and exposed along the basin margins.

Within the ELPMA, there are two primary east-northeasterly trending anticlines and three primary east-northeasterly trending synclines, which are part of the Camarillo fold belt (DeVecchio et al., 2012). The major folds in the LPVB, from north to south, are the Long Canyon Syncline, the Long Canyon Anticline, the Las Posas Syncline, the Moorpark Anticline, and the Moorpark Syncline (Turner, 1975). Folds in the LPVB strongly affect the occurrence, movement, and quality of groundwater (Ventura County Public Works Agency [VCPWA], 1975) (**Figure 3-2**).

CH2M (2017) identified several internal and basin bounding faults that may influence groundwater flow in the LPVB. These faults include the Fox Canyon (only in the WLPMA), Berylwood, and

Fairview faults in the northern portion of the basin; the Little Simi Valley faults in the southern portion of the basin; and the Somis Fault, also called the Central Las Posas Fault, which is a basin bounding fault between the ELPMA and the WLPMA, as discussed in the next section.

As noted, the geology of the region is complex due to intense tectonic deformation associated with the San Andreas Fault Zone and the rotation of the Transverse Ranges. The details of the complex geologic history of the area are beyond the scope of this groundwater modeling report, so the emphasis is on connecting the geologic history to the hydrogeology and on the occurrence and movement of groundwater.

3.2 Extent and Boundaries

The LPVB is bounded on the north by non-water bearing rocks of the South Mountain and the Oak Ridge Mountains and on the south by the Springville and Santa Rosa Fault systems. To the east, water-bearing units of the LPVB pinch out against non-water bearing Tertiary units. The Somis Fault Zone separates the LPVB into the WLPMA and the ELPMA by forming a barrier to groundwater flow between the sub-basins in the deep, confined aquifers. From a surface water perspective, the ELPMA outlet is between the Las Posas and Camarillo Hills where Arroyo Las Posas exits the LPVB and enters the Pleasant Valley Basin, where its designation becomes Calleguas Creek.

3.2.1 Basin Boundaries

Various LPVB boundaries have been used historically (California Department of Resources [DWR], 1975; 2003; 2016). DWR's Bulletin 118 defines the basin boundary based on the alluvium and hence excludes outcrops of the FCA and GCA (DWR, 2003; 2016).

The FCGMA is an independent special district created by the California Legislature in 1982 via the FCGMA Act, Assembly Bill No. 2995, to manage and protect the groundwater resources of five groundwater basins underlying southern Ventura County, including parts of the LPVB (FGMA, 2015). The jurisdictional boundary of the FCGMA was established based on a vertical projection of the FCA. Over time, the FCGMA boundary has been revised to reflect updated knowledge of the extent of the aquifers. Local practitioners recognized that GCA outcrops are hydrologically connected to the basin, as the GCA underlies the FCA, but GCA outcrops are not included in basin boundaries defined by DWR or the FCGMA. The basin boundary defined by the FCGMA deviates from DWR's Bulletin 118 boundary in two areas. First, DWR's Bulletin 118 boundary extends east of the FCGMA jurisdictional boundary where the FCA thins. Second, the FCGMA jurisdictional boundary extends north and northeast of the DWR's Bulletin 118 boundary and includes outcrops of the FCA and the GCA.

In addition to the jurisdictional basin boundary, the FCGMA defined an expansion area, a land use management area, that includes the FCA outcrop and uphill areas to protect the quality of water recharging the FCA. The expansion area is defined as that portion of land beyond the outer limits of the FCA outcrop that lies between the FCA outcrop and the crest of the hill or 1.5 miles beyond the FCA outcrop (Los Posas Users Group [LPUG], 2012). The expansion area was established by the FCGMA in 1987 with passage of Ordinance 4.

The western extent of the ELPMA is based on the Somis Fault Zone, the geologic structure that forms a barrier to flow between the West and East Las Posas sub-basins within the deep confined aquifers (CH2M, 2017).

3.2.2 Boundary for Hydrogeologic Conceptual Model

The study area boundary for the hydrogeologic conceptual model and the numerical model of groundwater flow generally coincide with the ELPMA (**Figure 3-1**). Additional outcrops of the GCA are included north of DWR's Bulletin 118 (2016) and east and south of the FCGMA's expansion area.

3.3 Stratigraphy and Hydrogeology

The LPVB is an east-west trending structure that has been highly folded with intense folding in Pleistocene sediments. In addition to folding, the LPVB has been tilted, and thus the principle structures in the basin plunge westward to the Oxnard Plain. The tectonic history of the region resulted in aquifers that have been folded and faulted into sub-basins with varying degrees of hydraulic communication. As discussed above, the Somis Fault Zone separates the WLPMA and the ELPMA by forming a barrier to groundwater flow between the sub-basins in the deep, confined aquifers. This is evident in the water level offsets, which can be as much as 250 feet (ft) between the sub-basins (CH2M, 2017).

The primary source for the stratigraphy and hydrogeology of the LPVB comes from a conceptual hydrogeologic model of the WLPMA and the ELPMA developed by CH2M (CH2M, 2017). The CH2M geologic conceptual model was based on reviewing existing work and publications, compiling electric logs (e-logs) and other subsurface information, and developing a geologic model, which was implemented in Rockworks. Rockworks (developed by Rockware, Inc. in Golden, CO) is used for borehole database management, lithologic correlation, subsurface visualization, and the creation of grids, surface maps, isopach maps, and related analyses. CH2M (2017) developed a stratigraphic column as part of the geologic conceptual model, as shown in **Table 3-1**, along with the aquifers and confining units present in the LPVB and age-equivalent regional aquifers.

Surficial geology from CH2M (2017), based on pre-Dibblee investigations, is shown in **Figure 3-3**. The Saugus Formation is present along the Happy Camp Syncline (**Figure 3-2**) and between the southern outcrop of the FCA and Arroyo Las Posas. Near Arroyo Las Posas/Simi alluvial fan deposits, valley fill, landslide deposits, and younger and older alluvium are present. Older alluvium is present, for example, between the Epworth Gravels and Arroyo Las Posas/Simi. CH2M (2017) lumped the Pleistocene-aged alluvium, informally called older alluvium as represented by “Qoal,” when exposed at the surface with the Upper San Pedro/Saugus Formation. The lumped surficial geology is shown in **Figure 3-4** and is described by the column “CH2M Stratigraphic Column” in the stratigraphic column shown in **Table 3-1**.

The locations and extents of the FCA and GCA outcrops are key aspects of the hydrogeologic conceptual model, and the mapped extent of the FCA and the GCA varies among the digital geologic maps provided by CH2M as presented in **Figure 3-5**. For this study, the northern extent of the FCA and GCA outcrops is based on the work of Staal et al. (1990) as presented in CH2M’s pre-Dibblee surficial geologic map (**Figure 3-5A**). The southern extent of the FCA outcrop is based on the Dibblee surficial geologic maps (Dibblee, 1992, 1990) as presented in CH2M’s (2017) Rockworks surficial geology map (**Figure 3-5B**). The GCA outcrops are based on the work of Staal et al. (1990) as presented in CH2M’s (2017) pre-Dibblee surficial geologic map (**Figure 3-5C**).

The hydrogeology of LPVB is well characterized in CH2M (2017) and in the Final Draft V.1 Las Posas Basin-Specific Groundwater Management Plan (LPUG, 2012). A brief summary of the hydrogeology and aquifers is provided below. Details of the hydrogeologic surfaces are discussed in Section 4.0. Groundwater occurrence and movement is specifically addressed in Section 5.0.

3.3.1 Shallow Aquifer

The Shallow Aquifer is the uppermost water-bearing unit and extends from land surface to a depth of up to approximately 150 ft along the Arroyo Las Posas/Simi floodplain. The Shallow Aquifer consists of Pleistocene- and Holocene-age alluvium characterized by sand and gravel in the eastern portion of the basin, and a higher prevalence of clays and silts in the western portion of the LPVB (DWR, 2003). Groundwater is present in unconfined conditions and is recharged by native and non-native (discharge of treated municipal wastewater) flows in Arroyo Las Posas/Simi. Few wells pump from the Shallow Aquifer because, historically and currently, groundwater quality has been marginal compared to deeper aquifers (LPUG, 2012). Downward leakage from the Shallow Aquifer through the Upper San Pedro/Saugus Formation provides an important source of recharge to the FCA (LPUG, 2012). The filling of the Shallow Aquifer due to increases in non-native flows in Arroyo Las Posas/Simi is discussed in section 5.0.

3.3.2 The Epworth Gravels Aquifer

The Epworth Gravels Aquifer is a localized aquifer within the upper portion of the Upper San Pedro/Saugus Formation near Broadway Road (LPUG, 2012). The aquifer is located 2 to 3 miles north-northwest of Moorpark, and its areal extent is on the order of 6 square miles (VCPWA, 1975). The Epworth Gravels consists of about 200 ft of gravel, gravelly clay, and silt (VCPWA, 1975) of Late Pleistocene age. The limited extent of the Epworth Gravel deposits has led to the interpretation that the deposits are remnants of an alluvial fan which has been folded and eroded (VCPWA, 1975). Historically, the Epworth Gravels Aquifer has been an important source for water supply for the area it underlies. The Fairview Aquifer, a local unconfined aquifer that may provide downward leakage into the Epworth Gravels Aquifer (LPUG, 2012), was not evaluated separately by CH2M and was generally lumped with the Epworth Gravels Aquifer in the CH2M's hydrogeologic conceptual model (CH2M, 2017). In the following discussion, the term "Epworth Gravels Aquifer" denotes the combined Epworth Gravels and Fairview aquifers.

The Epworth Gravels Aquifer is separated from the underlying FCA by several hundred feet of the Upper San Pedro/Saugus Formation and the Epworth Gravels Aquifer is not believed to be in hydraulic communication with deeper aquifers such as the FCA (VCPWA, 1975, LPUG, 2012). Very low groundwater flow rates between the Epworth and the Upper San Pedro/Saugus Formation/FCA are evident in the several hundred feet of vertical head gradients across wells screened in the two aquifers.

3.3.3 Upper San Pedro/Saugus Formation

The Upper San Pedro/Saugus Formation consists of Early Pleistocene marine clays and sands and terrestrial fluvial sediments. The formation grades upward from a white gray sand and gravel basal layer into an overlying series of interbedded silts, clays, and gravels (Turner, 1975). The Upper San Pedro/Saugus Formation consists of low permeability sediments with lenses of permeable sediments (VCPWA, 1975) and is the age-equivalent of the Hueneme Aquifer present in the Oxnard Plain (VCPWA, 1975). The water-bearing zones of the Upper San Pedro/Saugus Formation are not well connected and are not considered an aquifer.

3.3.4 Clay Marker Bed

The Upper San Pedro/Saugus Formation is typically separated from the underlying FCA by a gray clay marker bed of Pleistocene age. The clay varies in thickness but is typically less than 25 ft thick and is locally continuous (CH2M, 2017) but may not be continuous beneath Arroyo Las Posas west of the Moorpark wastewater treatment plant (WWTP) based on water quality data.

3.3.5 Fox Canyon Aquifer

The FCA consists of Late Pleistocene marine shallow regressive sands at the base of the San Pedro Formation. The FCA consists of continuous white or gray sand and gravel with minor silt and clay interbeds and contains abundant marine fossils (VCPWA, 1975). The FCA was folded post-

deposition (VCPWA, 1975). The FCA is laterally continuous in the LPVB. At the northern and southern basin margins, the FCA exists under unconfined conditions, and the aquifer is exposed at the surface in outcrops. Away from the basin margins, the FCA exists under confined conditions. The FCA is reported as 200 to 300 ft thick in most areas of the basin, with local thicknesses of 500 to 600 ft (LPUG, 2012; CH2M, 2017). The FCA is thinner, typically less than 100 ft, in the southeast portion of the basin, where the top of the FCA rises up such the depth to the top of the FCA is on the order of 200 ft. In the northeast, the FCA pinches out near Happy Camp Canyon. As most wells in the LPVB are perforated in the FCA, it is the principal water-bearing unit in the LPVB. The Somis Fault Zone forms a barrier to groundwater flow between the eastern and western portions of the FCA, as evident in the water level offsets, which can be as much as 250 feet (ft) (CH2M, 2017).

3.3.6 Upper Portion of the Upper Santa Barbara

The FCA is separated from the underlying GCA by a clay-rich aquitard called the upper portion of the Upper Santa Barbara. The aquitard may not be present at all locations and varies in thickness. CH2M (2017) identified contiguous thicknesses of 150 to 250 ft near the Long Canyon Anticline and the Las Posas Syncline, but the average thickness in the study area is about 20 ft. Where present, the clay layer is expected to greatly limit hydraulic communication between the FCA and GCA (LPUG, 2012). To the east of Stockton Road, the FCA and GCA are believed to be in hydraulic communication (VCPWA, 1975), which is consistent with CH2M's isopach which shows a thinner, clay-rich upper portion of the Upper Santa Barbara in southeast portion of the LPVB. Most wells do not penetrate the full thickness of the FCA or penetrate the GCA, which results in some uncertainty regarding the continuity and thickness of the clay-rich unit (CH2M, 2017; LPUG, 2012).

3.3.7 Grimes Canyon Aquifer

The GCA consists of up to 300 ft (CH2M, 2017) of hardened sandstones and conglomerates of clay, silt, sand and gravel of Pleistocene age (LPUG, 2012; VCPWA, 1975) that is laterally continuous in the LPVB. Like the FCA, the GCA was folded post deposition. A relatively small number of wells penetrate the GCA, which limits information on the variation in thickness within the basin. Like the FCA, the GCA exists under unconfined conditions at the northern basin margin, where the aquifer is exposed at the surface in outcrops. Away from the northern basin margin, the GCA exists under confined conditions. The GCA is likely in hydraulic communication with the FCA to the east where the upper portion of the Upper Santa Barbara is interpreted to be thin or absent. As in the FCA, the Somis Fault Zone, likely, acts as a flow barrier between the eastern and western portions of the GCA (CH2M, 2017).

Underlying the GCA and outcropping to the east and northeast are non-water bearing Tertiary units (DWR, 2003), including the Modelo Formation consisting of marine mudstones, the Conejo

Volcanics consisting of terrestrial and marine extrusive and intrusive igneous rocks, and the Sespe Formation consisting of sandstone and cobble conglomerate.

DRAFT

Table 3-1 Regional Geology and Stratigraphic Column from CH2M (2017, Figure 6)

Geologic Time									
Period	Epoch	Geologic Formation of Pre-Dibblee Investigators ¹		Dibblee ²	Geologic Formations of Post-Dibblee Investigators ³	CH2M Stratigraphic Column ⁴	Regional Aquifer Designations ³	Regional Aquifer Systems ³	
Quaternary	Holocene	Recent Alluvium (Qal)		Alluvial Deposits (Qa)	Alluvium – recent (Qya)	Undifferentiated Alluvium (Qal) ⁷	Recent alluvial and semi-perched Oxnard	Upper Aquifer System (UAS)	
	Pleistocene (Late/Upper)	Older Alluvium and Terrace Deposits (Qt)		Older Surficial/Alluvial Sediments (Qoa)	Alluvium – older (Qoa)				Mugu
		San Pedro Formation	Epworth Gravels (Qspg)	Saugus Formation (QTs)	Saugus Formation (Qs)	Epworth Gravels (Qseg)	Hueneme	Lower Aquifer System (LAS)	
			Fox Canyon Member (Qspfc)	Las Posas Sand (QTlp)	Las Posas Formation (Qlp)	Clay Marker Bed (CL)			Fox Canyon
		Santa Barbara Formation	Grimes Canyon Member (Qsbgc)		Santa Barbara Formation (Qsb)	Upper Santa Barbara Formation (clay-rich) (Qsb)	Grimes Canyon		
						Grimes Canyon Aquifer (Qsbfc)			
	Pleistocene (Early/Lower)	Pico Formation (Tp)		Pico Formation (Tp) ⁵	Pico Formation (Tp)				
Tertiary	Pliocene	Repetto Formation				Undifferentiated Tertiary Formation (Effective Base of Fresh Water)	Not included in regional flow system	Not included in regional flow system model ⁶	
	Miocene	Santa Margarita Formation (Msm)		Sisquoc Formation (Tsq)	Tertiary Bedrock				
		Modelo Formation (Mmsh, Mms)		Monterey Shale (Tm)					
		Topanga Formation (Mtp)		Upper Topanga Formation (Ttus)					
		Conejo Volcanics (Tv)		Conejo Volcanics (Tcvb)					
		Vaqueros Formation (Mvq)		Topanga Sandstone (Tts)					
	Oligocene, Eocene	Sespe Formation (Os)		Sespe Formation (Tsp)					

1. From Ventura County Water Resources Management Study, Geologic Formations, Structures, and History in the Santa Clara-Calleguas Area (prepared by Mukae & Turner, for Ventura County Department of Public Works, 1975), and North Las Posas Basin Hydrogeologic Investigation (prepared jointly by the Calleguas Municipal Water District and the Metropolitan Water District of Southern California, 1989)
2. From Geologic Map of the Moorpark Quadrangle (Dibblee, 1992).
3. From Simulation of Groundwater/Surface Water Flow in the Santa Clara-Calleguas Basin, Ventura County, California (Hanson et al., 2003) and Geologic Map of the Santa Paula 7.5' Quadrangle (Tan et al., 2004). The regional aquifer designations are informational as they are not all present in the Las Posas Valley Basin study area.
4. The stratigraphic column represents the horizons for which elevations will be selected and entered into Rockworks, where present. Some horizons are not present at all locations.
5. Dibblee (1992) infers that the Pico Formation may be in the Pliocene.
6. The Santa Margarita Formation sandstone is included in the northeastern Santa Rosa Valley as Layer 2 of Lower Aquifer System within the model.
7. For purposes of creating the Conceptual Model in Rockworks, where older alluvium is exposed at the surface, it was grouped with the Upper San Pedro/Saugus Formation.

4.0 HYDROGEOLOGIC STRUCTURE AND PROPERTIES

4.1 Updates to Geologic Structure

INTERA received geologic surfaces and hand-drawn contours of the FCA and the GCA as part of CH2M's hydrogeologic conceptual model (2017). The hand-drawn contours of the top elevations of the FCA and GCA incorporated faulting and were produced by Mr. Thomas Hopps, a senior-level structural/petroleum geologist with considerable experience in the Ventura Basin. INTERA reviewed the prior interpretations and updated the geologic surfaces based on further analysis of available data. Updates and final geologic surfaces were kept consistent, as much as possible, with CH2M hydrogeologic conceptual model and hand-drawn contours. The updates to geologic surfaces are described with regard to the data sources used, the geologic analyses performed, and a summary of the major refinements to the geologic surfaces and isopachs in the following sections.

4.1.1 Data Sources

Data sources for the updates to geologic structure are based on surficial geologic maps, geophysical logs, well construction information, a 10-meter (m) digital elevation model (DEM), and data from CH2M in the form of geologic surfaces, isopachs, and control points. A surficial geologic map from Staal et al. (1990) was used to define the location of the outcrops for the FCA and the GCA in the north. In the south, the FCA outcrops were based on Dibblee (1992, 1990). Faults, represented as offset elevation contours on the top elevation of the FCA and the GCA, were incorporated into the update of geologic structure using the hand-drawn contours by Hopps (CH2M, 2017). Hopps (CH2M, 2017) produced contours of the top elevation of the FCA (CH2M 2017, Figure 18b) and contours of the top elevation of the GCA (CH2M, 20017, Figure 21b) with a 100-ft contour interval.

In general, the hand-drawn contours from CH2M and Hopps (CH2M, 2017) were used preferentially, whenever available, over the Rockwork surfaces or isopachs. For example, hand-drawn isopach contours of the Shallow Aquifer from CH2M (2017, Figure 16b) with a 50-ft contour interval and hand-drawn isopach contours of the Epworth Gravels Aquifer from CH2M (2017, Figure 17b) with a 100-ft contour interval were used. The Rockworks isopachs and control points (CH2M, 2017) were used for the clay marker bed (Figure 24), FCA (Figure 20), Upper Santa Barbara Formation (Figure 25), and the GCA (Figure 23) if hand-drawn contour maps were not available.

4.1.2 Geologic Analysis

Using the geologic top surfaces and isopachs described above, geologic surfaces were adjusted such that:

- Elevations were less than or equal to the 10-m DEM and matched surficial topography along outcrops,
- Interpolation artifacts in the CH2M surfaces were smoothed out,
- Extents of geologic surfaces agreed with the surficial geology,
- CH2M geologic picks at ASR wells agreed with the geologic surfaces,
- All isopachs maintained a minimum thickness of 5 ft to provide continuous layers for the numerical model,
- Undifferentiated Alluvium not overlying the Shallow or Epworth Gravels aquifers was remapped as the underlying stratigraphic unit so the Undifferentiated Alluvium isopach could be used to represent the Shallow Aquifer in the groundwater flow model, and
- The Upper San Pedro/Saugus Formation was subdivided vertically into two equal parts to provide refinement for vertical flow in the groundwater flow model. For ease of discussion, these will be henceforth referred to as the top layer and bottom layer of the Upper San Pedro/Saugus Formation.

Updates were made to the top and bottom of the FCA near the Long Canyon Anticline and the Moorpark Anticline to provide additional refinement to the nearby geologic structural trends and well logs. Well logs were combined in cross-sections along structure and perpendicular to structure and the picks at the top of FCA were evaluated in concert with available groundwater elevation data. The overall effect of these minor revisions was to raise the elevation of the top and bottom of FCA (and corresponding overlying and underlying units) along the Moorpark Anticline, especially to the east. CH2M's (2017) picks at the ASR wells were not adjusted and were kept consistent with the updates to the geologic surfaces.

Additional minor updates were made to the bottom elevation of the Epworth Gravels Aquifer near the Fairview fault to smooth out variability in the isopach and bottom elevations and achieve consistency with measured groundwater elevations that indicate saturation in the Epworth Gravels Aquifer. CH2M's (2017) borehole picks and location of the Fairview fault, which truncates the Epworth Gravels Aquifer, were honored, but the bottom elevation of the Epworth Gravels Aquifer was smoothed between control points such that the western half of the isopach of the Epworth Gravels Aquifer was made thicker by lowering the bottom elevation of the Epworth Gravels Aquifer.

4.1.3 Geologic Surfaces and Isopachs

The stratigraphic column for the updated geologic surfaces is listed in **Table 4-1** under the heading "Hydrostratigraphic Column for Flow Model." The top elevation of geologic surfaces and the bottom elevation of the GCA are shown in **Figures 4-1** through **4-8**. The isopachs of each

hydrostratigraphic unit are shown in **Figures 4-9** through **4-14** and select features of the isopachs are described below.

Alluvium and Epworth Gravels Isopach:

- Thicker portions of the alluvium are mostly located north of Arroyo Las Posas/Simi,
- Alluvium is up to 150 ft thick with a contiguous area and thicknesses of 150 to 200 ft occurring between Spring Rd. and Grimes Canyon Rd. near Arroyo Las Posas/Simi.

Table 4-1 Stratigraphic Column from CH2M (2017, Figure 6) and Hydrostratigraphic Column for Groundwater Flow Model

Geologic Time		CH2M Stratigraphic Column ¹	Hydrostratigraphic Column for Flow Model ²	Flow Model Layer	Regional Aquifer Designations ³	Regional Aquifer Systems ³					
Period	Epoch										
Quaternary	Holocene	Undifferentiated Alluvium ⁴	Shallow Aquifer	1	Recent alluvial and semi-perched	Upper Aquifer System (UAS)					
					Oxnard						
	Pleistocene (Later/Upper)	Epworth Gravels	Epworth Gravels	Epworth Gravels	1	Hueneme	Lower Aquifer System (LAS)				
								Upper San Pedro/Saugus Formation	Top Layer of the San Pedro/Saugus Formation	2	
									Bottom Layer of the San Pedro/Saugus Formation		3
								Clay Marker Bed	Clay Marker Bed (aquitard)	4	
								Fox Canyon Aquifer	Fox Canyon Aquifer	5	
								Upper Santa Barbara Formation (clay-rich)	Upper Santa Barbara Formation (aquitard)	6	Grimes Canyon
								Grimes Canyon Aquifer	Grimes Canyon Aquifer	7	
								Tertiary	Pliocene	Undifferentiated Tertiary Formation (Effective Base of Fresh Water)	Not included in groundwater flow model
Miocene											
Oligocene, Eocene											

1. The stratigraphic column represents the horizons for which elevations will be selected and entered into Rockworks, where present. Some horizons are not present at all locations.
2. Gray shading indicates a notable update from the CH2M (2017) stratigraphic column.
3. From Simulation of Groundwater/Surface Water Flow in the Santa Clara-Calleguas Basin, Ventura County, California (Hanson et al., 2003) and Geologic Map of the Santa Paula 7.5' Quadrangle (Tan et al., 2004). The regional aquifer designations are informational as they are not all present in the Las Posas Valley Basin study area.
4. For purposes of creating the Conceptual Model in Rockworks, where older alluvium is exposed at the surface, it was grouped with the Upper San Pedro/Saugus Formation.
5. The Santa Margarita Formation sandstone is included in the northeastern Santa Rosa Valley as Layer 2 of Lower Aquifer System within the model.

- The Epworth Gravels isopach forms a bowl that is as much as 350 to 500 ft thick on the north of the Fairview fault and thins northward as topography steepens.

Clay Marker Bed Isopach:

- The clay marker bed has an average thickness of 20 ft.
- Thicknesses of 35 to 55 ft occur between the Fairview fault and the Las Posas Syncline.

Upper San Pedro Formation/Saugus Formation Isopach:

- The Upper San Pedro/Saugus Formation has an average thickness of 410 ft.
- The thicker portions of Upper San Pedro/Saugus Formation occur along the Las Posas Syncline, the Fairview fault, and the Long Canyon Syncline while the Upper San Pedro/Saugus Formation thins along the Moorpark Anticline.
- In the southwest portion of the basin, near the arroyo, the Upper San Pedro/Saugus Formation thins considerably and is 5 ft thick (the specified minimum thickness).

FCA Isopach:

- The FCA has an average thickness of 275 ft.
- Locally, the FCA's thickness is as much as 500 to 640 ft in two areas. One area is between the Long Canyon Anticline and the Las Posas Syncline near the Somis Fault Zone. The second area of significant thickness occurs in a long narrow band that trends northeast-southwest between the northern portion of ASR well field No. 2 and the southern extent of the northern FCA outcrops.
- The isopach contours are nearly parallel to the eastern portion of the Moorpark Anticline. Thicknesses of 150 to 200 ft occur between Arroyo Las Posas and the southern extent of ASR well field No. 1.
- The FCA thickness is 180 to 240 ft at ASR well field No. 1 and 280 to 580 ft at ASR well field No. 2.

Upper Santa Barbara Formation Isopach:

- The formation has an average thickness of 45 ft.
- Local thicknesses of 250 to 350 ft occur between the Long Canyon Anticline and the Las Posas Syncline.

GCA Isopach:

- The GCA has an average thickness of 110 ft.

- Maximum thicknesses of 275 to 355 ft occur in a contiguous feature between the FCA outcrop in the north and the Las Posas Syncline to the south. This feature trends northeast-southwest and is evident in the CH2M (2017) isopach map.
- The GCA is greater than 150 ft thick in the northern portion of ASR well field No. 2.

The folding and faulting of the geologic surfaces is illustrated in two hydrogeologic cross-sections – one cross-section is oriented north-south (**Figure 4-15**) and the other is oriented west-east (**Figure 4-16**). The north-south cross-section runs from the basin boundary along the GCA in the north, through the Epworth Gravels Aquifer, across the Moorpark Anticline, and terminates at the FCA outcrop along the southern basin boundary, as shown in **Figure 4-15**. This figure illustrates how the Epworth Gravels Aquifer terminates against the Fairview fault.

The second hydrogeologic cross-section runs from the basin boundary in the east, across the Moorpark Anticline, between ASR well fields No. 1 and 2, through the Las Posas Syncline, across splays from the Somis Fault Zone, and terminates against the western basin boundary, which is coincident with the Somis Fault Zone as shown in **Figure 4-16**. The cross-section shows that Upper San Pedro/Saugus Formation, the FCA, and the GCA are all thin units in the east and thicken to the west. The location of the maximum thickness of each unit varies spatially but occurs west of the Las Posas Syncline.

4.2 Initial Hydraulic Properties

Initial hydraulic properties for the groundwater flow model were based on available data from specific capacity testing, pumping tests, and grain size analysis. Initial hydraulic properties were refined during calibration and constrained by the hydraulic property data. In general, the modeling strategy was to start simple and add additional complexity to the spatial distribution of hydraulic conductivity as warranted by the misfit between the simulated and observed values of hydraulic head.

4.2.1 Hydraulic Conductivity

Aquifer permeability can be inferred from available data, which includes specific capacity testing at wells, constant rate pumping tests at ASR wells (CH2MHILL, 2001) and at Shallow Aquifer monitoring wells (Fugro Consultants, 2014; Hopkins, 2013), and from grain size analysis of the Shallow Aquifer (Fugro Consultants, 2014). CH2M compiled the specific capacity testing data and converted them to hydraulic conductivity for the FCA and the GCA based on the thickness in their hydrogeologic conceptual model (CH2M, 2017). INTERA estimated hydraulic conductivity from previously analyzed aquifer tests and reproduced CH2M's (2017) hydraulic conductivity estimates from specific capacity data for the FCA as shown in **Figure 4-17**. At the ASR wells, INTERA estimated a range of hydraulic conductivity using transmissivities derived from aquifer test analyses (CH2MHILL, 2001) and the sum of individual well screen intervals as shown in

Figure 4-17. The range of hydraulic conductivity at each ASR well is based on the range in transmissivities using the Cooper-Jacob (1946) and Theis (1935) solution methods. Using the total length of screen to convert between transmissivity and hydraulic conductivity typically overestimates hydraulic conductivity, as the thickness of the aquifer that contributes to flow at the well is greater than the length of the screen interval. Additionally, many of the wells are screened in both the FCA and GCA so that the transmissivity should be interpreted as an effective transmissivity rather than as a transmissivity representative of only the FCA. **Figure 4-17** shows higher conductivity areas (> 51 feet per day [ft/day]) between the Las Posas Syncline and the Moorpark Syncline in the central portion of the study area.

There are fewer specific capacity measurements in the GCA, but the zone of higher hydraulic conductivity is similar to that in the FCA. Five ASR wells between the Las Posas Syncline and the Moorpark Anticline had hydraulic conductivities between 7.2 and 9.4 ft/day (CH2M, 2017). Between the Long Canyon Anticline and the Moorpark Anticline, there are five wells with hydraulic conductivities between 3.6 and 7.2 ft/day (CH2M, 2017).

For the Alluvium and Upper San Pedro/Saugus Formation, CH2M (2017) developed relative hydraulic conductivity values, which were assigned as low, medium, or high based on the specific capacity data within the footprint of the Shallow Aquifer. A similar analysis was performed for the Lower San Pedro/Saugus Formation (CH2M, 2017). For both maps, the hydraulic conductivity values are higher in the east and decrease to the west.

Constant rate pumping tests were performed in the Shallow Aquifer near the Arroyo at three monitoring wells between Balcom Canyon Road in the east and Somis Road in the west, as part of Phase 1 of the Shallow Monitoring Well Network Installation Program (Fugro Consultants, 2014). The hydraulic conductivity inferred from the pumping tests varied between 5.1 and 83 ft/day (Fugro Consultants, 2014). The lower end of the range came from a well completed in fine-grained materials. The upper end of the range came from a well completed in relatively coarse-grained materials. These single-well pumping tests cannot provide estimates of storage properties.

Using monitoring wells, test wells, and test holes near Arroyo Simi and Hitch Boulevard, the hydraulic conductivity of the shallow alluvium was estimated as 259 ft/day, and the deeper alluvium was estimated as 15 ft/day based on application of the Hazen approximation (Hazen, 1911) of hydraulic conductivity from effective grain size analysis by Hopkins Groundwater Consultants (2013, Table 5). Well interference and potential drawdown effects were simulated by Hopkins Groundwater Consultants (2013) using hydraulic conductivity values of 100, 120, and 200 ft/day for the Shallow Aquifer based on the study findings.

The available data on hydraulic conductivity were integrated and used to assign initial estimates of hydraulic conductivity for each model layer as shown in **Table 4-2**. For aquifers, the ratio of

horizontal to vertical hydraulic conductivity is 10:1, while the aquitards were simulated as isotropic.

Table 4-2 Initial Assignment of Hydraulic Conductivity to Groundwater Flow Model

Aquifer or Hydrostratigraphic Unit	Model Layer	Zone	K _x	K _y	K _z	Specific Storage (1/ft) and (Specific Yield)
			Hydraulic Conductivity in feet per day			
Shallow Aquifer	1	-	50	50	5	(0.25)
Epworth Gravels Aquifer	1	-	50	50	5	(0.25)
Top Layer of the Upper San Pedro/Saugus Formation	2	below Epworth Gravels Aquifer	1x10 ⁻¹	1x10 ⁻¹	1x10 ⁻²	1x10 ⁻⁵
	2	below Shallow Aquifer	1x10 ⁻¹	1x10 ⁻¹	1x10 ⁻²	1x10 ⁻⁵
	2	north of Shallow Aquifer	1	1	1x10 ⁻¹	1x10 ⁻⁵ (0.25)
Bottom Layer of the Upper San Pedro/Saugus Formation	3	-	5	5	5x10 ⁻¹	1x10 ⁻⁵
Clay Marker Bed	4	-	1x10 ⁻³	1x10 ⁻³	1x10 ⁻³	1x10 ⁻⁵
Fox Canyon Aquifer	5	-	20	20	2	1x10 ⁻⁵ (0.25)
Upper Santa Barbara Formation	6	-	1x10 ⁻³	1x10 ⁻³	1x10 ⁻³	1x10 ⁻⁵
Grimes Canyon Aquifer	7	-	20	20	2	1x10 ⁻⁵ (0.25)

K_x is the horizontal hydraulic conductivity in the x-direction

K_y is the horizontal hydraulic conductivity in the y-direction

K_z is the vertical hydraulic conductivity

4.2.2 Storage Properties

Constant rate pumping tests at the ASR well fields provided local estimates of storage properties (CH2MHILL, 2001) for the FCA and GCA. Outside of the ASR well fields, little information was available to infer storage properties, with the exception of pumping tests performed as part of the Moorpark desalter pilot well test project (Hopkins Groundwater Consultants, 2014). Test Well No. 2 is screened in the Shallow Aquifer and storage coefficients of 0.0045 to 0.008 were estimated (Hopkins Groundwater Consultants, 2013, Table D3), and the average value is representative of a leaky or semi-leaky confined aquifer condition (Hopkins Groundwater Consultants, 2013). Interpretation of the storage values is complicated by the fact that the observation well MW-2 (screen depth 240 to 300 ft) is completed in the older alluvium while the test well was completed in both the older and younger alluvium (Hopkins Groundwater Consultants, 2013), which have substantially different hydraulic properties.

A specific yield value of 0.25 was assumed based on textural information and a specific storage of 1×10^{-5} per foot was assigned for an initial estimate of storage as shown in **Table 4-2**, which is consistent with the storage range of 5×10^{-3} to 7×10^{-5} from aquifer testing at wells ASR-5 and ASR-6 (CH2MHILL, 2001).

DRAFT

5.0 GROUNDWATER OCCURRENCE AND MOVEMENT

Groundwater occurrence and movement are presented by characterizing the primary groundwater recharge and discharge mechanisms, by describing changes in groundwater elevations over time, and by discussing spatial trends using contour maps of groundwater elevations. The underlying data sources for the occurrence and movement of groundwater are primarily measured water levels and, secondarily, the water quality sampling in wells.

5.1 Primary Groundwater Recharge Mechanisms

Primary groundwater recharge mechanisms include natural recharge, focused recharge along Arroyo Las Posas/Simi, and return flows as shown in **Figure 5-1**. Natural recharge occurs as diffuse areal recharge and as focused recharge in areas where precipitation runs off the land surface, primarily during storm events, and converges in low channels like tributaries. Focused recharge of native and anthropogenic water occurs along Arroyo Las Posas/Simi and includes discharges from the Simi Valley Water Quality Control Plant (SVQWCP), discharges from dewatering wells operated by the City of Simi Valley, and treated wastewater discharged to percolation ponds at the Moorpark WWTP. Most of the return flows are derived from percolation of irrigation water applied to agricultural lands; a smaller amount is derived from landscape irrigation in developed areas. If irrigation water percolates below the root zone, it may transport through the unsaturated zone and eventually reach the water table. In areas where the water table is deep (several hundred feet below ground surface) or saturated portions of the aquifer are overlain by aquitard material, the time scales of this mechanism could span decades or even centuries (Izbicki and Martin, 1997).

5.2 Primary Groundwater Discharge Mechanisms

Primary groundwater discharge mechanisms include pumping and, to a much lesser extent, evapotranspiration of groundwater by phreatophytes near Arroyo Las Posas/Simi as shown in **Figure 5-2**. Most of the pumping is extracted from the FCA and used for agriculture. Both losing and gaining stream reaches occur along Arroyo Las Posas, indicating portions of the arroyo discharge groundwater to surface water (Engle, 2012; 2013). However, because there is more recharge than discharge of groundwater along the Arroyo, it is characterized overall as a losing stream and the percolation of streamflow is a recharge mechanism.

5.3 Historical Groundwater Elevations

In the Shallow Aquifer, the predominant direction of groundwater flow is from east-northeast to west-southwest. In the FCA, south of the Moorpark Anticline, flow is from south-southeast to north-northwest. North of the Moorpark Anticline in the FCA, the predominant direction of groundwater flow is from outcrops in the north towards the center of the cone of depression

associated with pumping, which was located east of the ASR wells in Fall of 2015 (Bondy Groundwater Consulting, 2016).

Historical groundwater elevations are available as early as 1909, and most of the early groundwater elevation measurements are coincident with the drilling of the well. Much later, there are sufficient groundwater measurements across the basin to infer spatial trends in groundwater elevations. In the early- to mid-1970s, groundwater elevation contours, shown in **Figure 5-3**, indicate a primarily east to west gradient as influenced by the topography and folding of sediments in the basin. Groundwater elevation contours in the FCA in the early- to mid-1970s are largely perpendicular to the ephemeral Arroyo Las Posas/Simi, indicating the arroyo is not a significant source of water to the underlying FCA. These contours are limited by the extent of the measured groundwater elevations, as the FCA extends east of the easternmost groundwater elevation contour.

Groundwater elevation contours in the FCA for 1991 (**Figure 5-4**) reflect conditions prior to operation of the ASR facility. By 1991, the Shallow Aquifer had largely filled throughout most of the basin, and groundwater elevation contours in the FCA were becoming more parallel to Arroyo Las Posas/Simi south of the Moorpark Anticline in the eastern portion of the basin, indicating leakage from the Shallow Aquifer through the Upper San Pedro/Saugus Formation to the FCA. Groundwater elevations in the FCA are between 200 and 250 ft above mean sea level (amsl) in the vicinity of the ASR well fields.

A similar contour map of groundwater elevations in the FCA for average groundwater elevations between 2000 and 2002 is shown in **Figure 5-5** and reflects conditions after the ASR facility began storing water. Between 2000 and 2002, the intersection of the 250 ft groundwater elevation contour at the arroyo has moved farther downstream relative to the 1991 contour map. This indicates rising groundwater elevations in the Shallow Aquifer in response to the progressive filling of the aquifer from the discharges from the SVWQCP in the Simi Valley Basin and leakage from the Shallow Aquifer in the FCA in the ELPMA. Groundwater elevations in the FCA are 200 ft amsl near the west side of the ASR well fields, indicating little cumulative extraction from the facility by 2001.

5.3.1 Change in Elevations with Time

Four of the most significant changes in groundwater elevations with time relate to the filling of the Shallow Aquifer from recharge along Arroyo Las Posas/Simi (**Figure 5-6**), leakage from the Shallow Aquifer into the FCA, and changing groundwater elevations in the FCA as a result of pumping and ASR operations. Additional significant changes in groundwater elevations occur in the Epworth Gravels Aquifer in response to historical pumping. This section describes a series of ordered hydrographs presented as the well locations (**Figures 5-7, 5-10, 5-12, and 5-14**) followed by select hydrographs for each aquifer (**Figure 5-8, 5-9, 5-11, 5-13, and 5-15**), ordered from land surface to the bottom of the water-bearing rocks.

- Filling of the Shallow Aquifer

The ephemeral portion of the Arroyo migrated progressively farther downstream over several decades, as indicated by the timing of rising groundwater elevations and as illustrated by depth to groundwater in the Shallow Aquifer (**Figure 5-6**). In the eastern portion of the study area, groundwater elevations rose in the Shallow Aquifer during the mid-1950s and late 1960s, with corresponding depths to groundwater of 40 and 10 ft bgs, respectively, as shown in the hydrograph for well 02N19W03A01S (**Figure 5-6**).

In the central portion of the study area, upstream of the Moorpark WWTP, groundwater elevations rose in the Shallow Aquifer during the 1970s and 1980s with depth to groundwater decreasing from 90 ft bgs to less than 30 ft bgs by the 1990s, as shown in the hydrograph for well 02N19W07A03S (**Figure 5-6**).

In the western portion of the study area, downstream of the Moorpark WWTP, the available measured groundwater elevations do not capture the beginning of the rise in groundwater elevations. However, by the late 1990s, groundwater elevations in this area rose to a depth of 20 ft bgs and have since decreased about 10 ft bgs, as shown in the hydrograph for well 02N20W12MMW2 in (**Figure 5-6**).

The filling of the Shallow Aquifer also impacted flows in the Arroyo. As groundwater elevations in the Shallow Aquifer rose and moved west, baseflow to the Arroyo increased in gaining portions of the stream. Historically, dry weather flows in the Arroyo did not extend past the LPVB boundary, but, in the early to mid-1990s, dry season flows began spilling into the northern portion of the Pleasant Valley Basin (Hopkins Groundwater Consultants, 2008).

- Epworth Gravels Aquifer

Groundwater elevations in the Epworth Gravels Aquifer dropped approximately 150 ft between 1930 and the mid-1970s in response to pumping as shown in the hydrograph for well 03N19W29E02S (**Figure 5-9**). Beginning in the mid-1970s, pumpers began shifting pumping from the Epworth Gravels Aquifer to the FCA (LPUG, 2012). Between the mid-1990s and 2010, groundwater elevations in the Epworth Gravels Aquifer have recovered as much as 50 ft, as shown in the hydrograph for well 03N19W29F06S (**Figure 5-9**).

- Upper San Pedro/Saugus Formation Groundwater Elevations

An examination of changes in groundwater elevation in wells screened in the Upper San Pedro/Saugus Formation provides important information on the spatial variation of the degree of hydraulic connection between the Shallow Aquifer and the FCA, which is influenced by the thickness of the Upper San Pedro/Saugus Formation and the sediment permeability.

Near the Arroyo, in the eastern and east-central portions of the study area, a rise in groundwater elevation of more than 100 ft occurs in the 1970s and early 1980s in the Upper San Pedro/Saugus Formation, as shown in hydrographs for wells 02N19W05K01S and 02N19W08G03S (**Figure 5-10**, **Figure 5-11a**). Near the Arroyo, in the central portion of the

basin, groundwater elevations rose about 60 ft between the late 1970s and the early 1980s as shown the hydrographs for wells 02N19W06N03S and 02N20W12G02S (**Figure 5-11a**).

North of the eastern and central portions of the Moorpark Anticline, groundwater elevations in the Upper San Pedro/Saugus Formation do not appear to be impacted by groundwater elevation trends in the Shallow Aquifer, as evidenced by declining groundwater elevations from the mid-1970s through the mid-1980s, as shown in the hydrograph for well 03N19W32G01S (**Figure 5-11b**). Similarly, groundwater elevations have gradually declined since the 1990s, as shown in the hydrograph for well 03N20W35R04S (**Figure 5-11b**).

Away from the Arroyo, near the Long Canyon Anticline for example, groundwater elevations in the Upper San Pedro/Saugus Formation are about 240 to 260 ft amsl, which is lower than other portions of the Upper San Pedro/Saugus Formation, as shown in the hydrograph for well 03N20W27H01S (**Figure 5-11b**).

An area with a greater degree of hydraulic connection between the Shallow Aquifer and the FCA is located adjacent to the Arroyo, as indicated by a groundwater rise in the Upper San Pedro/Saugus Formation that begins in the late 1960s, as shown in the hydrograph for well 02N20W12J01S (**Figure 5-11b**). Water quality data also support an area with a greater hydraulic connection between the Shallow Aquifer and the FCA in this area. The northern limit of chloride data sampled in wells that exceed 100 mg/L is much farther away from the Arroyo (Bondy Groundwater Consulting, 2016) in the area, with greater hydraulic connection between the Shallow Aquifer and FCA. Farther from the Arroyo and north of the Moorpark Anticline, the beginning of the groundwater rise is delayed until the 1980s, as shown in the hydrograph for well 02N20W03K02S (**Figure 5-11c**).

- Leakage into the FCA from the Shallow Aquifer

Rising groundwater elevations in the Shallow Aquifer enhanced leakage into the FCA via a larger vertical hydraulic gradient. Folding and faulting of the sediments between the Shallow Aquifer and the FCA affects the movement of groundwater. Of particular significance is the steep rise in elevation of the top of the FCA seen just south of the Arroyo (**Figure 4-5**) towards the FCA outcrop and the corresponding thinning of the Upper San Pedro/Saugus Formation, so much so that the Upper San Pedro/Saugus Formation is virtually absent along downgradient (southwest) reaches of the Arroyo past the Moorpark WWTP (**Figure 4-10**). Bachman described this thin area of the Upper San Pedro/Saugus Formation as an area where the Upper San Pedro/Saugus Formation was extensively eroded prior to deposition of overlying alluvial materials (Bachman, 2016).

In general, the distance from the Arroyo and geologic structures in the basin impacts the timing of changes in groundwater elevations in the FCA. For example, south of the Moorpark Anticline in the central and western portions of the study area, groundwater elevations increased during the late 1970s through the mid-1990s. North of the Moorpark Anticline and

south of the Las Posas Syncline, groundwater elevations increased during the late 1970s and the late 1990s. Farther north, between the Long Canyon Anticline and the Las Posas Syncline, groundwater elevations increased during the 1980s through the early 2000s. In the eastern portion of the study area, north of the Moorpark Anticline, there are groundwater elevations in the Upper San Pedro/Saugus Formation and the FCA that do not appear to be impacted by the filling of the Shallow Aquifer.

Near the Arroyo and south of the Moorpark Anticline, during the late 1970s through the mid-1990s, FCA groundwater levels rose about 200 ft, as shown in hydrographs for wells 02N20W17J01S, 02N20W09R01S, and 02N20W09Q05S (**Figure 5-12, Figure 5-13b**). The latter two wells show that groundwater elevations have decreased by more than 25 ft since mid-1990s.

North of the Moorpark Anticline and south of the Las Posas Syncline, during the late 1970s through the late 1990s, groundwater elevations rose about 150 ft east of the Moorpark Anticline, as shown in the hydrograph for well 02N20W09F01S (**Figure 5-13a**), and 125 ft in the FCA north of the Moorpark Anticline, as shown in the hydrographs for well 02N20W10D02S (**Figure 5-13b**). Groundwater levels in these wells have decreased by approximately 50 ft since the mid-1990s.

Farther north, between the Long Canyon Anticline and the Las Posas Syncline, during the early 1980s through the 2000s, groundwater elevations rose between 100 ft in the FCA as shown in the hydrographs for wells 02N20W03B01S (**Figure 5-13a**) and 03N20W34K01S and 03N20W34G01S (**Figure 5-13c**). Since the peak groundwater elevations in the early 2000s, groundwater elevations have fallen about 75 ft at these wells.

The eastern and central portions of the Moorpark Anticline limit the impact of fluctuations in the Shallow Aquifer on the FCA as shown in hydrographs for wells 03N20W36G01S and 03N19W32A01S (**Figure 5-13c**), although some of these wells may be screened in the Upper San Pedro/Saugus Formation.

• ASR Operation Effects on FCA Groundwater Levels

CMWD began storing water in the ELPMA via in-lieu deliveries and injection in the mid-1990s. The cumulative volume of stored water increased between the mid-1990s and 2007, peaking at 28,664 acre-feet (AF) in 2007. During this period of increasing storage, groundwater elevations in the FCA rose about 40 ft at well 03N20W35R01S and 50 ft at well 03N20W35R03S (**Figure 5-13d**). CMWD recovered much of its stored water between 2007 and 2010. In-lieu deliveries to Ventura County Water Work District (VCWWD) No. 1 wells in the vicinity of the ASR well fields also ceased in 2007, resulting in the resumption of pumping by VCWWD No. 1 at wells at approximately the same time CMWD recovery activities were being initiated. The majority of the recovery pumping occurred during the period of 2008

through 2010. Wells located west of the ASR facility show groundwater elevations in the FCA decreasing about 100 ft between 2005 and 2010 as shown in hydrographs for wells 03N20W35J01S (**Figure 5-13c**) and 03N20W36G01S (**Figure 5-13d**). These same wells show an approximate 60-foot recovery in groundwater elevations between 2011 and 2013. The groundwater elevations following recovery are believed to be approximately what they would have been without storage and recovery activities. This will be evaluated further with the model.

GCA

Groundwater elevations in the GCA have decreased as much as 50 ft between the mid-1970s and late-1990s, as shown in the hydrograph for well 03N20W23L01S (**Figure 5-14, Figure 5-15a**), which is located near the outcrop of the FCA. Groundwater elevations were more stable between the late-1990s and the 2010 at both wells 03N20W23L01S and 03N19W17Q01S (**Figure 5-15a**).

5.3.2 Variation of Elevations with Depth

Few long-term records of groundwater elevations are available for the Upper San Pedro/Saugus Formation. However, well 03N20W35R04S, located near the Las Posas Syncline (**Figure 5-10**) recorded a steady decline in groundwater levels since the early 1990s. The early 1990s will be used as a period to compare groundwater elevations among the Epworth Gravels Aquifer, the Shallow Aquifer, the Upper San Pedro/Saugus Formation, and the FCA. In the early 1990s, groundwater elevations were on the order of 310 ft amsl (**Figure 5-13b**), which is about 100 ft above groundwater elevations in the FCA as recorded in nearby well 03N20W35R01S (**Figure 5-11d**). Groundwater elevations in the Epworth Gravels Aquifer were 550 to 575 ft amsl in wells 03N19W29F06S and 03N20W25H01S (**Figure 5-9**), respectively. In the Shallow Aquifer, groundwater elevations were 575 ft amsl at well 02N19W03A01S in the eastern portion of the basin and were likely between 410 and 440 ft amsl in the central portion of the basin based upon wells 02N19W07A03S and 02N19W07G01S (**Figure 5-8a**).

5.4 Groundwater Levels and Flow Direction

5.4.1 Spatial Trends in Groundwater Elevations

Spatial trends in groundwater elevations are presented for both the Shallow Aquifer (**Figure 5-16**) and the FCA for 2015 (**Figure 5-17**) using contour maps from Bondy Groundwater Consulting (2016). Note that the extent of the contours is not coincident with the extent of the aquifers but rather the extent of the groundwater elevation measurements used to make the contour maps. In the Shallow Aquifer, groundwater elevation contours are essentially perpendicular to the Arroyo, and the groundwater gradient is steep in the west.

In 2015, the FCA groundwater elevation contours are nearly parallel to Arroyo Las Posas south of the Moorpark Anticline, indicating leakage from the Shallow Aquifer. Groundwater elevations are

lowest in the central portion of the ELPMA where much of the pumping in the basin occurs, as indicated by the 125 and 150 ft amsl contours of groundwater elevation.

The Shallow Aquifer and the FCA are in close hydraulic communication just downstream of the Moorpark WWTP, as indicated by the coincident locations of the 300 ft groundwater elevation contour in both the FCA and the Shallow Aquifer. In this area, the Upper San Pedro/Saugus Formation is less than 100 ft thick (**Figure 4-10**), and the clay marker bed may be thinner, faulted, or not present. Bachman (2016) described this as an area where the Upper San Pedro/Saugus Formation was extensively eroded prior to deposition of overlying alluvial materials.

5.4.2 Estimate of Travel Times

Estimates of travel times through the groundwater system are available from geochemical studies and water chemistry sampling in the LPVB. Geochemical studies and water chemistry sampling are used to infer relative differences in travel times, rather than absolute travel times, within the basin to infer the relative rates of movement of groundwater. A geochemical study by Izbicki and Martin (1997) used deuterium sampled from groundwater wells to determine the source and to trace the movement of groundwater in the basin. Also, radioactive isotopes of carbon (carbon-14) were used to determine the age of the water reported as the time since the groundwater was recharged. Note that carbon-14 ages for groundwater are subject to considerable uncertainty even when the chemistry along the path of the groundwater is understood. Using the carbon-14 ages, the water in the center of the basin near the Las Posas Syncline was found to be 3 to 4 times older than the water near the FCA outcrop in the north (Izbicki and Martin, 1997). The presence of tritium in the Upper Aquifer System (UAS) was also used to identify younger water near the arroyo south of the Moorpark Anticline (Izbicki and Martin, 1997) in the eastern and central portions of the study area. This was also evidenced by a delta deuterium measurement of groundwater in the UAS that showed water originating from surface water infiltration from Arroyo Simi and Arroyo Las Posas had moved across the Moorpark Anticline.

The findings of Izbicki and Martin (1997) are consistent with long-term monitoring of chloride concentrations in wells that exceed 100 mg/L (**Figure 5-18**), which were present on the north side of the Moorpark Anticline near well 02N20W01A01S and near the west end of the Moorpark Anticline near well 02N20W10G01S by the 1990s. As previously discussed, the source of the elevated chloride concentrations are anthropogenic contributions to streamflow (treated municipal wastewater and Simi Valley dewatering wells) that filled the Shallow Aquifer, percolated, and continue to flow north or northwest through the Upper San Pedro/Saugus Formation and the FCA. The long-term monitoring of chloride concentrations at wells provides a relative travel time for the arrival of elevated chloride concentrations at wells from Arroyo Las Posas/Simi. By the 1980s, the northern limit of the 100 milligrams per liter (mg/L) chloride concentration was about 1 mile north of the Arroyo to the west of Grimes Canyon Road and about 1/3 mile north of the Arroyo

near the Somis Fault Zone, which defines the western basin boundary, as shown in Figure 5-18 from Bondy Groundwater Consulting (2016). By 2012 and 2013, the northern limit of the 100 mg/L chloride concentration had moved north of the Moorpark Anticline near Balcom Canyon Road and Grimes Canyon Road, respectively, a distance of about 1.3 miles from the arroyo.

In summary, in the western portion of the study area, the FCA is closely hydraulically connected to the Shallow Aquifer and groundwater elevations rise in the FCA in the 1970s and 1980s in response to an increase in flows in Arroyo Las Posas/Simi caused by increasing municipal wastewater return flows.

DRAFT

6.0 CONCEPTUAL WATER BUDGET

A water budget accounts for the inputs, outputs, and changes in the total amount of water by breaking down the hydrologic cycle into components. The water balance equation is the basis of any water budget, which can be expressed as:

$$\Delta\text{Storage} = \sum\text{Inflows} - \sum\text{Outflows} \quad (\text{Equation 4-1})$$

For a groundwater budget, when the sum of the inflows exceeds the sum of the outflows, groundwater levels rise, and there is an increase in the amount of groundwater stored in aquifers. Conversely, when outflows exceed inflows, groundwater levels decrease, and there is a decrease in the amount groundwater stored in aquifers. By convention, the accounting of flows in a water budget is simplified and assumes no time lag for travel times from land surface to the groundwater system.

The “conceptual” water budget presented in this section was a pre-modeling water budget for the groundwater system based on available data. The water budget was developed independently of the groundwater flow model to guide and constrain calibration of the groundwater flow model. Both native and non-native flows are accounted for in the water budget. It is emphasized that neither this “conceptual” water budget nor its individual components are calibrated and should not be used or cited for other purposes. Again, the sole purpose for developing this “conceptual” water budget was to provide starting points for calibration of the numerical groundwater flow model.

6.1 Period of Record

The primary data for the water budget include precipitation, streamflow, groundwater levels, and pumping records. Precipitation records are available at several stations in the LPVB and surrounding hills. The longest precipitation records are from Ventura County Watershed Protection Department’s (VCWPD) site ID 190 Somis-Bard, which has recorded daily precipitation since 1955, and VCWPD’s site ID 002 Somis-Aggen Ranch, which has recorded daily precipitation since 1903 (**Figure 6-1**).

Average daily streamflow records from VCWPD are available at several stations in or near the LPVB (**Figure 6-1**) as listed from upstream to downstream in **Table 6-1** and shown in **Figure 6-2**. Over the period of record, streamflow data may not be continuous and may be missing for days or years. The streamgages within (or near) the LPVB (gages 801, 841A, 841) do not have overlapping periods of record.

Table 6-1 Period of Record for Daily Streamflow Gages Considered in the Water Budget Analysis

Gage Name	Gage ID	Period of Record
Arroyo Simi at Madera Road Bridge	803	1933 - present
Arroyo Simi at Moorpark – Spring St.	801	1933 - 1978
Arroyo Las Posas at Hitch Blvd	841	1990 - 2004
Arroyo Simi above Hitch Blvd	841A	2004 - present
Calleguas Creek above Hwy 101	806	1968 - 1997
Calleguas Creek at Hwy 101	806A	1997 - 2007

Groundwater elevation has been recorded in wells as far back as 1909 in the LPVB. Pumping records from the FCGMA begin in 1983 but are not considered reliable or comprehensive until 1984 or 1985. For this water budget, the most recent available reported pumping from the FCGMA was from 2015.

A conceptual water budget was computed from 1985 through 2015, largely based on the period of record for pumping and on the period of record for the use of imported water in the ELPMA from water purveyors from Dudek (2017). This period does not capture the beginning of the filling of the Shallow Aquifer in response to increases in baseflow due to anthropogenic inflows in the form of treated wastewater effluent. However, the water budget period does capture the late-time filling of the Shallow Aquifer and the dry season flows from Arroyo Las Posas spilling into the Pleasant Valley Basin in approximately 1994 (Hopkins Groundwater Consultants, 2008).

6.2 Water Budget Components

The major components of groundwater inflow (recharge) in the study area are:

- Recharge from precipitation
- Focused recharge along Arroyo Las Posas/Simi
- Recharge via percolation ponds at the Moorpark WWTP
- Recharge from return flows including recharge from agricultural return flows, septic systems, outdoor municipal and industrial (M&I) water use, and leakage from water distribution systems
- Injection via wells at the ASR facility

The major components of groundwater outflows (discharge) in the study area are:

- Groundwater pumping at wells
- Extraction via wells at the ASR facility
- Consumptive use of shallow groundwater by vegetation via evapotranspiration (ET)

Lesser components in the water budget include inflows as underflow from the Simi Valley Basin and outflows as underflow to Pleasant Valley Basin through the alluvium of the Shallow Aquifer. Each of the major water budget components are described below. The inflow terms are listed in **Table 6-2**, and the outflow terms are listed in **Table 6-3** along with change in storage.

DRAFT

Table 6-2 Water Budget Inflows in Acre-Feet Per Year

Source (when not this study)	Recharge	Based on DBS&A (2017)	Septic Return Flows	Based on DBS&A (2017)	Based on Dudek (2017)	Hydrometrics (2016)	Percolation of Dry Weather Streamflow	Moorpark Net Infiltration from Percolation Ponds ²	CMWD	Total Inflow	Total Inflow Includes Use of Imported Water in ELPMA from Purveyors	CMWD
Calendar Year		Urban M&I Irrigation Return Flows		Ag Irrigation Return Flows	Leakage from Water Distribution Systems	GW Inflow from Simi Valley in Shallow Aquifer			Injection at ASR Wells			In Lieu Deliveries from SWP in ELPMA ¹
1985	3,362	584	385	1,917	427	5	8,903	1,646	0	15,583	23,589	0
1986	6,728	594	385	1,676	434	5	9,815	1,681	0	19,637	27,209	0
1987	4,024	705	385	1,900	515	5	10,382	1,793	0	17,916	26,594	0
1988	4,280	737	385	2,113	539	5	10,627	1,925	0	18,687	28,282	0
1989	2,042	770	385	2,419	563	5	10,222	1,910	0	16,408	26,611	0
1990	1,952	819	385	2,283	598	5	10,019	1,859	0	16,061	26,682	0
1991	5,983	588	385	1,978	429	5	9,436	1,798	0	18,805	27,031	0
1992	7,560	559	385	1,646	408	5	10,374	1,859	0	20,938	29,482	0
1993	8,115	555	385	1,788	406	5	10,874	1,930	66	22,194	31,033	0
1994	4,061	605	385	1,890	442	5	10,182	2,101	344	17,915	26,071	0
1995	9,661	542	385	1,563	396	5	10,091	2,197	371	23,014	30,426	276
1996	6,994	439	385	1,471	321	5	9,915	2,108	250	19,781	27,665	5,501
1997	4,733	497	385	2,009	363	5	10,476	2,221	250	18,719	27,476	3,047
1998	10,127	423	385	1,774	309	5	11,354	2,440	3	24,381	31,393	507
1999	3,316	574	385	2,212	419	5	10,712	2,193	114	17,737	26,702	0
2000	4,909	499	385	2,170	365	5	10,807	2,230	3	19,143	28,422	1,871
2001	7,177	530	385	1,637	387	5	12,708	729	2	22,832	31,988	140
2002	3,166	715	385	2,292	522	5	12,569	655	435	20,090	31,831	0
2003	4,580	609	385	1,961	445	5	11,054	2,405	1,186	20,225	30,840	1,379
2004	6,196	589	385	2,283	430	5	10,521	2,143	942	21,352	32,785	2,302
2005	9,957	515	385	1,734	376	5	10,972	2,189	1,704	25,648	35,198	2,390
2006	5,408	555	385	2,250	406	5	10,348	2,142	4,194	23,551	34,096	2,174
2007	2,487	856	385	2,483	625	5	11,089	2,077	57	17,986	30,124	571
2008	5,241	1,051	385	2,369	768	5	10,212	2,083	11	20,042	31,916	445
2009	3,911	1,364	385	2,399	996	5	10,249	2,068	0	19,310	30,171	352
2010	7,912	1,191	329	2,163	870	5	10,382	2,057	0	22,853	31,734	401
2011	4,554	651	329	2,215	476	5	10,694	1,962	764	19,688	27,895	452
2012	3,519	632	329	2,705	462	5	9,694	1,821	1,577	18,922	27,653	437
2013	1,214	666	329	2,897	487	5	9,617	1,682	1,462	16,676	25,827	491
2014	3,376	680	329	2,791	497	5	9,123	1,559	3,838	20,638	30,119	510
2015	2,145	551	317	2,633	402	5	8,818	1,563	703	15,575	23,763	433
Ave (1985-2015)	5,119	666	374	2,117	487	5	10,395	1,904	590	19,752	29,052	764

Ag = Agriculture; ASR = aquifer storage and recovery; CMWD = Calleguas Municipal Water District; DBS&A = Daniel B. Stephens & Associates; ELPMA = East Las Posas Management Area; GW = groundwater; M&I = municipal and industrial; SWP = state water plan; 1 = already accounted for in ASR injection term. 2 = already accounted for in the “percolation of dry weather streamflow” term.

Table 6-3 Water Budget Outflows and Change in Storage in Acre-Feet Per Year

Source (when not this study)	Dudek (2017)	GW ET by Phreatophytes	Hydrometrics (2016)	CMWD	Total Outflow	Dudek (2017)	Total Outflow Includes Use of Imported Water in ELPMA from Purveyors	CMWD In Lieu Use in ELPMA ¹	Change in Storage
Calendar Year	Pumping in ELPMA [includes ASR]		GW Outflow to Pleasant Valley in Shallow Aquifer	Extraction at ASR Wells		Use of Imports in ELPMA from Water Purveyors			
1985	-19,103	-971	-131	0	-20,205	-8,006	-28,211	0	-4,622
1986	-17,214	-1,009	-131	0	-18,354	-7,572	-25,926	0	1,283
1987	-19,676	-1,047	-131	0	-20,854	-8,678	-29,532	0	-2,938
1988	-21,277	-1,085	-131	0	-22,493	-9,595	-32,088	0	-3,806
1989	-24,089	-1,123	-131	0	-25,343	-10,203	-35,546	0	-8,935
1990	-23,072	-1,161	-131	0	-24,364	-10,621	-34,985	0	-8,303
1991	-19,186	-1,199	-131	0	-20,516	-8,226	-28,742	0	-1,711
1992	-15,297	-1,237	-131	0	-16,665	-8,544	-25,209	0	4,273
1993	-16,299	-1,275	-131	-1	-17,705	-8,839	-26,544	0	4,490
1994	-18,682	-1,313	-131	-78	-20,126	-8,156	-28,282	0	-2,211
1995	-15,390	-1,350	-131	0	-16,871	-7,412	-24,283	-276	6,142
1996	-12,556	-1,388	-131	-261	-14,075	-7,884	-21,959	-5,501	5,706
1997	-17,648	-1,426	-131	-163	-19,205	-8,757	-27,962	-3,047	-486
1998	-16,060	-1,464	-131	-61	-17,655	-7,012	-24,667	-507	6,725
1999	-20,477	-1,491	-131	-105	-22,099	-8,965	-31,064	0	-4,362
2000	-18,664	-1,817	-131	-1	-20,612	-9,279	-29,891	-1,871	-1,469
2001	-14,180	-1,625	-131	0	-15,936	-9,156	-25,092	-140	6,896
2002	-20,514	-1,688	-131	0	-22,333	-11,741	-34,074	0	-2,243
2003	-16,947	-1,710	-131	-23	-18,788	-10,615	-29,403	-1,379	1,436
2004	-18,929	-1,822	-131	-17	-20,882	-11,433	-32,315	-2,302	470
2005	-14,473	-1,736	-131	-12	-16,340	-9,550	-25,890	-2,390	9,308
2006	-18,945	-1,567	-131	-3	-20,643	-10,545	-31,188	-2,174	2,908
2007	-23,952	-1,742	-131	-2,220	-25,825	-12,138	-37,963	-571	-7,839
2008	-25,990	-1,809	-131	-5,119	-27,930	-11,874	-39,804	-445	-7,888
2009	-31,860	-1,732	-131	-9,763	-33,723	-10,861	-44,584	-352	-14,413
2010	-29,082	-1,652	-131	-9,032	-30,865	-8,881	-39,746	-401	-8,012
2011	-22,363	-1,644	-131	-1,186	-24,138	-8,207	-32,345	-452	-4,449
2012	-26,204	-1,675	-131	-406	-28,010	-8,731	-36,741	-437	-9,088
2013	-28,114	-1,763	-131	-1,043	-30,008	-9,151	-39,159	-491	-13,332
2014	-26,978	-1,868	-131	-900	-28,977	-9,481	-38,458	-510	-8,339
2015	-24,890	-1,708	-131	-99	-26,729	-8,188	-34,917	-433	-11,154
Ave (1985-2015)	-20,584	-1,487	-131	-984	-22,202	-9,300	-31,502	-764	-2,450

ASR = aquifer storage and recovery; CMWD = Calleguas Municipal Water District; DBS&A = Daniel B. Stephens & Associates; ELPMA = East Las Posas Management Area; ET = evapotranspiration; FCGMA = Fox Canyon Groundwater Management Agency; GW = groundwater; 1 = already accounted for in ASR pumping.

6.2.1 Recharge from Precipitation

Precipitation falling on the ground may infiltrate through the root zone and recharge the groundwater system. Groundwater recharge is often referred to as deep percolation, indicating percolation occurring below the root zone and below the zone where ET may occur. Precipitation falling on the ground surface may also run off and converge in tributaries, be consumed via ET, be held in storage in the root zone, or be held in storage in the vadose zone above the groundwater system.

The amount of precipitation that eventually becomes recharge is determined by many factors, including the amount, intensity, and timing of precipitation; soil properties such as the storage capacity and depth of soils; topography; the amount of ET by vegetation; the permeability of the aquifer; and land use changes that affect the infiltration capacity of the land surface. Recharge was calculated using a two-step approach with two datasets. The first dataset is the Basin Characterization Model (BCM), a publicly-available dataset for the California hydrologic region which includes all basins draining into the state created by (Flint and Flint, 2014; Flint et al., 2013). The BCM is a grid-based energy balance model that calculates the groundwater water balance. It simulates physical processes like snow accumulation, snow melt, sublimation, and the Priestley-Taylor equation (Priestley and Taylor, 1972) for simulation of potential evaporation. In the BCM, the subsurface is divided into three conceptual groundwater reservoirs: surface, shallow, and deep groundwater reservoirs. Inputs to the BCM include: (1) a 30-m DEM, (2) spatially distributed monthly Parameter-elevation Regressions on Independent Slopes Model (PRISM) precipitation (Daly, 2008), (3) the National Land Cover Database, (4) atmospheric conditions including minimum and maximum air temperature, (5) Soil Survey Geographic (SSURGO) database (Soil Staff Survey, 2016), and (6) mapped surficial geology. One of the outputs of the BCM is temporally varying, gridded, in-place recharge that represents potential natural recharge, which is the precipitation that infiltrates below the root zone.

Because VCWPD precipitation gages were not included in the BCM model, recharge was scaled by the VCWPD precipitation and the BCM precipitation to produce estimates of recharge for the water budget. The BCM average precipitation and recharge from 1981 to 2010 (the most recent climate normal period) was scaled by annual point precipitation data from VCWPD to provide an estimate of recharge through time for 1985 through 2015. Climate normal are three-decade averages of climatological variables. The VCWPD precipitation gage with the longest record is the Somis-Bard gage (Station 190) which is located in the eastern portion of the WLPSA (**Figure 6-1**). This gage was used to linearly scale the average precipitation and average recharge from the BCM to provide a time series of recharge in the study area that incorporates the VCWPD precipitation data (**Figure 6-3**).

Groundwater recharge from precipitation is highly variable over time, and the average annual recharge from precipitation between 1985 and 2015 was 5,119 AF. Higher recharge rates can be seen just below the mountain front where soils are thicker and slopes are less steep, which provides enhanced recharge capacity (**Figure 6-4**).

Given the scale of the BCM, focused recharge along Arroyo Las Posas/Simi or tributaries to the Arroyo are not included in the BCM other than as local changes in soil properties. Focused recharge from Arroyo Las Posas/Simi and tributaries to the Arroyo are described in the next section.

6.2.2 Focused Recharge from Arroyo Las Posas/Simi

Arroyo Simi is a 19-mile-long creek that originates at Corriganville Park by the Santa Susana Pass and flows westward until it converges with Arroyo Las Posas near Hitch Road in the City of Moorpark. Arroyo Simi is a tributary to Calleguas Creek, which flows to the Pacific Ocean near Point Mugu. Current streamflow in Arroyo Las Posas/Simi is a combination of natural flows and anthropogenic flows from five sources: discharge from the SVWQCP, discharge from the Moorpark WWTP via percolation ponds, discharge from a network of dewatering wells in Simi Valley that began operating in 1987 (Todd Groundwater, 2016), tributary inflows within the ELPMA that include agricultural and municipal runoff, and very minor inflows from agricultural drains (Engle, 2012).

Historically, the Arroyo was ephemeral and dry during most of the year and flowed during the winter or periods of heavy rain. As baseflow increased over time due to anthropogenic inflows (associated with urbanization in Simi Valley and Moorpark) and rising water levels in the Shallow Aquifer, the ephemeral portion of the Arroyo was pushed progressively farther downstream over several decades such that dry season flows in Arroyo Las Posas began to overflow into the Pleasant Valley Basin in approximately 1994 (Hopkins Groundwater Consultants, 2008). Based on stream gaging, Hydrometrics (2016) estimated the baseflow at Madera Road in the Simi Valley Basin to be on the order of 2 cubic feet per second (cfs) in 1979, which increased to approximately 5 cfs by 2000, and has been about 5 cfs since 2000.

More stormflow bypasses the ELPMA as a result of the filling of the Shallow Aquifer relative to historical conditions because elevated groundwater levels reduce the storage capacity for stormflow percolation in the ELPMA. Over time, increases in anthropogenic discharges to the Arroyo have increased water levels in the Shallow Aquifer and the FCA, along with chloride concentrations near the Arroyo (Bachman, 2016; Izbicki and Martin, 1997) which is due, in part, to stormflows with lower chloride concentrations bypassing the ELPMA. Water percolating from Arroyo Las Posas/Simi must move primarily vertically through the Upper San Pedro/Saugus Formation before leaking into the FCA. The conceptual model is that recharge into the FCA is likely to be the highest where the Upper San Pedro/Saugus Formation is thinnest (**Figure 4-10**).

Focused recharge occurs along the losing portions of Arroyo Las Posas/Simi, meaning the surface water body is losing water to the groundwater system. The most detailed temporal and spatial information about gaining and losing reaches of the Arroyo comes from streamflow measurements conducted by Larry Walker and Associates (Engle, 2012; 2013) during August 5 to October 3, 2011 and from July 3 to December 14, 2012. Streamflow measurements were made during periods without stormflow, and a flow difference approach was used to infer gaining and losing reaches of the Arroyo and quantify groundwater-surface water interactions.

The flow difference approach to quantifying groundwater-surface water interactions assumes that inflows and outflows to streams from other sources (like inflows from agricultural drains, tributaries, or evaporation) are either quantified and accounted for, or are negligible relative to measured differences in streamflow and unaccounted for. Errors in streamflow measurements are usually between 5 and 15% and largely depend on the number of flow measurements that are made across the stream (Cey et al., 1998; Langhoff et al., 2006).

Larry Walker and Associates' (Engle, 2012; 2013) streamflow measurements identified gaining and losing reaches of the Arroyo (**Figure 6-5**) during baseflow (dry weather) conditions. In general, Arroyo Las Posas/Simi was losing (groundwater system was gaining) between the eastern study area boundary and Larry Walker gaging site G4 located approximately 1-mile downstream of VCWPD streamgage 801 (Arroyo Simi at Moorpark – Spring St) (**Figure 6-5**). Downstream of gaging site G4, the Arroyo gained flow (groundwater system was losing) or was noted as “little change” all the way to Larry Walker gaging site G8 located about a half-mile downstream of the Moorpark WWTP. Farther downstream, a small 1.5-mile stretch of the Arroyo was noted as losing (groundwater system was gaining). Farther downstream near the western basin boundary (Larry Walker gaging sites G8 to G11), the flow different results were deemed inconclusive (Engle, 2012; 2013).

The gaining section of the Arroyo (groundwater system was losing) is consistent with the chloride water quality data that show elevated concentrations of chloride in the 175 to 200 mg/L range as sampled in 2003 and 2014 in the FCA (Bondy Groundwater Consulting, 2016). The elevated concentrations, faster travel times in this area as shown from measured concentrations in wells over time, and little difference in groundwater elevations indicate the Shallow Aquifer and the FCA are in greater hydraulic communication. In this area, the Upper San Pedro/Saugus Formation is less than 100 ft thick due to erosion (Bachman, 2016) (**Figure 4-10**), and the clay marker bed may be thinner, or faulted, or not present in this area.

Focused recharge from percolation of streamflow in Arroyo Las Posas/Simi for baseflow conditions was estimated by scaling reach-specific streamflow differences measured by Larry Walker and Associates (Engle, 2012; 2013) for 2012 to either: (1) annual SVWQCP discharge to the Arroyo or (2) annual discharge to the Moorpark percolation ponds, depending on the location

of the reach. For the calculations, the Arroyo was divided into three reaches defined by the location of the Larry Walker streamgage sites: G1 to G4, G4 to G7, and G7 to G11 (**Figure 6-5**). Essentially, this approach scales the measured flow differences (net infiltration) reported by Larry Walker and Associates for dry flow conditions (Engle, 2012, 2013), by reach over time, to estimate the amount of percolation of streamflow for each year in the water budget period.

Discharge from the SVWQCP is the source of most of the water in the Arroyo between streamgage sites G1 and G4. To estimate the annual percolation of streamflow for this reach, a linear scaling factor was developed between the daily discharge from the SVWQCP and the daily measured flow differences (net infiltration) reported by Larry Walker and Associates (Engle, 2012, 2013) for this reach. The scaling factor was applied to the annual SVWQCP discharges to the arroyo, for each year of the water budget period, to estimate the amount of percolation of streamflow for the reach. The computed scaling factor was 0.8, meaning that the net percolation of streamflow between gages G1 and G4 was 80% of the SVWQCP discharge to the arroyo. Thus, for each year in the water budget, the annual SVWQCP discharge to the arroyo was multiplied by 0.8 to estimate the annual percolation of streamflow for the reach of the Arroyo between streamgage sites G1 and G4.

A similar calculation was performed for the remaining two arroyo reaches (streamgage sites G4 to G7 and G7 to G11) using the discharge to the Moorpark percolation ponds, rather than the discharge from the SVWQCP, to develop a scaling factor for each reach. For each year of the water budget period, the estimated amount of streamflow percolation in each of the three reaches was summed to calculate the total amount of focused recharge from percolation of streamflow in Arroyo Las Posas/Simi in the ELPMA for baseflow conditions. Over the water budget period, the average annual focused recharge from Arroyo Las Posas/Simi was estimated to be 10,395 AF.

The approach for estimating focused recharge from percolation of streamflow represents baseflow conditions. Additional recharge occurs during stormflow conditions when runoff and tributary inflows reach Arroyo Las Posas/Simi, which typically only occurs during the winter or during heavy periods of rain. Without tributary stream gaging information, it was not prudent to estimate the tributary recharge component of the water budget for this study. A previous geochemical study by Izbicki and Martin (1997) reported the tritium composition of groundwater in wells in the LPVB and determined, based on the absence of tritium, that recharge from “infiltration of runoff from intermittent streams along the flanks of South Mountain” was not an important source of recharge to the Lower Aquifer System (LAS) (Upper San Pedro/Saugus Formation, Clay Marker Bed, FCA, and GCA).

Much of the tributary inflows to Arroyo Las Posas/Simi is expected to leave the ELPMA as streamflow. Bachman (2016) analyzed baseflow and stormflow at the VCWPD Hitch gage (841 and 841A) from 1994 through 2010 and determined that about half the flow in the arroyo was baseflow and half was stormflow. Happy Camp Canyon has both a larger drainage area and

connected areas of sandy alluvium with higher soil hydraulic conductivity (Soil Survey Staff, 2016) that could provide focused recharge. Historically, this was referred to as Happy Canyon Creek, an intermittent stream (Wood, 1913). Similarly, Long Canyon and Balcom Canyon may provide focused recharge although the soils have higher clay content and lower permeability than near Happy Canyon.

6.2.3 Recharge at Moorpark Wastewater Treatment Plant Percolation Ponds

VCWWD No. 1, a provider of water and sanitation services in the city of Moorpark and vicinity, owns and operates the Moorpark WWTP, which was originally constructed in 1965 as an interim treatment facility with a capacity of 1.0 million gallons per day (mgd) (Padre Associates, 2013). Treated effluent from the Moorpark WWTP is discharged to percolation ponds (storage basins) originally constructed in 2002, discharged to Arroyo Las Posas, or used for reclaimed water that is supplied to the Moorpark Country Club Estate for irrigation of the golf course. When the percolation pond capacity is exceeded, tertiary treated wastewater is discharged directly to Arroyo Las Posas/Simi. This occurs infrequently and has occurred once between 2002 and 2013 (Padre Associates, 2013). Historically, the effluent water quality discharged to the Moorpark WWTP percolation ponds was of significantly better quality than the Shallow Aquifer groundwater immediately up-gradient of the facility because the effluent source water is high quality out-of-basin water that comes from Metropolitan (Padre Associates, 2013). For simplification, the direct discharges to Arroyo Las Posas/Simi are included in the water budget category of “percolation of dry weather streamflow.”

Annual flows discharged to the settling and percolation ponds are available from VCWWD No. 1 for the period 1960 through 2015. The water in the percolation ponds may be lost through direct evaporation from the surface of the ponds or percolation to the subsurface. Some of the water discharged to the percolation ponds is believed to return to Arroyo Las Posas/Simi because the water table is generally shallow, and this portion of the Arroyo was identified as a gaining reach (Engle, 2012; 2013).

Evaporation from the pond surfaces was estimated from precipitation, pan evaporation, and pond areas derived from aerial imagery (**Figure 6-6**). The total area of the active percolation ponds ranged between 16 and 32 acres based on aerial imagery from six images between 1994 and 2016 (from May 1994, June 2002, August 2006, April 2011, July 2014, and February 2016). Annual pan evaporation rates from VCWPD evaporation station 171 (Fillmore-Fish Hatchery) were used to estimate evaporation from the ponds. This station was selected because it is close to the Moorpark WWTP percolation ponds and it is at a similar elevation relative to other nearby pan evaporation stations. From 2009 through 2015, long-term pan evaporation rates at station 171 were used because pan evaporation data were not reported during this period. Because pan evaporation rates are typically higher than actual evaporation rates due to the heating of the pan during the day,

the annual average evaporation rates were multiplied by a pan evaporation factor of 0.75. On an annual basis, the amount of treated effluent percolating to Arroyo Las Posas/Simi was estimated as the difference between the amount of treated effluent percolated to the ponds, the amount of direct precipitation falling on the ponds, and the amount of evaporation from the ponds.

During 2001 and 2002 there were direct discharges from the Moorpark WWTP to Arroyo Las Posas totaling 1,647 and 1,613 AF, respectively. For simplification, the direct discharges to the Arroyo are included in the water budget category of “percolation of dry weather streamflow.” Over the water budget period of 1985 to 2015, average annual percolation at the Moorpark WWTP percolation ponds was estimated as 1,904 AF.

Percolation at the Moorpark WWTP percolation ponds was estimated as part of the conceptual model and is included in the water budget table. Note, however, that the estimates for percolation at the Moorpark WWTP percolation ponds are not included in the total inflows for the water budget because this flow to the groundwater system has already been accounted for as focused recharge from Arroyo Las Posas/Simi, as discussed in the previous section.

6.2.4 Recharge from Return Flows

For the water budget, return flows were estimated for agricultural return flows, urban municipal and industrial (M&I) return flows, septic return flows, and distribution system leakage as described below. For return flows to reach the groundwater system, they must percolate through the subsurface after accounting for any runoff or ET losses and arrive at the water table. Movement of water through the unsaturated zone is very slow and, consequently, in parts of the basin with a greater depth to water, it may take hundreds of years for return flows to arrive at the water table (Izbicki and Martin, 1997).

Where the depth of water is shallower, for example, near the Arroyo, the travel time to the water table is much less. For example, water sampled in wells near the Arroyo was determined to have been recharged less than 50 years ago based on the tritium signature (Izbicki and Martin, 1997). Conceptually, the timing of return flows varies spatially with depth to water, permeability and saturation of the subsurface. By convention, however, all water budget, terms, including return flows, are assumed to instantaneously recharge the groundwater system. Return flows from irrigation of agriculture, septic systems, urban M&I irrigation, and leakage from water distribution systems are shown in **Figure 6-7**.

Agricultural Return Flows

Irrigation water applied to the land surface may percolate below the root zone and reach the groundwater if the water is not consumed by vegetation. The source of agricultural return flows includes both water pumped from the basin and water imported from outside of the basin. Various water purveyors in the ELPMA purchase imported water from the CMWD, who in turn purchases

it from Metropolitan. Water from Metropolitan comes primarily from the California State Water Project and enters CMWD's service area through a pipeline at the eastern end of the service area.

As part of the preliminary draft water budget prepared by Dudek for the FCGMA (Dudek, 2017), Daniel B Stephens & Associates applied the Distributed Parameter Watershed Model, which is run with daily time steps, to estimate the groundwater budget for several basins, including the ELPMA. From this model, the average agriculture return flows was 10.5% of the average applied water for agriculture uses (water from FCGMA and imported water for agricultural uses) in the ELPMA during the period from 1985 to 2015 (Dudek, 2017). INTERA applied this return flow rate to the annual applied water for agricultural uses tabulated by Dudek (2017) and estimates average annual agricultural return flows of 2,117 AF in the ELPMA over the water budget period of 1985 to 2015.

An important conceptual question is whether return flows from historical irrigation of agricultural lands, a significant portion of the water budget, have already arrived at the water table. The timing of the arrival of return flows is expected to differ based on the depth to water and permeability of the sediments between the land surface and the water table, which is a function of saturation, as discussed in the first paragraph of section 6.2.4. Based on the isotopic sampling from Izbicki and Martin (1997) and water quality sampling in wells (Bondy Groundwater Consulting, 2016) in the study area, the conceptual model is that return flows occurring above the Shallow Aquifer and the Epworth Gravels Aquifer could have arrived at the water table based on estimated travel times (Izbicki and Martin, 1997). Agricultural return flows occurring above the Upper San Pedro/Saugus Formation may not have reached the water table in areas where the water table is deep (more than 200 ft bgs) and overlain by clay confining beds. For areas where the Upper San Pedro/Saugus Formation is very thin or absent, and the Shallow Aquifer is not present, there has been little historical irrigation for agriculture.

Urban M&I return flows

In the urban setting, outdoor water use may percolate to groundwater if water remains after evapotranspiration and runoff losses. In the study area, M&I outdoor water use is predominately used for irrigation of landscape vegetation but also includes car washing and the filling of swimming pools. In the study area, most of the M&I water use is derived from imported water. Of the M&I water use, 65% was assumed to occur outdoors for irrigation (Dudek, 2017) and 10.5% of the outdoor use was assumed to percolate to groundwater (Dudek, 2017). For the water budget period of 1985 to 2015, the average annual M&I return flow was 666 AF. For comparison, outdoor water use in the nearby Simi Valley Basin was assumed to be 70% of total urban water supplies, and 10% of the outdoor use was assumed to percolate to groundwater (Todd Groundwater, 2016).

Septic Return Flows

Septic system returns to the groundwater system occur at residences with wells and at residences served by public water supplies. Water from the septic field may travel through the unsaturated zone to the groundwater system if the groundwater system is relatively shallow and ET demands do not consume all the water. Septic return flows were estimated based on the amount of indoor water use on a per capita basis, average household size, and the location of septic system use within the study area.

For VCWWD No. 1 (Moorpark), sewer service exists only within the city limits and residences outside of the city limits use septic system. For VCWWD No. 19 (Somis), it was assumed that 100% of the residences use septic systems and none of the residences are connected to sewers. It was further assumed that only 30% of the septic usage in VCWWD No. 19 occurs within the ELPMA. The Environmental Health Division of Ventura County reports about 1,147 permits for onsite wastewater treatment systems in Moorpark (data accessed on 12/30/2016 at <http://www.vcenvhealth.org/isds/>). Using 2015 as an example, the residential water demand was estimated to be 146.4 gallons per capita per day (gpcd) (Psomas, 2014). The average household size was assumed to be 3.31 people (U.S. Census, 2015). Assuming these values for the residential water demand and household size, the average household would use 0.54 acre-feet per year (AFY). Assuming 35% of the water demand is for indoor use (Hydrometrics, 2016) and 100% of the indoor use returns to the groundwater system, then 0.19 AFY per septic system would be available for percolation. The annual volume of septic returns to the groundwater system was estimated as 218 AFY for the 1,147 septic systems in VCWWD No.1. A similar calculation was performed for VCWWD No. 19, and the values for both Districts were summed to estimate the septic return flows for the study area as presented in **Table 6-4**. As the return flows are a small component of the total water budget, septic return flows from 2005 were applied to 1985 through 2004, recognizing the diminishing returns of effort to improve the accuracy of the water budget with additional historical information. For the water budget, the estimated septic system return flow was 385 AF in 1985 and decreased to 317 AF in 2015. The average annual septic system return flow was estimated as 374 AF over the water budget period.

For comparison, a summary of the estimates of septic return flows made by Daniel B. Stephens & Associates as part of the preliminary draft of the GSP for the LPVB (Dudek, 2017) is provided. Daniel B. Stephens & Associates (Dudek, 2017) estimated septic return flows based on the number of septic systems in the ELPMA and household water use. If septic systems were present within any parcel within a tract as estimated from the Ventura County septic database, it was assumed that all parcels in the tract contained septic systems. This approach resulted in an estimated total of 1,002 septic systems in the ELPMA. Household water use and annual disposal was estimated to decrease from 0.21 AFY per septic system for 1985 to 1997, 0.20 AFY per septic system for 1988 to 2010, and 0.16 AFY per septic system from 1998 to 2015 based on

DeOreo and Mayer (2012). The estimated percolation from all septic systems in the ELPMA was 210 AF in 1985 decreased to 155 AF in 2015, which reflects additional urbanization of the basin. The average annual septic system percolation in the ELPMA was estimated as 196 AF.

Table 6-4 Basis for Septic System Return Flow Rates

Year	Residential Water Use (gpcd)	Septic Return Flows in VCWWD No. 19	Septic Return Flows within VCWWD No. 1	Sum of VCWWD No. 1 and No. 19
		Septic Return Flows in Acre-Feet Per Year		
2005	177.9	265	121	385
2010	151.7	226	103	329
2015	146.4	218	99	317

Distribution System Return Flows

Return flow to the groundwater system can occur through pipeline leakage of water distribution systems. Leakage losses of 5% of metered water supply values were assumed in the ELPMA (Hydrometrics, 2016). Over the water budget period of 1985 to 2015, the average annual percolation from distribution systems was estimated as 498 AF. For comparison, water system losses in the nearby Simi Valley Basin ranged from 2.9 to 6.4% from 2004 to 2009 (Todd Groundwater, 2016). Assuming an average water distribution system loss of 5%, an average of 490 AFY recharges the groundwater system over the period 2000 to 2009 (Hydrometrics, 2016).

6.2.5 Well Production

The amount of pumping in the study area was derived from pumping reported by the FCGMA. Wells within the study area were identified and pumping was summed annually from the biannual pumping periods reported by the FCGMA. Pumping was also aggregated by the use type as shown in **Figure 6-8**. The vast majority of the pumped water is used for agriculture with lesser amount for M&I and domestic pumping that averages 70 AFY. The amount of pumping from the Shallow Aquifer and the Epworth Gravels Aquifer is shown in **Figure 6-9**. For the water budget (but not the numerical model of groundwater flow, where pumping is specific to each model layer), the remaining pumping in the Upper San Pedro/Saugus Formation (clay marker bed, FCA, and GCA) was aggregated into a single category representing the LAS as shown in **Figure 6-9**. This simplified distribution of pumping to aquifers was computed from well screen information and the total depth of the well if well screen information was not available, and the thickness of the Shallow and Epworth Gravels Aquifers. Most of the pumping is from the LAS with smaller amounts of pumping from the Shallow and Epworth Gravels aquifers since 2003.

6.2.6 Evapotranspiration Losses

ET of groundwater by vegetation occurs when the water table is near the land surface, such as near surface water bodies, and roots can penetrate the saturated zone below the water table allowing vegetation to directly transpire water from the groundwater system. In general, transpiration varies based on temperature, relative humidity, wind and air movement, soil moisture availability, and plant type.

Consumptive use of groundwater by deep-rooted vegetation called phreatophytes occurs near Arroyo Las Posas/Simi in riparian areas where groundwater is near land surface. Phreatophytes are characterized by high biomass, deep roots, and high water use relative to other plants. A common phreatophyte with a high rate of water use in the study area is *Arundo donax* (*Arundo*) (giant reed, giant cane), a large, non-native grass found in many coastal watersheds in southern California. *Arundo* typically becomes dormant in the colder months and a hard freeze can cause a dieback to the ground (California Invasive Plant Council, 2011).

In 2010 the occurrence of *Arundo* was mapped at a fine scale using high-resolution aerial imagery and field verification (California Invasive Plant Council, 2011). From this study, 75 acres of *Arundo* and 279 acres of other phreatophytes were identified across the WLPMA and ELPMA (LPUG, 2012). The rates of consumptive water use by phreatophytes in the published literature vary widely depending on the method used, the density and age of the vegetation, and the local climatic conditions. Water use by *Arundo* water use was estimated using the average leaf area values developed for the study and published leaf transpiration values to determine a stand-based transpiration value (California Invasive Plant Council, 2011). Annual water use consumption by *Arundo* was estimated at 24 acre-feet per acre (ac-ft/ac) (20 millimeters per day [mm/day]) and water use consumption by native phreatophytes was estimated at 4 ac-ft/ac (3.3 mm/day) (California Invasive Plant Council, 2011). These values yield 2,916 AFY of consumptive use by phreatophytes in ELPMA based on current conditions in Arroyo Las Posas. Historically, when Arroyo Simi/Las Posas was ephemeral and the water table was deeper, consumptive use by phreatophytes would have been much less. As *Arundo* annually consumes about 6 times as much water as native phreatophytes (California Invasive Plant Council, 2011) and detailed mapping of *Arundo* is available in the basin, all riparian vegetation was assumed to be *Arundo* to simplify estimates of groundwater ET for the water budget.

To estimate ET of groundwater by phreatophytes for the water budget, there are several factors to consider, including:

- ET rates of phreatophytes over time due to seasonal variation in weather (humidity, temperature, and precipitation),
- the length of the growing season during which ET occurs,

- the area of phreatophytes over time in the study area.

Because transient consumptive water use by phreatophytes was desired for the water budget, additional methods of estimating ET losses from phreatophytes were employed. Water use consumption was estimated using annual average reference ET (ET_o) values from the California Irrigation Management Information System (CIMIS) to reflect variations in the consumptive use of phreatophytes over time in response to factors like air temperature, precipitation, and wind speed. Daily reference ET values were reported by CIMIS at station 152 (Camarillo) for the period 2000 to 2015. To determine the ET of a specific vegetation type or crop, the measured ET_o values are multiplied by a crop coefficient to determine the ET from the crop as:

$$ET_c = ET_o * K_c, \text{ where} \quad \text{(Equation 4-3)}$$

ET_o=reference crop ET

K_c=crop coefficient

ET_c=ET for specific crop or vegetation

ET_c was calculated from the CIMIS data using an average crop coefficient of 1.26 for *Arundo* (Triana et al., 2015) for the growing season, which was identified as part of a lysimeter study under non-limiting water conditions (soil moisture was maintained near field capacity). The CIMIS daily values were aggregated to annual ET_c values for 214 days of the growing season for phreatophytes between March 25 and October 24 for each year the CIMIS station was active.

Because ET is temperature dependent, a linear regression relationship was developed for 2015 between ET_o at two different CIMIS stations (152 – Camarillo and 217 – Moorpark) with elevations (130 and 718 ft amsl, respectively) that bracket the representative elevation of areas with groundwater ET along Arroyo Las Posas/Simi (444 ft amsl). This regression relationship was applied uniformly from 2000 through 2015 assuming elevation was a proxy for temperature.

Estimates of the area of *Arundo* in the floodplain come from two sources. The first source of the area of *Arundo* is from a study by Wildscape Restoration (2015) that estimated the area of *Arundo* using aerial imagery, satellite imagery, high resolution oblique imagery, and field observations and estimated the water savings that could be obtained by removing *Arundo* from portions of the Simi Valley Basin and the LPVB, which are both part of water budget study area. Information on the changes in vegetated area in the stream channel comes from an analysis of aerial photos between 1980 and 2005, which were used to map the growth of *Arundo* in Arroyo Las Posas from VCWPD Hitch gage (841 and 841A) to the Pleasant Valley Basin (Huber, 2006). This study shows increasing establishment of vegetation in the stream channel over time (**Table 6-5**). Channel vegetation also periodically diminished in response to large natural flow events such as the event that occurred before February 2005. The 2005 vegetated areas from Huber (2006) were linearly scaled to represent the entire study using the subset of the total *Arundo* in Arroyo Las Posas and

Arroyo Simi mapped by Wildscape Restoration (2015) that was coincident with the study area (444 acres).

Table 6-5 Open Channel and Vegetated Areas in the River Channel of Arroyo Las Posas from Huber (2006)

Date	Arroyo Las Posas		
	Open Channel Area (acres)	Vegetated Area (acres)	Ratio of Vegetated to Total Area
1980	231	149	0.392
1985	244	136	0.358
1998	175	205	0.539
2002	84	296	0.779
February 2005	163	217	0.571
September 2005	114	266	0.700

Incorporating the estimated area of *Arundo* over time and ETC values based on CIMIS data with the other scaling approaches described above resulted in annual estimates of groundwater ET by phreatophytes that varied between 971 AF in 1985 to 1,868 AF in 2014.

6.2.7 Injection and Extraction at ASR wells and In-Lieu Deliveries

Imported water purchased from Metropolitan is stored underground in the Las Posas ASR Project in the ELPMA so that it will be available for subsequent use. CMWD operates the 18-well ASR facility that consists of two well fields near Grimes Canyon Road. Imported water stored by CMWD is documented with the FCGMA. Water recovered from the ASR facility supplies the CMWD service area during planned and unplanned shutdowns of its wholesale imported water system (LPUG, 2012). Artificial recharge of treated imported water into the FCA and the GCA occurred at CMWD’s Fairview Well between 1993 and 1999 and has occurred at the ASR facility since 1999 (Bachman, 2012). The annual amount of ASR injection and ASR extraction from 1985 through 2015 is shown in **Figure 6-10**. ASR extractions were largest during the period 2007 to 2010.

Imported water purchased from Metropolitan has also been delivered to basin pumpers in the ELPMA in lieu of pumping their own wells. By deferring in-basin production, more water is left in storage for future use. Water stored through in-lieu methods is designated for emergency operations such as earthquakes or pipeline breakages (Bondy Groundwater Consulting, 2016).

6.2.8 Underflow

Underflow is the amount of water entering a basin in the subsurface. Lesser components in the water budget include inflows as underflow from the Simi Valley Basin and outflows as underflow to the Pleasant Valley Basin through the alluvium of the Shallow Aquifer. As the hydraulic

gradient is not steep and the alluvium is not deep, the amount of underflow from the Simi Valley Basin to the LPVB is small and was estimated by the State Water Resources Control Board (SWRCB) (1956) as 100 AF per season. Hydrometrics (2016) estimated 5 AFY from a Darcy flux calculation based on a hydraulic gradient of 0.005 ft/ft, a 1,000 ft width of the of the floodplain, a saturated alluvium thickness of 5 ft, and a hydraulic conductivity of 25 ft/day.

Underflow in the alluvium from the study area into the Pleasant Valley Basin was estimated by Hydrometrics (2016) as 131 AFY using a Darcy flux calculation based on a hydraulic gradient of 0.0025 ft/ft (similar to the gradient of Arroyo Las Posas), a roughly 5,000-foot width of the floodplain, a hydraulic conductivity of 25 ft/day, and a saturated thickness of alluvium of 50 ft. Underflow may occur in the Upper San Pedro/Saugus Formation between the ELPMA and the WLPMA. It may occur either in the southwest corner of the study area or along the northern portion of the Somis Fault Zone below the northern FCA outcrop. Without more detailed groundwater elevation data in the Upper San Pedro/Saugus Formation near the basin boundaries, it is not possible to quantify the amount of underflow through the Upper San Pedro/Saugus Formation without numerical modeling.

6.2.9 Change in Storage

Annual change in storage was computed from the water budget as a change in storage from estimated basin inflows and outflows, as shown in **Figure 6-11**. Over the water budget period, the average annual change in storage was estimated to be -2,450 AF. The corresponding average annual inflows and outflows was estimated to be 19,752 and -22,202 AF, respectively, excluding the use of imported water in the ELPMA from water purveyors.

6.2.10 Water Budget Limitations

The accuracy and certainty of estimated water budget terms varies and depends on many factors, including the underlying data sources, the data resolution, the spatial scale of the data, how closely the underlying data are connected to the physical process represented by the water budget term, and the level of effort required to incorporate complex physical processes or temporal changes relative to the improvements yielded in the water budget. For example, estimates of recharge at the basin scale are typically based on indirect measures of recharge such as measured precipitation and, consequently, recharge is one of the more uncertain terms in the water budget.

In some cases, water budget terms were estimated coarsely with regard to both accuracy and certainty when the groundwater flow model, not the water budget, was determined to be a more effective way to estimate the water flux. The estimate of focused recharge along Arroyo Las Posas/Simi is an example of such a water budget term. The complex spatial and temporal interaction of the surface water in the Arroyo, groundwater levels, and flux through streambed are best estimated by the calibrated groundwater flow model. Note, the water budget approach to estimating focused recharge from percolation of streamflow in Arroyo Las Posas/Simi represents

baseflow conditions (aka dry weather flows) and does not include stormflow when runoff and tributary inflows reach Arroyo Las Posas/Simi. Thus, the stormflow contributions to storage in the groundwater system are not accounted for in the water budget calculations. During stormflow events, in actuality, some of the stormflow in Arroyo Las Posas/Simi would exit the ELPMA as streamflow, some stormflow would be stored in the unsaturated zone as bank storage (and, perhaps, later discharge to the Arroyo), and some stormflow would recharge the groundwater system adding to groundwater storage. The groundwater flow model would be a more effective way to estimate these wet-weather recharge contributions.

Finally, it is important to note that the water budget does not account for travel times from land surface to the groundwater system. Thus, there is more year-to-year variation in the water budget than expected. For example, recharge estimates in the water budget vary considerably from year to year in response to precipitation but, in reality, travel through the unsaturated zone creates a more uniform water content with depth and results in a near steady-state flux of recharge to groundwater system.

7.0 MODEL DESIGN

Model design represents the process of translating the conceptual model for groundwater flow in the aquifer into a numerical representation of the flow system. The conceptual model for flow defines the processes and attributes required of the code to be used. In addition to selection of an appropriate code, model design includes definition of the model grid and layer structure, the model boundary conditions, initial conditions, and the model hydraulic parameters. This section describes these elements of model design and their implementation.

7.1 Code and Processor

MODFLOW-NWT (Niswonger et al., 2011) was selected as the numerical code to simulate groundwater flow in the ELPMA. MODFLOW is a finite-difference groundwater-flow code that solves the three-dimensional form of the continuity equation that governs flow through saturated porous media. The benefits of using MODFLOW include: (1) MODFLOW incorporates the necessary physics of groundwater flow, which are the basis for the conceptual model (described in Sections 3 to 5 of this report); (2) MODFLOW is the most widely accepted groundwater flow code in use today; (3) MODFLOW was written and is supported by the United States Geological Survey (USGS) and is public domain; (4) MODFLOW is well documented (Harbaugh et al., 2000); (5) MODFLOW has a large user group; and (6) there are several mature graphical user interface programs written for use with MODFLOW.

MODFLOW-NWT is a Newton-Raphson formulation for MODFLOW-2005 (Harbaugh, 2005), which improves the solution of the unconfined groundwater-flow systems. MODFLOW-NWT treats nonlinearities of cell drying and rewetting by use of a continuous function of groundwater head (even under unsaturated conditions), rather than the discrete approach of drying and rewetting used by earlier versions of MODFLOW. Unlike older versions of MODFLOW that either inactivated unsaturated cells or used rewetting functions (that can introduce mass-balance errors and numerical instabilities), MODFLOW-NWT uses the “Upstream-Weighting” (UPW) package to calculate intercell conductances, hydraulic heads, and flow in (but not out of) unsaturated cells. MODFLOW-NWT was selected to simulate unconfined groundwater flow conditions in the Shallow Aquifer and Epworth Gravels Aquifer, as well as potentially in the outcropping and uplifted parts of the deeper aquifer system. The solver used for the model was the Orthomin/stabilized conjugate-gradient χ MD solver. Default values for solver settings, corresponding to “complex” models (see Niswonger et al., 2011, for details) worked well for this model. Head- and flux-convergence tolerance were kept at 0.05 ft and 1000 cubic feet per day (ft³/day), respectively.

The MODFLOW datasets were developed to be compatible with Groundwater Vistas for Windows Version 6.96 Build 39 (Rumbaugh and Rumbaugh, 2005). The model was built and run on a

Windows 10 Pro computer with a 64-bit, 4-core, 2.50 GHz Intel® Core™ i7 Processor with 8.00 GB of memory. MODFLOW is not typically a memory-intensive application in its executable form. However, if any preprocessor (such as Groundwater Vistas) is used for this size and complexity of model, at least 512 megabytes of random access memory (RAM) is recommended.

7.2 Model Layers and Grid

MODFLOW requires a rectilinear grid. The grid created for the model had a north-south/east-west orientation, with an origin at 1,914,525.3 ft northing and 6,259,774.5 ft easting in the California State Plane, NAD 1983, Zone 5 coordinate system. The grid spacing was kept uniform at 200 ft by 200 ft throughout the model domain.

The model has 213 rows and 339 columns for a total of 72,207 grid cells per layer. The model consists of 7 layers, with a total of 505,449 grid cells. Layer designations are shown in **Table 7-1**. Note that the Upper San Pedro/Saugus Formation overlying the FCA was split into two layers because a wide range of responses were evident in water levels from wells screened in the Upper San Pedro/Saugus layer. Some wells in the upper part of the layer (for example, 02N19W06N03S) near the Arroyo showed responses very similar to wells in the Shallow Aquifer. However, wells deeper in the Upper San Pedro/Saugus Formation and further away from the Arroyo (03N20W35R04S) showed virtually no response to the filling of the Shallow Aquifer. Given this difference in vertical response within the same formation, it was decided to split the layer into two (“Top Layer of the Upper San Pedro/Saugus Formation” and “Bottom Layer of the Upper San Pedro/Saugus Formation”, respectively) to better capture the different responses in the upper and lower parts of the Upper San Pedro/Saugus Formation.

Layer 1 cells were active in areas corresponding to the Shallow Aquifer and the Epworth Gravels Aquifer. For computational efficiency, model cells in the Epworth Gravels Aquifer were made inactive wherever the thickness of the layer was 5 ft or less. Furthermore, during model testing most of the northern fringe of the Epworth Gravels Aquifer was seen to be unsaturated, due to steeply rising bottom elevations reaching up to more than 1,000 ft amsl in the north. Water level elevations in the Epworth Gravels Aquifer range from 625 to 525 ft amsl; hence, the cells with bottom elevations above 650 ft amsl were made inactive, as these cells were not expected to saturate during model simulations and would only add to the computational burden of the model. Likewise, the Upper Santa Barbara Formation and GCA are virtually non-existent towards the south-east, with thicknesses of 5 ft or less in the geologic model (**Figures 4-6 and 4-7**). Cells with 5 ft or less thickness were made inactive for computational efficiency. All cells outside the aquifer extent for a given layer were made inactive. With these changes, of the 505,449 grid cells a total of 182,918 remained active. **Figures 7-1 to 7-5** present the active areas for each of the model layers. **Table 7-1** presents the model layering scheme for the groundwater model, as well as the number of active cells per model layer.

Table 7-1 Model Layers and Active Cells

Model Layer	Stratigraphic Unit(s)	Active Cells	Layer Type
1	Shallow and Epworth Gravels Aquifers	8,386	Unconfined
2	Top Layer of Upper San Pedro/Saugus Formation	29,133	Confined
3	Bottom Layer of the Upper San Pedro/Saugus Formation	29,132	Confined
4	Clay Marker Bed	29,143	Confined
5	Fox Canyon Aquifer	30,249	Convertible
6	Upper Santa Barbara Formation	26,382	Confined
7	Grimes Canyon Aquifer	30,493	Confined

Layer 1 (Shallow and Epworth Gravels Aquifers) was treated as an unconfined layer and Layer 5 (FCA) was simulated as a “convertible layer,” such that the storage and hydraulic properties would be adjusted whenever heads fell below the top elevation. Note that, ideally, the Upper San Pedro/Saugus Formation layers would have been treated as convertible, but the switch from confined to unconfined creates numerical discontinuities and leads to much longer convergence time (sometimes even failing to converge). While the Upper San Pedro/Saugus Formation layers (layers 2 and 3) were treated as confined layer for numerical reasons, hydraulic transmissivities and storage properties were adjusted so that they were comparable to unconfined systems. Furthermore, the Upper San Pedro/Saugus Formation is expected to be confined underneath the Shallow Aquifer. In other areas, where the Upper San Pedro/Saugus Formation outcrops, unconfined conditions exist; but, in these areas, water levels do not fluctuate much due to the absence of significant pumping stresses in the Upper San Pedro/Saugus Formation, hence, the confined assumption of head independent transmissivities seems reasonable under prevailing conditions.

Likewise, the GCA is expected to be unconfined where it outcrops. However, the base of the GCA is not very well defined due to limited data. Making the unit unconfined or convertible, without accurate knowledge of the base of the unit can lead to errors and inconsistencies. Hence, the GCA was treated as a confined system with constant transmissivities, which can be calibrated to match transient head responses in the aquifer.

7.3 Simulation Period and Stress Periods

The period of record and key transient trends in the history of the basin were presented in Sections 6.1 and 5.3, respectively. The 1970s and 1980s were a key period due to the rising water levels and the filling of the Shallow Aquifer. However, comprehensive water level and production records were available starting in the mid-1980s. At the time of model development, the latest year

with complete production records was 2015. As such, the simulation period for the model was from 1970 to 2015. This period was sufficient to capture the key transience in the basin history while allowing the model to be based on and calibrated to the most comprehensive and reliable available dataset.

A stress period in MODFLOW defines the time period over which boundary and model stresses remain constant. Each stress period may have a number of computational time steps, which are some fraction of the stress period. The groundwater flow model had a total of 552 monthly stress periods beginning in January 1970 and ending in December 2015. In addition, each stress period consists of daily time steps adaptively selected by the MODFLOW-NWT solver to ensure convergence.

7.4 Flow Model Design

This section discusses implementation of boundary conditions and parameters for the groundwater model. A boundary condition can be defined as a constraint put on the active model grid to characterize the interaction between the active simulation grid and the surrounding environment. There are generally three types of boundary conditions: specified head (First Type or Dirichlet), specified flow (Second Type or Neumann), and head-dependent flow (Third Type or Cauchy). The no-flow boundary condition is a special case of the specified flow boundary condition. Boundaries can be either time independent or time dependent. An example of a time-dependent boundary is a pumping flow boundary (e.g., grid cell with a well) or a time-varying specified head boundary. For this model, boundaries requiring specification included: lateral and vertical boundaries for each layer, surface water boundaries, inflows from recharge boundaries, outflows from evapotranspiration, and inflows/outflows from groundwater injection/extraction.

7.4.1 No-Flow, Specified Head, and General Head Boundaries

Specified head and general head boundaries are useful in specifying hydraulic connections between a given basin and adjacent basins or hydrologic units. Given the geologic setting, little to no underflow occurs along the northern, eastern, and southern boundaries (see discussion in Section 6.2.8). Very little underflow is known to occur between Simi Valley and the Las Posas Basin (Hydrometrics, 2016). As such, this interface is assumed to be a no-flow boundary. Note, surface water does flow from Simi Valley to the East Las Posas Sub-Basin and is simulated using streamflow routing as discussed in the following sub-section. Underflow occurs in the Shallow Aquifer at the boundary between the East Las Posas Sub-Basin and Pleasant Valley Basin and was estimated to be approximately 130 AFY by Hydrometrics (2016). There is significant faulting that likely acts as a barrier to flow across the boundary in deeper units. Hydrographs and water levels contours from Hopkins Groundwater Consultants (2008) show head gradients across the East Las Posas and Pleasant Valley boundary of more than 100 ft in the 1980s and 1990s. As such, the boundary between the East Las Posas Sub-Basin and Pleasant Valley Basin is modeled as a no-

flow boundary for the deeper units (Upper San Pedro/Saugus Formation, Clay Marker Bed, FCA, Upper Santa Barbara Formation, GCA) and a specified head boundary for the Shallow Aquifer. The specified head boundary in the Shallow Aquifer is set at a constant value of 90 ft amsl, which is more than 150 ft bgs in that area. This value is much lower than water levels in upgradient sections of the Shallow Aquifer (water level elevations in the Shallow Aquifer are 250 ft amsl or more when saturated). As such, the specified head boundary acts as a free outflow boundary allowing water to flow out of the Shallow aquifer whenever the cells along the boundary are saturated. **Figure 7-6** shows the specified head boundary in the Shallow Aquifer along the southern boundary with the Pleasant Valley Basin.

The Somis Fault Zone along the western boundary acts as a flow-barrier in the deeper water bearing formations (FCA and GCA), as evidenced by the hundreds of feet of head difference between the West and East Las Posas Sub-Basins. Underflow may occur along this boundary in saturated portions of the Upper San Pedro/Saugus Formation, overlying the deeper units. To simulate the underflow in the Upper San Pedro/Saugus Formation, a general-head boundary (GHB) was implemented across the East and West Las Posas Sub-Basins boundary in the bottom layer of the Upper San Pedro/Saugus Formation (model layer 3). The GHB is similar to a specified head boundary, except that it also includes a conductance term that can be modified to control flow across the boundary. Initial simulations without the GHB indicated that several sections of the Upper San Pedro/Saugus Formations (layers 2 and 3) were unsaturated along the boundary. Since GHBs require boundary cells to be saturated (the head of a GHB cell has to be above the bottom elevation for the given boundary cell) at all times, GHBs were defined only for cells that remain saturated during model simulations. The head for the GHB was defined at a few feet above the bottom elevation of the cell, such that underflow would occur whenever the surrounding area in the Upper San Pedro/Saugus Formation was saturated. **Figure 7-7** shows the GHBs in the bottom layer of the Upper San Pedro/Saugus Formation (model layer 3).

7.4.2 Arroyo Las Posas/Simi Streamflows

In general, water discharges from streams when the groundwater elevation is less than the surface water elevation and flows into the stream when groundwater elevations are higher than the stream elevation. This process is proportional to the difference between the groundwater and surface water elevations and depends on the effective hydraulic conductivity of the interface between the surface water and groundwater elements. If groundwater elevations fall below the bottom of the stream-channel, then the stream gets hydraulically disconnected from the groundwater system but still continues to lose water through streambed seepage. These groundwater and surface-water interactions are shown in **Figure 7-8**.

The Arroyo Las Posas/Simi is an important source of recharge to the Las Posas groundwater basins. Under low flow conditions, the groundwater also discharges to the Arroyo in certain

reaches (Engle 2012; 2013). Winter storms contribute significant flows to the Arroyo. Low flows in the Arroyo have steadily increased due to anthropogenic discharges (Section 6.2.2). Surface-water/groundwater interaction along the Arroyo is compounded by the fact that for most parts the Arroyo does not have permanent embankments, and flow conditions can alter channel width and geometry. As such, both the stage in the Arroyo and the wetted area (through which recharge or discharge occurs) is dependent on prevalent flow conditions and can change from wet to dry conditions and from one year to another. To accurately model the interaction of surface water flows with the groundwater system, it was important to capture this transience in flows, stage, and streambed geometry.

The enhanced MODFLOW streamflow routing (SFR2) package (Niswonger and Prudic, 2005) was found suitable to simulate the complex interaction between groundwater and surface water along the Arroyo. The SFR2 package uses the continuity equation (conservation of mass) to route surface water flow through one or more simulated rivers, streams, canals, or ditches (which may or may not be interconnected). Streams are divided into segments and segments into reaches. A stream water budget for each stream reach, as well as the leakage rate between a stream reach and corresponding groundwater model cell, is computed each iteration of a time step and at the end of each time step. This approach allows for the addition and subtraction of water from runoff, precipitation, and evapotranspiration within each reach. For each reach, the locations, length, streambed elevation, slope, streambed thickness, and hydraulic conductivity are fixed over the length of the simulation. However, for each segment that the reach is associated with, SFR2 includes several options for simulating stream depths, widths and releases/diversions. Different options may be used for different segments of the stream and may change from one stress period to another.

When creating the SFR2 package, LIDAR data, obtained from CMWD, were used to delineate the Arroyo channel and obtain streambed elevations (the LIDAR data were post-processed to remove artifacts from various man-made structures). Streambed elevations were also qualitatively compared to observed water levels to assess gaining and losing portions of the stream in relation to streambed elevations. **Figure 7-9** shows a cross-section running east to west, Arroyo streambed elevations, key features along the stream, and historical water levels. Reach lengths and slopes were calculated once the reaches had been delineated from the LIDAR coverage.

Segments define the stream units for which inflows/outflows, and the flow-stage/flow-width relationships can be specified. The Arroyo was divided into 18 segments based on streambed and channel characteristics as assessed from areal imagery during different time periods (dry and wet months from 2005 to 2015), discussions with the CMWD groundwater manager (Mr. Bryan Bondy), presence of known tributaries, and gage locations. **Figure 7-10** shows the discretized segments for the Arroyo Las Posas/Simi. For each segment, average channel width was measured

from areal imagery of the Arroyo during a range of dry and wet periods (January 2005; September 2007; April 2011; December 2013; and May 2015). Flows for the corresponding period were collected from streamgage data available for upstream gage 803 and mid-point gage 841/841A. Regression relationships between flow and width were developed for each segment based on the developed dataset. In general, a monotonic trend was seen between flow and width for all segments, with the wet-period (January 2005) width ranging from 30 ft (Segment 1) to 350 ft (Segment 3) and dry-period (May 2015) width ranging from 4 ft (Segment 3) to 20 ft (Segment 11). These flow-width relationships were input into the SFR2 package as a table specifying widths for a set of flow values (see Section 8.2.2, for details). The flow-width relationships were kept the same for all stress-periods; however, the flow-width relationships were applicable over a range of flows, encompassing both low- and high-flow conditions. The flow-width relationship was further modified during calibration to match flows and water levels during high-flow and low-flow conditions.

Flow-depth relationships were derived from rating curves available for three streamgage locations (803, 841/841A, and 806) on the Arroyo, upstream, mid-point, and downstream of the Las Posas Basin. In general, gage 803, the most upstream gage, had the highest stage for a given flow and gage 806 had the lowest stage for a given flow, with gage 841/841A in the middle. For each segment, the stage for a given flow was interpolated from the stages at the three gages (for the same flowrate) using inverse distance weighting. This allowed us to create a unique flow-depth relationship for each segment, which transitioned from the rating curve of gage 803, to gage 841/841A, to gage 806 for upstream to downstream segments.

ET losses in the Arroyo were specified in the SFR package. Pan ET rates were obtained from the VCWPD's Hydrologic Data Webpage (for the Fillmore-Fish Hatchery station located just north of the basin). Pan ET rates ranged from a high of 7.5 inches/month in July to a low of 3 inches/month in January.

The inflow to the SFR package consisted of surface-water flows from the Simi Valley. As discussed in Section 6.2.2, inflows to Arroyo Las Posas/Simi consisted of natural inflows, discharges from the SVWQCP, and discharges from the Simi dewatering wells. Flow data at gage 803 incorporates natural flows and discharges from the Simi dewatering wells. However, the gage is upstream of the SVWQCP discharge point; hence, these releases were added to the observed flows at the 803 gage. SVWQCP discharges are only available starting in 1980. Based on information provided by VCWWD, the SVWQCP was designed in 1964 (by Pomeroy Johnston & Bailey) and probably online sometime in 1965. Hence, SVWQCP discharges were scaled linearly from 0 in 1965 (when the plant went online) to 1980 values.

Finally, any losses to the groundwater upstream of the basin boundary were accounted for using the average loss rate between gages 1 and 2 from the study by Larry Walker and Associates (Engle 2012; 2013). The net flowrate was applied as inflow to the first segment of the SFR2 package.

An initial streambed conductivity of 1 ft/day and a streambed thickness of 1 ft were assumed for all reaches. Conductivity values were subsequently modified during calibration.

7.4.3 Groundwater Injections and Extractions

Groundwater extractions and injection were simulated using the WEL package. Production data for extraction wells has been collected by the FCGMA starting in 1983. A total of 184 wells had production data between 1983 and 2015. Production and ASR wells are shown in **Figure 7-11**. Production data were comprised of 6-month total production volumes for each well. Since the model had monthly stress-periods, pumping was evenly divided across each of the six months. Injection and extraction information was available at daily and monthly timescales for the ASR wells. For these wells, net extraction/injection for each month was calculated and used in the model.

Where available, screen elevation information was used to associate pumping from groundwater wells to one or more model layers. The assignment was made by evaluating the screened interval in each model layer and apportioning pumping based on screened transmissivity (i.e., screened thickness multiplied by the conductivity of the corresponding model layer). Several production wells did not have screen information. For these, a stepwise approach was taken to determine production intervals. First, available water level data for the well was reviewed to determine if water level trends could inform the screened interval for the well. Second, if available, total depth of the well was used to determine the deepest productive (Shallow Aquifer, FCA, or GCA) model layer the well could have been screened in and thus pumping was assigned to that layer. Where no information was available, a production interval was assigned based on the location of the well and the pumping intervals of the neighboring wells in the area.

Based on discussions with the CMWD groundwater manager, 1984 was assumed to be the first year with reliable pumping records. However, the model simulation period starts in 1970. Hence, pumping estimates were needed from 1970 to 1984. An “analogous” year approach was implemented to estimate historical pumping. This approach is outlined in the steps below:

- Years between 1970 and 1984 were compared to years between 1985 and 1990 in terms of precipitation and estimated ET (based on annual average temperature). Each year between 1970 and 1984 was assigned to an “analogous” year between 1985 and 1990, based on similarity of precipitation and ET.

- Historical areal imagery was reviewed to determine which areas were agricultural in the 1970s. Discussions were also held with the CMWD groundwater manager to discuss historical agriculture and groundwater production trends.
- In areas that were agricultural in the 1970s and remained agricultural after 1985, pumping from the analogous year was assigned to the corresponding pre-1984 year. Note that it is possible that the historical pumping was from an older (perhaps abandoned well). Information on well-drilling and abandonment dates was sparse prior to 1985. Hence, it was not possible to accurately associate historical pumping to older wells. A simplifying assumption was made to associate the historical pumping to active wells that are in areas that have been historically agricultural and would have pumped water from older wells on the property that may not be part of current records.
- Certain areas like the City of Moorpark and the ASR wellfields were historically agricultural but no longer pump water for agricultural production. Hence, in such areas post-1985 pumping would not be representative of pre-1985 conditions. For these areas, agricultural parcels were delineated from 1970 areal imagery. Pumping from 1970 was assigned at the rate of 3 ac-ft/ac of land (estimate of historical average agricultural demand in the ELPMA). For the agricultural parcels in the City of Moorpark, pumping was linearly ramped down to zero in 1984, by which time the area was urbanized. For the ASR wellfields, the pumping was kept constant and then made zero in 1984, when the FCGMA records start. For each agricultural parcel, the historical pumping was assigned to known inactive and abandoned wells within or adjacent to the parcel.
- VCWWD wells supply water to several agricultural and municipal customers. Due to this, VCWWD production is less susceptible to seasonal demand cycles. Hence, 1984 was assumed to be a representative year for VCWWD wells, and pre-1984 years were assigned 1984 pumping rates. The only exception to this was well 03N20W35J01S, which had a much higher than average pumping in 1984. For this well, analogous years between 1985-1990 were used to assign pumping prior to 1984. For all VCWWD wells, drill-dates were checked to ensure that pumping was only assigned in the period after the wells were drilled, as it is unlikely that older wells would have pumped at similar rates as the VCWWD wells prior to their drill-dates.

Groundwater wells were implemented as “Analytic Element Wells” in Groundwater Vistas. This utility automatically allocates total pumping for a given well across multiple screened aquifers, by apportioning pumping based on screened aquifer transmissivity. The utility also facilitates pumping reallocation across model layers during the calibration process, as Groundwater Vistas automatically apportions pumping rates based on specified hydraulic conductivities in screened aquifers before running the model.

7.4.4 Areal Recharge and Return Flows

Recharge was simulated using the RCH package, which applies a given rate of recharge to the top most active cell. Note, that with MODFLOW-NWT, even dry cells receive recharge, allowing them to get saturated under wet conditions.

The methodology for estimating areal recharge, recharge from the Moorpark percolation ponds and recharge from return flows was discussed in Sections 6.2.1, 6.2.3 and 6.2.4, respectively. Areal recharge was based on the estimates from the BCM (Flint et al., 2013; Flint and Flint, 2014) scaled by precipitation from VCWPD precipitation gage. The recharge from the BCM is an estimate of water penetrating below the root zone (Flint and Flint, 2014). This recharge is much more variable and transient than is expected for deep percolation to the groundwater table. The thick vadose zone that overlies much of the water table in this basin is expected to smooth out the recharge signal. This is evident from water level observations in the basin that do not show any response to precipitation or seasonal variability. Moreover, geochemical studies (Izbicki and Martin, 1997) indicate that much of the groundwater away from the Arroyo is at least several decades old. Hence, a long-term average (50 year) was calculated from the BCM recharge estimates and used as the baseline areal recharge for the model.

Due to its coarse scale, the BCM does not account for focused recharge from tributaries. High water levels to the east of the model domain indicate higher recharge rates, likely from the Happy Canyon Creek, which has a larger drainage area and connected areas of sandy alluvium with higher soil hydraulic conductivity (Soil Survey Staff, 2016) that could provide focused recharge. Initial testing with the model indicated the need for more recharge in the east. Hence, additional recharge along tributaries (especially along the Happy Canyon Creek) was added to the model.

Recharge also includes agricultural return flows in areas with a shallow water table or high permeability soils (areas corresponding to the Shallow Aquifer and the Epworth Gravels Aquifer). Return flows were estimated as a fraction of pumping in agricultural areas. Return flow fractions of both 8 and 16% were created. The corresponding recharge was uniformly spread over the agricultural parcels in these areas.

The Epworth Gravels Aquifer, is relatively isolated from the rest of the LPVB. Areal recharge and return flows are the primary recharge mechanisms and pumping is the primary discharge mechanism. Water level trends show declining water levels from 1970 through the late 1990s and rising trends after 2000 as pumping rates declined (**Figure 5-9**). Declining trends in water levels indicate that there is more pumping than recharge, while rising trends indicate that recharge is overtaking discharge from pumping. Average production from the Epworth Gravels Aquifer between 1970 to 1998 was estimated to be 1,500 AFY. Average production from 1999 – 2015 was approximately 1,200 AFY. Given trends in water levels, recharge was estimated to be between 1,200 and 1,500 AFY. The active domain for the Epworth Gravels Aquifer has an area of

approximately 950 acres. Dividing the recharge rate with the area gives a recharge rate of 19 to 15 inches per year (in/yr). Hence, a constant rate of 17 in/yr was assumed for the Epworth Gravels Aquifer. Note that this recharge rate would be inclusive of return flows.

Finally, discharges from the Moorpark WWTP were included in the recharge package. Information provided by Ms. Susan Pan from the Public Works Agency, County of Ventura, indicated that only the percolation ponds (1-7 & 28-30) to the east were active (See **Figure 6-6**), hence recharge from Moorpark WWTP discharges was only applied to cells corresponding to those percolation ponds.

7.4.5 Evapotranspiration from Phreatophytes

ET from phreatophytes (predominantly *Arundo*) along the Arroyo was simulated using the EVT package. Details on how the ET rate was estimated is presented in Section 6.2.6. The EVT package requires an extinction depth, at which groundwater depth ET losses become zero. An extinction depth of 6 ft bgs was assumed for this model. EVT cells were created in areas with significant *Arundo* density along the Arroyo. ET rates were based on the *Arundo* density and water use studies summarized in Section 6.2.6. **Figure 7-16** shows the locations of the EVT cells.

7.4.6 Hydraulic Properties

The UPW package was used for specifying hydraulic properties for the model, which consisted of horizontal and vertical hydraulic conductivities, specific yields (for unconfined/convertible layers), and specific storage (for confined/convertible layers). Initial hydraulic properties were presented in Section 4.2.

The Horizontal Flow Barrier package (HFB) was included to simulate significant faults and other discrete flow restricting features. The locations and conductance of the faults were adjusted during model calibration to match observed heads and head differences across faults.

8.0 MODEL CALIBRATION

The modeling approach comprised development and calibration of the groundwater flow model. In the context of groundwater flow modeling, calibration is typically defined as the process of producing agreement between model simulated and observed heads and discharges through the adjustment of aquifer parameters, boundary conditions, and estimated recharge terms within prescribed ranges.

8.1 Calibration Approach

Groundwater models are inherently non-unique, meaning that multiple combinations of hydraulic parameters and aquifer stresses can reproduce essentially equivalent heads and flow fields. To reduce the impact of non-uniqueness, a calibration method described by Ritchey and Rumbaugh (1996) was employed. This method includes (1) calibrating the model using parameter values (e.g., hydraulic conductivity, storage coefficient, and recharge) that are consistent with site-specific estimates (either through measurements or those developed as part of the conceptual model), (2) calibrating to multiple hydrologic conditions, and (3) using multiple calibration performance measures to assess calibration.

Calibration consisted of the conventional “trial and error” approach, which entails making informed and hydrogeologically realistic incremental changes to the various model parameters and evaluating the effects of each successive trial on the state variables as well as the effect on any other calibration metrics. With this type of “manual” calibration, the modeler is directly modifying parameter values, typically one at a time, based on knowledge of the conceptual model framework and sometimes including refinement of the conceptual model itself. This is in contrast with automated calibration with a software tool such as PEST (Doherty, 2004), which was not used for the current model. The initial setup for PEST can be time consuming and does not necessarily guarantee an improved calibration and may be most valuable for any final refinement once a reasonably close manual calibration has been accomplished. PEST could certainly be applied to the calibrated ELPMA model in the future if extension the calibration period or calibration refinement was desired based on future needs or additional data.

As a precursor to calibration, preliminary sensitivity analyses were performed for the flow model. This entailed varying model parameters to assess which produced the most significant change in the hydraulic heads and flow to and from the Arroyo. Findings from the sensitivity analysis are presented in subsequent sections, when discussing model calibration.

Calibration commenced with a steady-state model with assumed average production rates and surface water flows prior to 1970. Large scale hydraulic properties such as hydraulic conductivities and recharge were modified until the model converged to plausible hydraulic head distributions

(with respect to pre-1970 historical water levels). Apart from providing a better estimate for regional hydraulic properties and recharge, this was a necessary first step to develop a stable numerical model that could then be used for transient calibration. The steady-state model was also useful in providing initial head distributions, which were further modified during the calibration phase (Section 8.3).

Transient calibration was an iterative process. The calibrated process proceeded by first focusing on the Arroyo, as this is the primary source of recharge to the basin during the calibration period. Primary calibration parameters of the SFR package included riverbed conductivity, the flow-width relation, and (to a lesser degree) the flow-depth relationship (Section 8.2.2). Hydraulic conductivities and specific yield of the Shallow Aquifer were also modified to achieve appropriate head response in shallow wells (Section 8.4). Streamflow characteristics such as outflow from the basin and net discharge from the Arroyo to the groundwater system was monitored for dry and wet conditions. The streamflow and groundwater budget were regularly checked to ensure that it was as close as possible to the conceptual groundwater budget. Calibration in the Shallow and Epworth Gravels Aquifers also entailed modifications to diffuse recharge from precipitation and/or return flows (Section 8.2.1). Subsequently, calibration proceeded to deeper units (Section 8.4). For these units, hydraulic conductivities, specific storage, and specific yield were refined during calibration of the transient flow model by matching observed heads to those simulated. Vertical conductivities of underlying units were modified to either allow inflow into deeper units or reduce inflow and build groundwater elevations in shallower units. As hydraulic, storage, and recharge properties were modified, refinements were made to the SFR package to improve local calibration. This iterative cycle was repeated until calibration was achieved as assessed by quantitative metrics at target wells (8.1.1) as well as several semi-qualitative and qualitative measures (Sections 8.1.2 and 8.1.3).

Throughout this process, model results (consisting of calibrated model parameters, simulated hydraulic heads/gradient, and water budget components) and areas of uncertainty were presented to and discussed with the CMWD Groundwater Manager, to ensure the model was plausible and consistent with current understanding of the hydrogeology in the Basin.

8.1.1 Calibration Targets

Calibration requires development of calibration targets and specification of calibration measures. To address the issue of non-uniqueness, it is best to use as many types of calibration targets as possible. The primary data type for flow calibration were hydraulic head (water level) measurements. Simulated heads were compared to observed heads at specific observation points through time (hydrographs) to ensure that simulated heads were consistent with hydrogeologic interpretations. Another important metric for flow model calibration include lateral and vertical head gradients, especially between the Upper San Pedro/Saugus Formation and the FCA.

Therefore, simulated head gradients were compared against those observed and aquifer parameters were adjusted accordingly. Other calibration measures included Arroyo flows and infiltration rates, gaining and losing reaches within the Arroyo, and groundwater velocities (as assessed from observed water quality trends).

A total of 120 groundwater wells were included in the model as calibration targets with about 8,000 total head observations. There were several target wells without screen information. These wells were assigned to aquifers based on water level elevations. There were also a few wells with screens in multiple aquifers. In such cases, the observed water level is expected to be a weighted average (by transmissivity) of heads in individual screened aquifers, (if screened portions of the aquifers are in connection with the water in the well-bore). Such targets were used in a qualitative fashion, to ensure that observed water levels were in between the simulated water levels in the top and bottom screened aquifers. Finally, several calibration target wells showed pumping impacts on the water levels. While the model does include pumping, the simulated head represents an average hydraulic head within the grid cell. During pumping, heads within the well are lower than surrounding aquifer heads due to well-losses. Finally, the calibration dataset included several observations that seemed spurious or noisy. As much as possible, the noise and outliers were removed from the calibration dataset. Wells used for calibration are shown in **Figures 8-1 to 8-5**, with key wells labeled. Key wells represent wells with a sufficient period of record and number of measurements over the simulation period to allow the model to be calibrated with respect to salient spatial and temporal water level trends in the ELPMA (as discussed in sections 5.3 and 5.4). The figures also show that many of the calibration target wells are production wells, hence water levels may be impacted by pumping and well-losses. Salient water level trends in key wells are summarized in Section 5.3 and 5.4.

8.1.2 Quantitative Calibration Measures

Traditional calibration measures (Anderson and Woessner, 1992), such as the mean error and the mean absolute error, quantify the average error in the calibration process. The basis for these statistics is the head residual, which is simply the difference between the simulated head (h_s) and observed or measured head (h_m):

$$residual = (h_s - h_m) \quad \text{(Equation 8-1)}$$

The mean error (ME) is the mean of the residuals:

$$mean\ error = \frac{1}{n} \sum_{i=1}^n (h_s - h_m)_i \quad \text{(Equation 8-2)}$$

where n is the number of calibration measurements. The mean absolute error (MAE) is the mean of the absolute value of the residuals:

$$MAE = \frac{1}{n} \sum_{i=1}^n |h_s - h_m|_i \quad \text{(Equation 8-3)}$$

The root mean square error (RMSE) is the square root of the sum of the squared residuals divided by the number of observations:

$$RMSE = \left[\frac{1}{n} \sum_{i=1}^n (h_s - h_m)_i^2 \right]^{1/2} \quad (\text{Equation 8-4})$$

Both the RMSE and mean absolute error are routinely used as basic calibration metrics for heads, and we looked at both during calibration. The scaled RMSE is given by:

$$\text{Scaled MAE} = \frac{ME}{\text{Observation Range}} \quad (\text{Equation 8-5})$$

For groundwater flow models, the typical calibration criterion for heads is a scaled RMSE or scaled MAE equal to or less than 10% of the observed head range in the aquifer being simulated (Anderson and Woessner, 1992).

The mean absolute error is useful for describing model error on an average basis but, as a single measure, it does not provide insight into spatial trends in the distribution of the residuals. An examination of the spatial distribution of residuals is necessary to determine if they are randomly distributed over the model grid and thus are not spatially biased. Plots of head residuals were used to judge the spatial aspects of the calibration.

During the calibration process, it is important to check the overall water and mass balance errors periodically to ensure that the difference between simulated inflow and outflow is small. Typically, the overall percent difference should be less than 1%, and ideally less than 0.1% (Anderson and Woessner, 1992). The calibrated flow model had a mass balance error of less than 0.1%.

8.1.3 Qualitative and Semi-Quantitative Calibration Measures

In addition to the quantitative metrics discussed above, several qualitative and semi-qualitative measures were also considered when assessing calibration. These are listed below:

- During every significant calibration update, the resulting spatial distributions of hydraulic properties were presented to and discussed with the CMWD Groundwater Manager to ensure that the resulting hydraulic conductivity and storage property fields were plausible and consistent with current understanding of basin geology and structure.
- During every significant calibration update, the simulated groundwater and surface water budget components were compared against the conceptual model and discussed with the CMWD Groundwater Manager to ensure that the simulated flows were plausible and consistent with the current understanding of the basin water budget. Different water budget components were constrained based on the level of uncertainty therein. Thus, water budget components with higher uncertainty (such as wet weather recharge from the Arroyo) were allowed more variation during the calibration phase, while water budget components with

high certainty (such as extraction rates at production wells or recharge from the Moorpark Percolation Pond) were more tightly constrained during calibration.

- Hand-drawn annual water level contour maps (**Figures 5-3, 5-4, 5-5, 5-16, and 5-17**) were compared with simulated head contours for the same time periods to check lateral head gradients and flow directions in the model.
- Simulated versus observed vertical head gradients were compared at the USGS multiport monitoring wells as well pairs screened in different units.
- Simulated versus observed streamflows were compared at the Hitch gage, which is located within the model area.
- Losing and gain reaches of the Arroyo (as simulated by the SFR2 package) were compared against the Larry Walker Study (Engle 2012, 2013). Similarly, the net infiltration rate and total recharge from the Arroyo were compared against estimates from the Larry Walker Study (Engle 2012, 2013).
- Simulated temporal trends in outflows from the Arroyo (into the Pleasant Valley Basin) were compared against current understanding of and published literature (Hopkins Groundwater Consultants, 2008) on historical surface water outflows from the Basin.
- Particle track simulations were undertaken to visualize flow paths from the Arroyo to the Shallow Aquifer and the FCA. Simulated flow paths and groundwater velocities (assessed via particle track simulations) were evaluated with respect to observed spatial and temporal trends in water quality across the Basin.

8.2 Calibration of Boundary Conditions

The model was not sensitive to variations in either the specified head boundary along the southern boundary with the Pleasant Valley Basin or the GHBs in the Upper San Pedro/Saugus Formation along the western boundary with the WLPMA. Other boundary packages are discussed below.

8.2.1 Recharge

Recharge consisted of areal recharge, return flows, and recharge from the Moorpark percolation ponds. Given the nature of the physical processes involved, there is considerable uncertainty in the net amount of recharge (from all sources) reaching the water table. Note, that the model responds to the spatial and temporal distribution of the aggregate recharge from all sources, and cannot distinguish between different sources of water. Hence, a phased strategy was implemented when calibrating recharge. Recharge distributions were created for each individual recharge source. Calibration commenced by starting with the largest contributor of areal recharge – diffuse

precipitation-based recharge; smaller recharge components were then added progressively until calibration was achieved in terms of water levels and water budget.

Diffuse precipitation-based recharge is the primary mechanism for areal recharge in much of the basin not receiving focused recharge from the Arroyo. Using the BCM-based recharge estimates led to much lower groundwater elevations than observed in the 1970s. Moreover, water levels continued to decline with pumping even with perennial flows in the Arroyo, counter to what is observed in water level records. As noted in section 6.2.1, BCM does not account for recharge from tributaries or overland flow. Hence, additional recharge was added along tributaries. In particular, the eastern and north-eastern parts of the basin are expected to receive recharge from the Happy Camp Canyon Creek. Thus, additional recharge was added to the model in the east along the Happy Camp Canyon Creek to raise water levels to the east. A total of approximately 2,500 AFY of additional recharge was added along tributaries as part of this calibration phase.

Return flows are expected to be significant in areas with permeable soils and/or a shallow water table. Preliminary conceptual modeling of the travel time for a pulse of saturation to travel through a 1-D unsaturated soil column with typical properties for the Upper San Pedro/Saugus Formation gave periods of several decades to centuries. Hence, agricultural return flows were only applied to the Shallow and Epworth Gravels Aquifers. Agricultural return flow rates of 8 and 16% of pumping were tested. Initial heads and the rising water level trends in the Shallow Aquifer were better simulated with the 8% agricultural return flows.

The Epworth Gravels Aquifer was determined to be very sensitive to recharge rate. The Epworth Gravels Aquifer receives recharge from precipitation, runoff/overland flow, and return flows. For ease of calibration, a uniform recharge rate was assumed for the Epworth Gravels Aquifer and the rate varied (between 14 and 18 in/yr) until simulated heads matched the temporal trends observed in the aquifer. A net recharge rate of 17 in/yr yielded the best results with respect to temporal trends in water levels in the Epworth. Note that, for numerical stability, the extent of the Epworth Gravels Aquifer was reduced to the saturated portions of the aquifer. Thus, actual recharge rates over the entire extent of the Epworth Gravels Aquifer are actually less than the 17 in/yr estimated.

No changes were made to recharge from the Moorpark percolation ponds during the calibration phase. Since the model calibrated well the lower bound on agricultural return flows, additional recharge from smaller recharge terms (M&I or septic return flows) were not deemed necessary for the model. Calibrated recharge fields for 1970 and 2010 are shown in **Figure 8-6** and **8-7**.

8.2.2 Streamflow Parameters

Perennial flows in the Arroyo Las Posas/Simi are a significant source of recharge to the groundwater basin. Flow from streams is a head-dependent boundary condition, depending on the difference between groundwater and surface water elevations as well as the riverbed conductance

(as long as the stream is not disconnected from the aquifer, after which point the stream discharges at a constant rate), defined as follows:

$$C = KwL / m \quad \text{(Equation 8-6)}$$

Where K is the riverbed conductivity, w is the channel width at the reach, L is the length of the reach, and m is the riverbed thickness. In the above formulation, m can be kept constant during calibration and changes can be made to K and w , L is fixed as it depends on how much of the stream intersects with the grid. The riverbed conductivity does not change over time and hence represents a parameter that controls the overall flux to or from the reach.

Recharge from the Arroyo Las Posas/Simi and heads in the Shallow Aquifer were very sensitive to the riverbed conductance for the stream reaches. In general, higher conductances (ranging from 2 to 5 ft/day) were required to get enough recharge from the Arroyo to the Shallow Aquifer. Conductivities were also varied spatially to control localized recharge and calibrate heads in shallow groundwater wells. These conductivities seem reasonable given that the riverbed sediment mostly comprises sands and silts. Table 8-1 shows the conductivities for each of the 18 segments.

For the Arroyo, the channel width (w) depends on flow and is defined by a table of flow and width values. The flow-width relation can be used to control flow in and out of the stream channel under different flow conditions. Using a higher w for high flow conditions allows for more high flows to recharge the basin. Similarly, using a higher w for low flow conditions allows for more flow (in or out depending on the head gradient) under low flow conditions. The flow-depth relationship was varied segment-by-segment to calibrate heads in the Shallow Aquifer and to match flow characteristics in the Arroyo. For example, dry weather flows were known to not spill over into the Pleasant Valley Basin until the early to mid-1990s (Hopkins Groundwater Consultants, 2008). To simulate these conditions the channel width for low flow conditions was increased to allow for more conductance/higher groundwater discharge during low-flow conditions.

Table 8-1 Calibrated Riverbed Conductivity in SFR Package

SFR Segment	Conductivity (ft/day)
1 - 4	5
5	4
6-8	3
9	2.5
10-13	2
14-15	3
16	5
17-18	4.5

Another key transience in the system is the gradual filling of the Shallow Aquifer, starting in the 1970s and extending through the 1980s. The timing and magnitude of this phenomenon was sensitive to the riverbed conductivity and flow-width relationships for the Arroyo as well as hydraulic conductivities and specific yield in the Shallow Aquifer. Reducing the width during high-flow conditions was instrumental in not filling the Shallow Aquifer too soon (driven by recharge from winter storm flows). This is consistent with the high-intensity/short-duration storms that are typical in the area. Most of the storm flows do not remain in the basin long enough to percolate significant volumes into the groundwater system.

Flows in the Arroyo are characteristic of a braided stream channel. Due to the absence of permanent river banks, the stage in the Arroyo does not change by more than a few feet (at most) between low and high flow conditions. During high flow conditions, surface water spills over the banks of the active channel expanding the width and limiting stage. Hence, the flow-depth relationship was not varied during the calibration process. Calibrated flow-width and flow-depth relations are shown in **Figure 8-8** and **8-9**.

The study by Larry Walker and Associates (Engle 2012; 2013) was used as a qualitative guide to assess gaining and losing reaches of the Arroyo. In general, the losing reaches were simulated as such by the model. As part of calibration, streambed elevations were dropped by an average of 5 ft to better match gaining sections of the Arroyo along segments 8, 9, and 10 (between Larry Walker and Associates gages 4 and 6). Note, localized interaction between surface-flow and groundwater can be highly complex, driven by channel geometry, bathymetry, riverbed characteristics, and small changes in the gradient between the stream stage and groundwater elevations. Additional grid and streambed/groundwater property refinement would be needed to accurately simulate the localized interaction between the Arroyo and the groundwater system.

8.3 Initial Conditions

Considerable time and effort was spent calibrating the spatial distribution of initial heads in each of the aquifers. Model results were seen to be particularly sensitive to initial head conditions, especially in the unconfined units (Shallow and Epworth Gravels Aquifers), as this defines the starting storage and initial transmissivity of the system. Estimation of initial head conditions was compounded by the fact that the basin was not in steady-state in the 1970s. In fact, significant pumping is known to have occurred during and before that time. Water levels in the west were much lower in the 1970s than in the 1980s, before perennial flows in the Arroyo recharged the western part of the basin and water levels in the eastern part of the basin were in decline due to continued pumping (see **Figures 5-13a to 5-13d**). Due to the sparseness of the pumping and water-level datasets prior to 1970, it was difficult to extend the model prior to 1970 to pre-development conditions. To estimate initial heads a hybrid approach was utilized - a steady-state model was created with the best guess of 1970s pumping and initial conductivity field. Hydraulic conductivity, recharge, and pumping were varied to get the general flow trends as expected (flow from the outcrops towards the pumping centers). Specified head boundaries (based on observed and extrapolated heads in the 1970s) were added to areas with high head residuals. This allowed the hydraulic head field to match observed 1970s water levels while also being hydrologically consistent with the flow regime. This approach was preferred over simply interpolating head data because interpolation often leads to hydrologically inconsistent initial head fields. The initial head field was then used for the transient calibration. In areas where the transient model showed high residuals during the initial stress-periods, the initial heads were manually modified (within limits) to improve calibration during the early period. Calibrated initial heads are shown in **Figures 8-10 to 8-14**.

8.4 Hydraulic Properties

Key hydraulic properties for the groundwater basin are horizontal and vertical hydraulic conductivities, specific yield (for unconfined portions of the aquifers), and specific storage (for confined portions of the aquifers). Sharp contrasts in horizontal conductivities (along fault lines) were simulated using HFBs with low intercell conductivity values.

8.4.1 Hydraulic Conductivities

Hydraulic conductivity controls the flow of water through the groundwater system in response to hydraulic head gradients. As expected, the model was sensitive to the hydraulic conductivity distribution. Calibration commenced assuming uniform hydraulic conductivities as presented in Table 4-2. **Figure 4-17** shows the spatial distribution of hydraulic conductivity estimates for the FCA, from specific capacity and aquifer test data. Note that interpreting specific capacity and aquifer test results is complicated by the fact that several are from wells screened in multiple aquifers and, hence, represent an aggregate hydraulic transmissivity across screened aquifers. Furthermore, specific capacity values are impacted by well losses and hence do not provide an

independent estimate of formational permeability. However, certain general trends could be discerned from the data. Conductivities ranged from hundreds of feet per day to less than 5 ft/day. High transmissivities/conductivities were observed in and around the ASR wellfields, as well as in the western and southwestern portion of the basin. It is noted that the cluster of wells with high transmissivities/conductivities south of the Moorpark Anticline are screened in the Upper San Pedro/Saugus Formation. Lower conductivities were observed north of the Fairview fault and in the central portion of the basin between the Long Canyon Anticline and the Las Posas Syncline. Especially low transmissivities/conductivities were observed southeast of the Moorpark Anticline, where the FCA is thought to be unproductive (based on the low density of production wells in the area and confirmed through discussions with the CMWD Groundwater Manager).

Note that lateral groundwater flow is driven by the transmissivity - a function of the hydraulic conductivity and saturated thickness - of the hydrologic unit. While, the focus of the calibration was on hydraulic conductivities, similar results could have been achieved by varying the thickness of the hydrologic unit. Hence, changes made to conductivities, as part of calibration, may well be indicative of variation in stratigraphy at certain locations. This is particularly true along features like the Moorpark Anticline, where variations in water levels and stratigraphy may exert control on groundwater flow by impacting the saturated thickness (and hence transmissivity) across the Anticline.

Shallow Aquifer

Calibration of the Shallow Aquifer, focused on matching observed water levels as well as the rising trend in water levels in the 1970s and 1980s (**Figures 5-8a** and **5-8b**). Gaining and losing reaches from the study by Larry Walker and Associates (Engle 2012; 2013) were used qualitatively, to raise water levels along gaining sections and lower water levels along losing sections (during dry weather flows in the 2011 and 2013) during calibration. Much of the production in the Shallow Aquifer occurs in the central portion of the basin. This area was given relatively high conductivity values (50 – 100 ft/day). Calibrated horizontal and vertical hydraulic conductivities in the Shallow Aquifer are shown in **Figures 8-15** and **8-16**. **Figure 8-17** shows the transmissivity of the Shallow Aquifer.

Epworth Gravels Aquifer

Heads in the Epworth Gravels Aquifer were very sensitive to the vertical conductivity between the Epworth Gravels Aquifer and (top layer of) the Upper San Pedro/Saugus Formation. Given the vertical head gradient of several hundred feet and the fact that heads in the Epworth Gravels Aquifer do not respond to pumping or injection events in the lower formations, it is safe to assume that there is little to no vertical hydraulic connection between the Epworth Gravels Aquifer and the deeper aquifers. Hence, a vertical conductivity of 1×10^{-4} was used for the Epworth Gravels

Aquifer. Heads in the Epworth Gravels Aquifer were mildly sensitive to the horizontal conductivity, as drawdowns at pumping wells were influenced by this parameter. A calibrated value of 40 ft/day was used for the horizontal conductivity of the Epworth Gravels Aquifer. Horizontal and vertical conductivities for the Epworth Gravels Aquifer are shown in **Figures 8-15** and **8-16**. **Figure 8-17** shows the transmissivity of the Epworth Gravels Aquifer.

Upper San Pedro/Saugus Formation

Several wells in the top layer of the Upper San Pedro/Saugus Formation (for example, wells 02N19W06N03S in **Figure 5-11a**) showed water level trends very similar to those seen in the Shallow Aquifer. These wells were also in the area with high specific capacity values in the Upper San Pedro/Saugus Formation (**Figure 4-17**). Based on these water levels, it was assumed that in this area, the top layer of the Upper San Pedro/Saugus Formation was in hydraulic connection with the Shallow Aquifer. Alternatively, the Shallow Aquifer may be deeper in this area than conceptualized in the geologic model, and the wells may be screened in the Shallow Aquifer. From a modeling standpoint, a high conductivity zone (with a corresponding high vertical conductivity) was added to the model in this area, to allow the Shallow Aquifer and the top layer of the Upper San Pedro/Saugus Formation to essentially behave as one unit.

The deeper portions (corresponding to the bottom layer) of the Upper San Pedro/Saugus Formation have few long-term water level measures. Well 02N19W05K01, screened in the bottom layer of the Upper San Pedro/Saugus Formation and located east and north of the Arroyo (**Figure 5-11a**), shows a similar trend to the Shallow Aquifer. Well 02N20W12J01S (**Figure 5-11b**), also screened in the bottom layer of the Upper San Pedro/Saugus Formation, has declining water level trends in the 1940s, 1950s, and 1960s, followed by rising water levels in the 1970s and 1980s. At well 02N20W12J01S water level elevations in the bottom layer of the Upper San Pedro/Saugus Formation are more than 100 ft lower than well 02N20W12G02S, which is located just north (on the other side of the Arroyo) but screened in the top layer of the Upper San Pedro/Saugus Formation. This indicates that the vertical hydraulic connection within the Upper San Pedro/Saugus Formation is limited and vertical gradients exist within the Formation. Geologically, the Upper San Pedro/Saugus Formation is known to be a low permeability unit with interspersed sand and clay layers. Hence, horizontal and vertical conductivities in the bottom layer of the Upper San Pedro/Saugus Formation were kept low in this area (between 0.1 to 1 ft/day). USGS monitoring well 03N20W35R04S, located in the central portion of the basin and north of the Moorpark Anticline, is the one well in the bottom layer of the Upper San Pedro/Saugus Formation that has long-term water level records starting in 1990s. The water levels show a steady decline over the period of record. There is no apparent impact of rising water levels in the Shallow Aquifer and very little impact of injection and pumping events at the ASR wellfields. This indicates (1) a degree of hydraulic isolation from the southern portion (south of the Moorpark Anticline) of the

Upper San Pedro/Saugus Formation, and (2) vertical hydraulic isolation from the FCA (presumably due to the underlying Clay Marker Bed). Accordingly, water levels at well 03N20W35R04S were most sensitive to changes in the vertical conductivity of the Clay Marker Bed and horizontal transmissivities along the Moorpark Anticline. To achieve calibration, the vertical conductivity along the Moorpark Anticline was reduced to between 0.1 to 0.01 ft/day along the anticline in both layers of the Upper San Pedro/Saugus Formation. Note that the Upper San Pedro/Saugus Formation layers were modeled numerically as confined layers with constant transmissivities (unlike unconfined layers where transmissivities are proportional to water levels). Model results indicate that water levels are below the base of the Upper San Pedro/Saugus Formation along much of the Moorpark Anticline (i.e., the area is unsaturated). Hence, the low conductivities required to calibrate water levels in the Upper San Pedro/Saugus Formation north of the Moorpark Anticline are representative of unsaturated conditions (with low conductivities) along the anticline.

North of the Moorpark Anticline, a few pumping wells are screened only in (mostly bottom layer of) the Upper San Pedro/Saugus Formation. To allow for pumping at these wells, a zone of relatively high conductivities (5 ft/day) was added to the bottom layer of the Upper San Pedro/Saugus Formation.

Finally, water levels in the southwestern and western portions of the FCA show rising trends in water levels starting from the mid-1970s to the 1990s (**Figures 5-13a** and **5-13b**) in response to the Shallow Aquifer filling in response to perennial flows in the Arroyo from discharges of treated municipal wastewater. This is borne out by the water quality signature in the FCA, where high total dissolved solids (TDS) water has been observed in wells near the Arroyo (**Figure 5-18**). Hence, the FCA is in hydraulic connection with the Shallow Aquifer in the southwest and receives recharge from the Arroyo via the Shallow Aquifer. To allow for this hydraulic connection, vertical conductivities in the Upper San Pedro/Saugus Formation layers (model layers 2 and 3) were increased to 1 ft/day in an area southwest from the Moorpark WWTP. Calibrated horizontal conductivity, vertical conductivities, and transmissivities for the Upper San Pedro/Saugus Formation layers are shown in **Figures 8-18** to **8-23**.

Clay Marker Bed

Vertical conductivities of the Clay Marker Bed control the flow of water from the Upper San Pedro/Saugus Formation to the FCA. Consequently, heads in the Upper San Pedro/Saugus Formation (along with the overlying Shallow Aquifer) and the FCA were very sensitive to the vertical conductivities of the Clay Marker Bed. Furthermore, water from Arroyo Las Posas/Simi is an important source of recharge to the FCA, as evident from the water quality signature in FCA wells close to the Arroyo (**Figure 5-18**). Hence, changes to the Clay Marker Bed below the Arroyo (especially, in areas to the south-west where the FCA is in uplift and closer to ground surface) also

impacted flow from the Arroyo into the FCA. During calibration, conductivities of the Clay Marker Bed were increased under the Arroyo along losing reaches of the Arroyo to induce increase the vertical gradient and simulate more stream losses, as was needed to achieve calibration. Conductivities of the Clay Marker Bed were kept low under the central portion of the Shallow Aquifer (and Arroyo) to maintain heads in the Shallow Aquifer (and allow for the filling of the Shallow Aquifer). The conductivities of the Clay Marker Bed were kept high along a stretch of the Arroyo west of the Moorpark WWTP, where the FCA is in uplift and is in hydraulic connection (and in some areas, in contact) with the Shallow Aquifer. Geologically, this may represent an area of erosional unconformity between the older FCA and the younger alluvium deposits. This area of “hydraulic connection” between the surficial system and the FCA was instrumental in calibrating water levels in FCA wells in the west and southwest, all of which show rising trends in water levels starting from the mid-1970s to the 1990s (**Figures 5-13a** and **5-13b**) in response to the Shallow Aquifer filling in response to perennial flows in the Arroyo from discharge of treated municipal wastewater.

Hydraulic conductivities were also varied (between 1×10^{-4} ft/day and 5×10^{-5} ft/day) north of the Moorpark Anticline to calibrate to the declining trend observed at USGS well 03N20W35R04S as well as the water levels/drawdowns in production wells in the FCA. Hydraulic conductivities of the Clay Marker Bed were increased along the northern outcrop of the FCA, to allow for leakage to the FCA and calibrate to observed water levels in the north. Finally, observed trends in the southeast portion of the FCA indicate sharp rise in water levels in response to the filling up of the Shallow Aquifer. To calibrate to this observed response, vertical conductivities of the Clay Marker Bed (and overlying Upper San Pedro/Saugus Formation) layers were raised to 1 ft/day. This area is directly underneath the Arroyo reach that was seen to be strongly losing during the study by Larry Walker and Associates (Engle, 2012; 2013). High vertical conductivities of the Clay Marker Bed and Upper San Pedro/Saugus Formation would allow for more vertical leakage from the Arroyo/Shallow Aquifer in this area.

The calibrated vertical conductivity of the Clay Marker Bed is shown in **Figure 8-24**.

Fox Canyon Aquifer

The FCA is the primary productive aquifer in the ELPMA. As expected, simulated water levels in the FCA were quite sensitive to changes in hydraulic conductivities. The hydraulic conductivities in the FCA control the flow of water (and the propagation of hydraulic pressure) within the FCA from sources of recharge (recharge from the Arroyo, leakage from the Shallow Aquifer and the Upper San Pedro/Saugus Formation, recharge from the outcrops, as well as injection into the ASR wellfields). The distribution of transmissivities from specific capacity and aquifer test data was used as a general guide for the spatial distribution of conductivities in the FCA. High conductivity zones (from 50 to 200 ft/day) were included in and around the ASR wellfields to match drawdown

and draw-up responses in the ASR wells and surrounding wells to injection/extraction events. Medium to high conductivity values (10 to 25 ft/day) were also included in the west where higher transmissivity was required to support pumping from several production wells without excessive drawdowns.

Water from the Arroyo directly and indirectly (through leakage from the Shallow Aquifer and Upper San Pedro Formation) recharges the FCA. This recharge caused water levels in the western portion of the FCA to rise in the 1980s and 1990s. Injection at the ASR wells, likely contributed to the increasing water levels in the early 2000s. Increased pumping (including extractions from the ASR wellfields) caused reductions in water levels in the mid to late 2000s and 2010s. Water level trends in the central and eastern portion have a different temporal trend. The recharge from the Arroyo does not seem to have impact water levels quite as much as water levels to the east. This is likely due to the Moorpark Anticline acting as a flow barrier under low groundwater levels. Injection at ASR wells caused water levels to peak in the early 2000s in and around the ASR wells. Extraction at the ASR wells led to sharp declines in water levels (more than 150 ft at and around the ASR wells) in the east. Due to continued recharge from the Arroyo in the southwest, the response to ASR pumping was less pronounced in wells to the west and southwest. Hydraulic conductivity distributions within the FCA were calibrated to match these temporal trends in water levels. An area of lower conductivity (5 – 10 ft/day) was included in the central portion of the basin to keep the responses of water levels to recharge and ASR pumping distinct in the eastern and western halves of the aquifer. The response to injection and extraction events is muted north of the Fairview fault. A combination of HFBs (discussed in the next sub-section) and lower conductivities north of the Fairview fault were included to calibrate the propagation of the ASR events to the north.

FCA wells south of the Moorpark Anticline (02N19W05M01S and 02N19W04K01S, for example) show rising water levels in the 1980s in response to the filling of the Shallow Aquifer. Few measurements from the 1970s and 1980s exist in wells east and north of the Moorpark Anticline (**Figures 5-13c** and **5-13d**). The few wells with early water levels (e.g., 03N20W35R01S, 03N20W36G01S, and 03N19W32A01S) do not show the rising trend seen in westerly wells (note that production wells 03N20W35R01S and 03N19W32A01S are screened both in the Upper San Pedro/Saugus Formation and the FCA, hence early water levels are likely an average of Upper San Pedro/Saugus Formation and FCA water levels). Note, that the FCA is modeled as a convertible layer, with head-dependent transmissivities. Eastern sections of the Moorpark Anticline go dry under low water level conditions. This mechanism was seen to control the propagation of the rising water levels across the eastern portion of the Moorpark Anticline.

Specific capacity data (**Figure 4-17**) suggest the eastern and southeastern portions of the FCA are not very productive. Water levels in a few wells southeast of the Moorpark Anticline (e.g.,

02N19W05M01S) show sharp increases in the 1970s. This response was simulated by having good vertical connection between the Shallow Aquifer and FCA but low horizontal conductivities in the FCA. A relatively high vertical conductivity (1 ft/day) was used in the Upper San Pedro/Saugus Formation and Clay Marker Bed in this area to allow for water levels in the FCA to respond to rising water levels in the Shallow Aquifer. Low conductivities (1×10^{-1} to 1×10^{-3} ft/day) in the southeast limited the propagation of this signal to the north of the Moorpark Anticline).

VCWWD production well 03N19W33P03S (**Figure 8-4**), located near the southeast edge of the basin, showed water level trends unlike any other well screened in the FCA. Water levels throughout the period of record were 400 ft amsl or higher (whereas water levels in the FCA are typically less than 250 ft amsl. Water levels at the nearest (less than a mile) monitoring well (03N19W32A01S) were more than 150 ft below observed water levels at 03N19W33P03S. The well had historical pumping going back to the 1970s and stopped pumping in the 1990s. Screen information was reviewed to make sure the well was indeed in the FCA. Hydrologically, for water levels to be this high in the FCA this area would (1) need to be hydraulically connected to the Shallow Aquifer (presumably receiving recharge from the Arroyo), and (2) hydraulically isolated from the rest of the FCA. Water levels in this area were simulated by increasing horizontal and vertical conductivities of the FCA and overlying units until head response at well 03N19W33P03S was matched. Moreover, low conductivities were added to the FCA north and west of well 03N19W33P03S to isolate the heads in this area from the rest of the basin.

The anisotropy ratio of vertical to horizontal conductivity was kept at 0.1, except in areas with very low conductivities (1×10^{-2} to 1×10^{-3} ft/day), which are expected to be predominantly silts and clays and hence have an anisotropy ratio of 1.

Calibrated horizontal and vertical conductivities in the FCA are shown in **Figures 8-25** and **8-26**. **Figure 8-27** shows the transmissivity of the FCA.

Upper Santa Barbara Formation

Vertical conductivities of the clay-rich Upper Santa Barbara Formation layer impact the vertical gradient between the FCA and GCA. In the southwest, FCA receives recharge from the overlying units and the Arroyo, leading to higher heads in the FCA compared to the GCA. Upper Santa Barbara Formation conductivities were decreased (1×10^{-5} ft/day) to reduce leakage from the FCA to the GCA, allowing heads in the FCA to build up as observed in the wells to the southwest. In areas with significant pumping in the FCA, the vertical gradient can reduce, such that heads in the FCA are lower than the GCA. In such areas, reducing the vertical conductivity of the Upper Santa Barbara Formation would reduce the flow of water *from* the GCA to the FCA and induce higher drawdown for a given amount of pumping. In these areas, the vertical conductivity of the Upper Santa Barbara Formation was calibrated to (1) keep heads in and around production wells in the

FCA at observed levels and (2) better match vertical gradient between the FCA and GCA, where data in the GCA is available (e.g., between USGS multiport wells 03N20W35R02S in the GCA and 03N20W35R03S in the FCA). Hydraulic conductivities of the Upper Santa Barbara Formation varied between 1×10^{-3} to 1×10^{-5} ft/day. The exception was near the northern and western edges of the basin, where higher Upper Santa Barbara Formation conductivities allowed for more recharge to reach the GCA, keeping heads close to observed levels. **Figure 8-28** shows the vertical conductivity of the Upper Santa Barbara Formation.

Grimes Canyon Aquifer

Only a few water level measurements in the central and northern portions of the GCA were available at the time of this study (**Figure 8-7**). The hydraulic conductivities in the GCA were calibrated to match water levels trends at these locations. High conductivities (40 – 80 ft/day) were included near the northern ASR wellfield to match observed water levels in GCA and FCA wells in the area. In the remaining part of the basin, conductivities in the range of 10 – 20 ft/day were used. The GCA receives recharge from the outcrops in the north and northeast, as well as from leakage from the FCA in the southwest, south, and southeast. Hydraulic conductivities in the range of 0.1 to 1 ft/day were needed in these areas to control the hydraulic gradient and heads towards the central part of the aquifer where data are available. **Figures 8-29, 8-30, and 8-31** show the calibrated horizontal conductivities, vertical conductivities, and the transmissivities in the GCA.

8.4.2 Hydraulic Flow Barriers (Faults)

HFBs were used to simulate faults that impede lateral flow. The default value for hydraulic conductivities for all faults was 0.1 ft/day. Hydraulic conductivities were reduced in areas that showed large horizontal gradients in hydraulic heads. As discussed in Section 7.4.1, the Somis Fault Zone forms the boundary between the East and West Las Posas Sub-Basins and was modeled as a no-flow boundary. Extensions of the Somis Fault Zone to the east were modeled with a hydraulic conductivity of 0.1 ft/day in the Upper San Pedro/Saugus Formation, FCA, and GCA. The Fairview fault impedes flow north of the ASR wellfields. The fault was included in the Upper San Pedro/Saugus Formation, and the FCA and was calibrated to a hydraulic conductivity of 1×10^{-3} ft/day to match (1) head response to injection/extraction events in wells north of the fault, and (2) head response to injection/extraction events in and around the ASR wellfields. Note that, due to the proximity of the ASR wellfields to the Fairview fault, lower hydraulic conductivities led to higher simulated drawdowns and draw-ups in and around ASR wells in response to extraction/injection events. An unnamed fault was included in the FCA just north of the western edge of the Moorpark Anticline (**Figure 3-2**). Peak water levels in well 02N20W10G01S, south of the fault, are 70 ft higher than peak water levels in well 02N20W10D02S (**Figures 5-12 and 5-13b**). The fault was extended to the east to calibrate to observed heads in wells just north of the fault (e.g., 02N20W03J01S and 02N20W02N03S).

Two unmapped faults were included in the model to better calibrate to observed water levels. The first fault, running along the Long Canyon Syncline was modeled with a hydraulic conductivity of 1×10^{-6} ft/day. The HFB was necessary to keep heads high at observed levels in wells 03N20W27H01S and 03N20W27H03S in the Upper San Pedro/Saugus Formation outcrop (**Figures 5-10** and **5-11b**). Similarly, the fault was required to keep heads high at observed levels in well 03N20W23L01S near the GCA outcrop (**Figure 5-14** and **5-15a**). This fault could be an extension of the Berylwood fault (**Figure 3-2**) currently mapped in the West Las Posas Basin. Another unmapped fault was included (using a hydraulic conductivity of 1×10^{-4} ft/day) west of well VCWWD well 03N19W33P03S, discussed in the previous section. This well displays water levels several hundred feet higher than nearby wells, indicating an impedance to flow northwest of the well. This fault could be associated with the Santa Rosa – Simi fault system (**Figure 3-2**).

Figure 8-32 shows the final calibrated HFBs in the model.

8.4.3 Storage Properties

Calibration commenced with assuming uniform storage properties of 0.25 for specific yield and 1×10^{-5} (1/ft) for specific storage. In general, higher specific storage was needed across the model to simulate the observed amplitude in water level fluctuations. The specific storage was increased to 5×10^{-5} (1/ft) for all confined/convertible layers. These values were found to be appropriate for the Upper Santa Barbara Formation, and the GCA. In other model layers, storage properties were refined to better match the observed amplitude in water level fluctuations in response to change in pumping stresses. Adjustments were also made to account for unconfined conditions in layers modeled as confined (for numerical purposes) and for higher clay content, which tend to increase the storage of the formation.

In the Shallow Aquifer, a zone of higher specific yield (0.275) was included in an area with production wells to better calibrate to response in water levels to transience in pumping and recharge from the Arroyo. In the Epworth Gravels Aquifer, specific yield was reduced to 0.225 to better match the falling and rising trends observed in hydrographs as a function of change in pumping. The Upper San Pedro/Saugus Formation is unconfined/semi-confined in much of the ELPMA. However, due to numerical reasons, both the Upper San Pedro/Saugus Formation layers were modeled as confined systems with constant specific storage. To compensate for this, a high specific storage (1×10^{-3} 1/ft) was used in areas expected to be unconfined in the Upper San Pedro/Saugus Formation layers.

A specific storage value of 1×10^{-4} 1/ft was used in areas underlying the Shallow Aquifer, where the Upper San Pedro/Saugus Formation is likely to be confined/semi-confined. Likewise, specific storage of 1×10^{-5} 1/ft was used underneath the Epworth Gravels Aquifer, where the Upper San Pedro/Saugus Formation is, most likely, confined. A low specific storage value, of 1×10^{-5} 1/ft was also needed in the northwestern outcrop of the Upper San Pedro/Saugus Formation to calibrate to

observed water levels in wells (03N20W27H01S and 03N20W27H03S) in that area. Note, that these values are consistent with those for sandy-clays and clays (Batu, 1998), which is the predominant lithology in the Upper San Pedro/Saugus Formation. For the FCA, higher specific storage of 1×10^{-4} 1/ft was used underlying the Shallow Aquifer and the Moorpark Anticline, to match water level fluctuations in observed hydrographs.

Calibration specific yields for the Shallow Aquifer, Epworth Gravels Aquifer, and FCA (modeled as a convertible layer) are shown in **Figures 8-33** and **8-34**. **Figures 8-35** to **8-40** show the specific storage values for the top and bottom layers of the Upper San Pedro/Saugus Formation, the Clay Marker Bed, the FCA, Upper Santa Barbara Formation, and GCA, respectively.

8.5 Model Calibration Results

The groundwater flow model simulates groundwater levels from January 1970 to December 2015. In addition to groundwater levels, the model also simulates the flow of water in the Arroyo as well as inflows/outflows to and from the stream channel. Note that the focus of the model is groundwater flow and any recharge or discharge processes that influence groundwater flow. Thus, while effort was made to calibrate flows in the Arroyo to observed flows at gage 841/841A (Hitch gage), the surface water flows were evaluated in the context of their contribution to the groundwater system.

Finally, particle tracking simulations were carried out using MODPATH (Pollock, 1994) to assess flow paths and groundwater velocities in the model. Of interest was the movement of high TDS water from the Arroyo to production wells in the FCA, as observed in water quality trends in such wells. Results from the above are presented in the following subsections.

8.5.1 Hydraulic Heads

Figures 8-41 to **8-57** show simulated heads in the Shallow Aquifer, Epworth, top and bottom layers of the Upper San Pedro/Saugus, FCA and GCA in January of 1970, 1990, and 2015. Heads in the FCA are also shown for December 2006 and January 2010 in **Figures 8-52** and **8-53** to show the response to ASR injection and extraction events.

The model successfully captures key water level trends for the period simulated. **Figures 8-41** to **8-43** show the filling the Shallow Aquifer in the 1970s and 1980s, with rising water levels east to west. **Figures 8-44** to **8-46** show water levels in the top layer of the Upper San Pedro/Saugus Formation. Water levels in the south and southeast are similar to water levels in the Shallow Aquifer, as the top layer of the Upper San Pedro/Saugus Formation is in hydraulic connection with the Shallow Aquifer in this area. **Figures 8-47** to **8-49** show water levels in the bottom layer of the Upper San Pedro/Saugus Formation. Note the rising water levels in the south and southwest, in response to filling of the Shallow Aquifer. However, water levels north of the Moorpark Anticline continue to decline. **Figures 8-50** to **8-54** show water levels in the FCA in January 1970, 1990,

2000, 2010, and 2015. Note the rising water levels in the south, southwest, and west from 1970 to 1990. The flow direction in 1970 was predominantly east to west, consistent with water level contours shown in **Figure 5-3**. By the 1990s, recharge from the Arroyo becomes a factor and a southeast to northwest head gradient is seen. Again, this is in agreement with hand-drawn contours shown in **Figure 5-4**. Note that the Moorpark Anticline starts off unsaturated in the 1970s and gradually becomes more saturated as water levels rise in the FCA. By 2006 (**Figure 8-52**), water levels have risen in the southwest due to surface water recharge and in the central part of the basin from ASR injection. Note that the Moorpark Anticline is nearly completely saturated. The head contour map for January 2010 (**Figure 8-53**), shows the decline in water levels in the central part of the ELPMA between 2007 to 2010 in response to groundwater extractions from the ASR wells, resumption of pumping at wells that participated in the in-lieu storage program, and drought conditions (**Figure 6-10**). Groundwater levels declined approximately 100 ft in the central part of the ELPMA. The Moorpark Anticline becomes unsaturated, limiting recharge to the area north of the anticline. **Figure 8-54** shows water levels in the FCA in January 2015. Water levels in central part of the ELPMA have partially recovered. The groundwater elevations following recovery are believed to be approximately what they would have been without storage and recovery activities. This will be evaluated further with the model. Simulated water levels and hydraulic gradients are comparable to hand-drawn contours for the year (**Figure 5-17**) from Bondy (2016).

Figures 8-55 to 8-57 show water levels in the GCA in January 1970, 1990, and 2015. Water level in the GCA show similar trends as in the FCA.

Figures 8-58 to 8-65 show simulated hydrographs from the calibrated model compared to observed hydrographs at key wells in each of the hydrologic units. **Figure 8-58** shows that the model captures observed water level trends in the Shallow Aquifer. Note that the early “spikes” in water levels seen in 02N20W09Q01S and 02N20W09Q04S represent simulated recharge from stormflows in the Arroyo during a period when the Shallow Aquifer is unsaturated. However, recharge from stormflows alone is clearly insufficient to sustain heads in the Shallow Aquifer and water levels are not sustained until the Arroyo flows become perennial due to discharges. As can be seen, the Aquifer cycles through wet and dry periods, gradually getting saturated over time as the Arroyo flows become perennial due to discharges. Once the aquifer is saturated, the response to stormflows is more muted because (1) the aquifer has less storage, (2) the gradient between the surface water stage and groundwater is less, and (3) saturated transmissivities are higher, and the pulse from a high flow event has a more diffuse impact in the aquifer.

Figure 8-59 shows simulated versus observed water levels in the Epworth. The decline and subsequent rise in the aquifer is captured by the model. However, the model tends to under-predict the rise in water levels in the 2000s and 2010s. Recharge in the Epworth was kept constant over

time during this round of calibration. Additional recharge may be necessary in the latter half of the simulation to better match the rise in water levels during that period.

Figure 8-60 shows simulated versus observed water levels in the top layer of the Upper San Pedro/Saugus Formation. All wells shown, except 02N20W03K02S, underlie the Shallow aquifer where the top layer of the Upper San Pedro/Saugus Formation is in hydraulic connection with the Shallow Aquifer. The model does well in simulating rising water levels in response to the Shallow Aquifer filling up at these wells. Well 02N20W03K02S is an anomaly in terms of water levels. Water levels are more than hundred feet below water levels in other wells. In fact, water levels look similar to those in the FCA even though the screen is well within the top layer of the Upper San Pedro/Saugus Formation.

Figure 8-61 shows simulated versus observed water levels in the bottom layer of the Upper San Pedro/Saugus formation. The model captures the rising water levels south of the Moorpark Anticline (e.g., 02N19W05K01S) while simulating declining trends at wells north of the anticline (e.g., 03N20W35R04S).

Figures 8-62a to 8-62d show simulated versus observed water levels in the FCA. The model calibrates well to rising trends in water levels to the west and southwest (e.g., 02N20W10D02S and 03N20W34G01S) driven by recharge from the Arroyo and leakage from the overlying Shallow Aquifer and Upper San Pedro/Saugus Formation. The model also simulates the sharp rise in water levels observed to the southeast (e.g., 02N19W04K01S), where the intermediate Upper San Pedro/Saugus and Clay Marker Bed were calibrated to have a high vertical conductivity and an HFB was added to build up heads. Trends at VCWWD well 03N19W33P03S (**Figure 8-62d**), where water levels are hundreds of feet higher than other nearby wells, are also reasonably well matched as a result of the connection established between the FCA and the Shallow as well as the control on flow imposed by the low conductivities and HFB, west of this well. The model accurately simulates draw-up and drawdown at the ASR wells (**Figures 8-62a and 8-62b**).

Figure 8-63 shows simulated versus observed water levels in the GCA. Overall the residuals in the GCA are higher than other layers, although the model simulates general trends in water levels at the wells. Several of the wells (e.g.) are near the outcrops where the base of the aquifer dips sharply, making stable simulation of groundwater heads challenging from a numerical stand-point. The base of the GCA is poorly defined in this area, and it is possible that residuals in the model may be linked to incorrectly specified base elevation for the aquifer. Well 03N20W27B01S in the northern outcrop displays anomalous water levels. Observed heads rise sharply from 200 ft to 700 ft amsl in the 1980s. It is possible that the water exists in perched conditions around this well. No attempt was made to calibrate to this well and it was not used to calculate calibration statistics.

Figure 8-64 show simulated and observed water levels at the USGS multiport well situated in the central portion of the basin. Results indicate that the model accurately simulates the vertical disconnect between the Upper San Pedro/Saugus (03N20W35R02S), and FCA (03N20W35R02S), while capturing the hydraulic connection between the FCA and GCA (03N20W35R02S).

Figure 8-65 shows simulated and observed water levels at several wells that are screened across multiple hydrologic units. The water level within the well-bore is a function of the water level in individual aquifers and the flow contribution from that layer to the well bore. The numerical model only calculates an average head at the 200 ft x 200 ft grid scale and does not account for well-bore effects or vertical flows from one formation to the other within the borehole. Nevertheless, simulated water levels are between the water levels in the screened layers, as expected. Early observed water levels indicate that during early periods when drawdown at the well is limited, the well is in communication with both the upper and lower units. With continued pumping water levels decline and at some point, the well becomes disconnected from the upper formation and tends to have water levels closer to the lower formation. The intent of this model is not to simulate bore-hole effects. Hence, the attempt during calibration was to keep observed water levels between simulated levels in the screened units. Residuals at these wells are not indicative of overall model error and were not used when calculating calibration statistics.

8.5.2 Calibration Statistics

Calibration residual statistics for each of the model layers and the entire model are presented in **Table 8-2**. **Figure 8-66a** and **8-66b** show the scatter-plots for observed versus simulated hydraulic heads.

Table 8-2 Calibration Residual Statistics

Layer	Mean Error (ft)	Mean Absolute Error (ft)	RMSE (ft)	Range of Observations (ft)	Scaled RMSE	Scaled MAE
1	-4.3	12.6	19.2	575	0.03	0.02
2	-3.8	8.9	12.2	238	0.05	0.04
3	-6.6	15.8	23.14	343	0.07	0.05
5	-2.9	18.0	23.8	491	0.05	0.04
7	-7.7	17.5	21.7	284	0.08	0.06
Model	-2.6	16.4	22.2	620	0.04	0.03

Calibration results indicate that the model is well calibrated. Overall, the model does not display strong bias (as indicated by the low mean error). The MAE of 16.4 and RMSE of 22.2 seem reasonable given that several of the wells are production wells that are likely impacted by

variability in pumping (not simulated in the model, which assumes constant monthly pumping rates) and well-bore effects (again not simulated by the model). The Scaled MAE and RMSE of 0.03 and 0.04 are well below the 10% threshold for scaled RMSE, which is the industry practice in groundwater modeling.

The highest residuals are in the bottom layer of the Upper San Pedro/Saugus Formation and the GCA. Given that residuals in the top layer of the Upper San Pedro/Saugus Formation and FCA are low, this is indicative of areas of more vertical separation (leading to higher vertical gradients) within the Upper San Pedro/Saugus formation. Additional vertical refinement may be necessary to reduce these residuals. In the absence of more geologic data across this interval, such vertical refinements were not feasible in this phase of the modeling.

In the GCA, high residuals are driven by wells near the outcrop where simulated water levels are lower than observed. As already discussed, the stratigraphy is not very well known in the GCA outcrop, and it is possible that errors in stratigraphy impact water levels in the outcrop area. Nevertheless, even for layers with high residuals the scaled MAE and RMSE are well below the recommended 10% threshold.

8.5.3 Streamflow

While simulating flows in the Arroyo Las Posas/Simi is not a primary goal of this model, groundwater gains from and losses to the Arroyo are important parts of the water budget for the system, especially during dry-weather/perennial flows. The Larry Walker Study (Engle 2012, 2013) measured streamflow at various gages during dry-weather flows (summer of 2011 and 2012). **Figure 8-67a and 8-67b** compare gaining and losing reaches from the model with gaining and losing reaches from the Larry Walker Study, based on average gain/loss for 2011. The model simulates the gaining reach upstream of the Hitch gage, where high water levels in the Shallow Aquifer contribute base-flow to the Arroyo under low-flow conditions. The gaining segment downstream of the Hitch gage, is not as well simulated by the model. There are short reaches that are gaining along that section, but the net effect is a losing segment, as simulated by the model. Discussions with the CMWD Groundwater Manager has indicated that some water discharged to the percolation ponds may move laterally in the shallow subsurface and become streamflow, as based on historical visual observations of seepage faces adjacent to the percolation ponds. This might explain why the Larry Walker Study (Engle 2012; 2013) observed gaining reaches along this stretch of the Arroyo, while the model (which applies the Moorpark WWTP discharges to the groundwater as part of the recharge package) simulates losing streamflow conditions. Future refinements to the model could include a better representation of the routing of the Moorpark WWTP discharges to the percolation ponds and/or Arroyo, as the case may be. However, it is emphasized that overall gain/loss of groundwater to/from the Arroyo is the critical factor for the model, which is not significantly affected by the details of water flow paths near the WWTP.

Figure 8-68 shows a comparison of streamflows gains/losses from the Larry Walker Study and the model. The net infiltration rate for reaches 1 through 9, was 5.4×10^{-4} from the model compared to 6.2×10^{-4} AFD/ft from the LWA Study. Note, the LWA Study did not explicitly account for evaporative losses and all losses were assumed to be due to infiltration. Hence, the LWA estimate is likely an upper bound on the infiltration rate (actual groundwater infiltration is likely less than the estimated values). The numerical model does explicitly account for evaporative losses and the simulated infiltration rate represents actual groundwater infiltration. Hence, the simulated (actual groundwater) infiltration rate compares favorably with the slightly higher LWA Study infiltration estimate, which did not account for evaporative losses. Note, that localized surface-water/groundwater interaction is a highly complex phenomenon driven by small differences in stream stage and groundwater heads. Discrete changes in riverbed elevation can change flow direction suddenly. Recall that the model does a simple mass-balance based routing as opposed to dynamic wave routing, which may be required to accurately estimate stage and width over the numerous drop-structures along the Arroyo. Given the scale of the model, the relative simplicity of the streamflow modeling approach, and the uncertainty in channel characteristics (channel geometry, riverbed elevation, riverbed conductance), this is an acceptable level of error. Improved results would need a finer resolution model with better definition of the Arroyo channel geometry and riverbed sediment characteristics, which is far beyond the scope of this study.

The Hitch gage (841/841A), located just upstream of model reach 12 (**Figure 7-12**), has long term flow records that can be compared to simulated flows in the stream. Inflows to the SFR package consist of flows at gage 803 (Arroyo Simi at Madera Road Bridge) and outflows from the SVWQCP. The SFR package routes these flows through the reaches and segments, accounting for groundwater gains and losses, as driven by the difference in stream stage and groundwater elevations. The model does not account for surface run-off from precipitation events. **Figure 8-69** compares streamflow from the model to measured streamflows at the Hitch Gage for the period of record (1990 to 2015). Inflow to the SFR package comprising of flows at 803 plus the SVWQCP discharges are also plotted on the graph. Results indicate that the model does well in simulating low-flow conditions in the Arroyo. The model does less well simulating peak flows at the gage. This is because the model does not account for stormflow and runoff contributions between the 803 and 841/841A gage. These flows could be estimated and added as inputs to the SFR package, but they would not significantly impact results because the basin is characterized by short-duration/high-intensity storm events during the winter months. These peak flows tend to flow very fast out of the basin and do not have sufficient time to infiltrate into the groundwater system.

Figure 8-70 shows simulated streamflows exiting the basin from the last reach in the SFR package. Results indicate that up until 1993 little to no dry weather flows exited the basin. This is consistent with the findings from Hopkins Groundwater Consultants (2008) that stated that dry weather flows began to spill over into the Pleasant Valley Basin in the early to mid-1990s. Hence, the model is

successfully able to simulate the temporal trends in surface water flows from the Las Posas Basins to the Pleasant Valley Basin.

Model calibration of water levels in the Shallow Aquifer, consistency with the LWA infiltration rate, and consistency of low flows at the Hitch gage, all indicate that the model is a reliable tool for this purpose.

8.5.4 Calibrated Water Budget

Figures 8-71 to 8-77 show the water budget for individual aquifers/hydrologic units as well as for the entire model. Salient trends for each aquifer/hydrologic unit are presented below:

Shallow Aquifer

Figure 8-71a shows the water budget for the Shallow Aquifer. Inflows from the Arroyo are the primary source of recharge into the Shallow Aquifer. When water levels are low, storm flows can contribute large recharge rates for short durations of time. However, long term groundwater levels only increased with increased perennial flows from the SVWQCP discharges (**Figure 8-70**). Much of the early recharge events contribute to storage in the Shallow Aquifer. Once the Shallow Aquifer is filled, leakage to underlying units increases, until it is balanced by net recharge from streamflow. As water levels in the Shallow Aquifer rise, recharge from high-flow events is less because: (1) the vertical gradient between the surface water and groundwater decreases, and (2) storage capacity of the Shallow decreases and more water flows out of the basin. This is evident from peak recharge rates being much lower in the period from 1990 to 2015 (when the Shallow was full), compared to recharge rates in the period 1970 to 1990 when the water levels in the Shallow Aquifer were rising. The average net rate of recharge from the streamflow into the Shallow Aquifer was approximately 12,750 AFY over the entire period of the simulation. The average recharge rate from 2000 to 2015 (after the Shallow Aquifer filled) was 12,400 AFY.

It is useful to compare simulated streamflow recharge with estimates from the Larry Walker Study (Engle 2012; 2103). The Larry Walker Study estimated a mean stream loss of 10,694 in the summer of 2011. Model simulated recharge during the same period were slightly higher, at 11,468 AFY. Note the Larry Walker Study was unable to estimate gain/losses between gages 9 and 11 (**Figure 8-67b**). This reach is likely a losing reach, and would account for higher streamflow losses from the Arroyo than estimated by the study, reducing the difference between simulated and measured streamflows. Overall, the model is seen to match observed recharge rates from the Larry Walker Study.

Other sources of recharge include areal recharge from precipitation (and tributaries during the wet season), return flows from agricultural pumping, and Moorpark WWTP percolation. All of these

together account for approximately, 2,800 AFY and 3,250 AFY for the entire simulation period and 2000 – 2015, respectively.

Leakage to underlying units is the primary form of outflow from the Shallow Aquifer. Average leakage for the simulation period was approximately 14,700 AFY, with an average of 15,440 AFY from 2000 – 2015. As expected, vertical leakage from the Shallow aquifer increases as water levels rise in the aquifer.

ET losses from the Shallow Aquifer increased over time (from 920 AFY in 1970 to 1,700 AFY in 2015) as the aquifer filled up, and the *Arundo* density increased (**Figure 8.71b**). Average ET losses were about 1,250 AFY for the entire simulation period.

Underflow into the Pleasant Valley Basin (via the constant head boundary applied to the southern boundary) was 1,130 AFY for the entire duration of the simulation, with a high of approximately 2,000 AFY in the 2005 going down to approximately 1,200 AFY in 2015 (**Figure 8.71c**).

Epworth Gravels Aquifer

Figure 8-72 shows the water budget for the Epworth Gravels Aquifer. Recharge rate was kept constant at 1,360 AFY. Pumping varied between 500 to 2700 AFY, with a declining trend from 1999 – 2013. Note the net positive change in storage during this period. Leakage through the bottom of the Epworth Gravels Aquifer was not seen as a significant outflow term.

Top and Bottom Layers of the Upper San Pedro/Saugus Formation

Figures 8-73 and **8-74** show the water budget for the top and bottom layers of the Upper San Pedro/Saugus Formation. The primary source of recharge to the upper part of the San Pedro Formation is the Shallow Aquifer. Inflows from the top layer (Shallow Aquifer) average 14,760 and 15,550 AFY for the entire period of simulation and 2000 – 2015, respectively. Areal recharge accounts for approximately 5,600 AFY, on average. Net outflow from the bottom of the Upper San Pedro/Saugus Formation (Layer 3) was about 14,600 AFY, on average.

Flow from the GHB along the western boundary was minimal, at about 110 AFY.

Fox Canyon Aquifer

Figure 8-75 shows the water budget for the FCA. Inflow from overlying layers was 16,500 AFY, on average through the simulation. The primary outflow was groundwater pumping which averaged at 16,500 AFY, fluctuating year to year from between 5,000 AFY to more than 30,000 AFY (inclusive of ASR extractions). Recharge from the outcrops is not an important contribution to the overall water budget. Of note, is the inflow of water from the GCA (labeled as bottom

inflow) in response to the ASR extractions. It is noted that, although **Figure 8-75** depicts an overall *increase* in groundwater storage within the FCA, many FCA wells within the central portions of the study area exhibited a net *decline* in groundwater elevation over the calibration period. These observations suggest that non-ASR FCA groundwater pumping in the central portion of the basin may not be sustainable at historical rates (groundwater elevation declines occurred despite a 11,402 AF net *increase* in storage via CMWD storage activities during the calibration period).

Grimes Canyon Aquifer

Figure 8-76 shows the water budget for the GCA. Inflow from overlying FCA is a significant contributor to the GCA water budget (2,000 – 4,000 AFY). The GCA also received direct recharge in the outcrops of approximately 1,700 AFY.

Model Water Budget

Figure 8-77 shows the water budget for the entire model. Water budget components are summarized in **Table 8-3**. Individual flow terms are discussed in the previous sections. Of particular interest is the net change in storage for the entire basin from year to year. The model indicates reductions in storage in the early part of the 1970s. With the filling of the Shallow Aquifer water levels rose on average through the 1980s, 1990s, and early 2000s. Increased groundwater extractions (including ASR extractions) led to lowering of storage from 2007 and 2010. A slight recovery was observed in 2011, but reduced inflows from the stream and recharge (driven by decreasing rates of discharge to the Arroyo and drought conditions)) combined with higher than average groundwater extractions led to reductions in storage from 2012 – 2015.

It is emphasized that the water budget presented in **Table 8-3** is for the entire model domain (ELPMA and associated outcrops). Importantly, much of the reported storage increase, particularly that which is associated with the Arroyo, has occurred in areas with little pumping (i.e. the Shallow Aquifer and southwestern portions of the Upper San Pedro Formation and FCA). As noted earlier, the majority of the groundwater pumping is from the FCA in the central portion of the basin and groundwater in storage within the Shallow Aquifer and Upper San Pedro Formation is not immediately available to the FCA in this area because low leakage rates limit groundwater flow between these units. It is noted that many FCA wells within the central portions of the study area exhibited a net *decline* in groundwater elevation over the calibration period, despite an overall increase in groundwater storage within the basin. Thus, conclusions should not be made based on the model-wide water balance results alone. Groundwater level trends should also be considered.

Table 8-3 Groundwater Budget (AFY) for the Model

Year	Recharge from Arroyo	Recharge (Includes Return Flows and Percolation Ponds)	Groundwater Injection at ASR Wells	Groundwater Extractions (Includes ASR Wells)	ET Losses from <i>Arundo</i>	Boundary Flow in Upper San Pedro/Saugus Formation	Boundary Flow in Shallow Aquifer	Change in Storage
1970	10,011	10,478	-	(18,006)	(922)	(97)	46	1,510
1971	5,689	10,469	-	(18,462)	(922)	(96)	45	(3,277)
1972	4,600	10,615	-	(18,289)	(922)	(96)	56	(4,036)
1973	9,370	10,514	-	(17,680)	(922)	(96)	37	1,224
1974	10,360	10,505	-	(17,553)	(922)	(96)	20	2,313
1975	9,074	10,668	-	(20,505)	(922)	(97)	25	(1,757)
1976	8,868	10,750	-	(21,113)	(922)	(97)	59	(2,455)
1977	11,123	10,652	-	(17,713)	(922)	(97)	71	3,114
1978	22,229	10,550	-	(17,168)	(922)	(97)	(176)	14,416
1979	15,311	10,638	-	(17,866)	(922)	(98)	(50)	7,013
1980	18,093	10,826	-	(19,228)	(922)	(99)	(320)	8,349
1981	12,273	11,027	-	(21,138)	(922)	(100)	17	1,157
1982	12,851	11,226	-	(17,492)	(922)	(101)	28	5,591
1983	19,878	11,584	-	(16,323)	(922)	(101)	(676)	13,440
1984	12,569	11,701	-	(19,528)	(922)	(102)	(194)	3,525
1985	12,194	11,798	-	(18,572)	(922)	(103)	(149)	4,246
1986	16,266	11,786	-	(16,794)	(958)	(104)	(648)	9,549
1987	14,764	12,092	-	(19,413)	(994)	(105)	(694)	5,650
1988	14,960	12,402	-	(20,938)	(1,030)	(106)	(897)	4,392
1989	13,114	12,459	-	(23,751)	(1,066)	(107)	(769)	(120)

Year	Recharge from Arroyo	Recharge (Includes Return Flows and Percolation Ponds)	Groundwater Injection at ASR Wells	Groundwater Extractions (Includes ASR Wells)	ET Losses from <i>Arundo</i>	Boundary Flow in Upper San Pedro/Saugus Formation	Boundary Flow in Shallow Aquifer	Change in Storage
1990	13,299	12,228	-	(23,074)	(1,102)	(108)	(926)	318
1991	14,521	12,049	-	(18,950)	(1,138)	(109)	(1,089)	5,284
1992	16,429	12,089	-	(15,318)	(1,174)	(110)	(1,593)	10,325
1993	14,848	12,241	66	(16,308)	(1,210)	(111)	(1,876)	7,650
1994	13,146	12,274	341	(18,633)	(1,246)	(112)	(1,753)	4,017
1995	13,520	12,352	375	(15,653)	(1,282)	(114)	(1,989)	7,209
1996	12,522	12,170	248	(12,280)	(1,318)	(115)	(1,938)	9,289
1997	12,002	12,434	253	(17,253)	(1,354)	(116)	(1,919)	4,047
1998	12,518	12,597	1	(15,750)	(1,389)	(118)	(2,091)	5,768
1999	12,126	12,374	146	(20,362)	(1,415)	(119)	(1,848)	904
2000	12,655	12,400	1	(18,919)	(1,637)	(119)	(1,850)	2,530
2001	13,050	12,436	-	(14,319)	(1,637)	(120)	(2,049)	7,359
2002	12,581	12,536	431	(20,447)	(1,637)	(121)	(1,799)	1,543
2003	12,090	12,504	1,192	(17,007)	(1,637)	(122)	(2,108)	4,912
2004	12,528	12,236	947	(18,915)	(1,637)	(123)	(2,055)	2,981
2005	12,034	12,277	1,792	(14,450)	(1,637)	(123)	(2,206)	7,686
2006	11,280	12,271	4,206	(19,012)	(1,637)	(124)	(2,144)	4,840
2007	11,752	12,226	168	(24,046)	(1,637)	(125)	(2,033)	(3,695)
2008	12,022	12,211	48	(25,190)	(1,637)	(126)	(2,058)	(4,730)
2009	12,409	12,190	257	(30,350)	(1,637)	(126)	(1,991)	(9,248)
2010	12,996	12,171	31	(27,022)	(1,637)	(127)	(2,066)	(5,654)

Year	Recharge from Arroyo	Recharge (Includes Return Flows and Percolation Ponds)	Groundwater Injection at ASR Wells	Groundwater Extractions (Includes ASR Wells)	ET Losses from <i>Arundo</i>	Boundary Flow in Upper San Pedro/Saugus Formation	Boundary Flow in Shallow Aquifer	Change in Storage
2011	12,673	12,066	739	(19,823)	(1,637)	(127)	(2,056)	1,835
2012	12,512	11,947	1,351	(22,905)	(1,637)	(128)	(1,887)	(747)
2013	12,115	11,839	528	(26,575)	(1,644)	(128)	(1,635)	(5,500)
2014	13,442	11,731	3,567	(25,930)	(1,637)	(128)	(1,502)	(457)
2015	12,089	11,692	689	(23,936)	(1,637)	(128)	(1,371)	(2,603)

DRAFT

8.5.5 Particle Tracks

Particle tracking simulations were carried out using MODPATH (Pollock, 1994) to assess flow paths and groundwater velocities in the model. The goal was to compare model simulated groundwater velocities with respect to basin-wide water quality assessments done by Bachman (2012) and Bondy Groundwater Consulting (2016), who estimated the rate of migration of high TDS (above 100 mg/L) water from the Arroyo to the Shallow Aquifer and the FCA from 1980 (when the earliest reliable records of water quality are available) through 2015 (**Figure 5-18**). Consistent with the Bachman (2012) and Bondy Groundwater Consulting (2016) study period, particles were released starting in 1980 and simulated through 2015. Particles were introduced all along the Arroyo, and the uppermost saturated unit under and surrounding the Arroyo to represent high TDS water from the various discharges. Bondy Groundwater Consulting (2016) indicated that relatively high TDS was already present in the deeper aquifers in 1980 (**Figure 5-18**). Additional particles were released along the extent of the 100 mg/L contour in 1980. A porosity of 0.25 was used for the particle tracking. **Figures 8-78 to 8-80** show simulated particles tracks from 1980 to 2015 in the Shallow Aquifer, Upper San Pedro/Saugus Formation, and the FCA compared to 100 mg/L contours from Bondy Groundwater Consulting (2016). Particle flow-lines are consistent with observed water quality trends in the south and southwestern portions of the basin. Particles are simulated to travel from the Arroyo, to the Shallow Aquifer, through the Upper San Pedro/Saugus Formation, and into the FCA towards production wells to the northwest and ASR wells to the north. In the southwest, the particles end very close to the 100 mg/L extent in 2015. Particles slightly overshoot the 100 mg/L extent for 2015 in the near the ASR well field. Flow in this area may be more impeded by the Moorpark Anticline than is simulated in the model. Higher values of porosity in this region may also be a cause for slower pore velocities. However, as a qualitative check on flow paths and velocities the particle track results are consistent with water quality trends observed in the basin.

8.6 Model Uncertainty

A model is, by definition, a simplified representation of (a complex) physical system. Model conceptualization and construction entails making assumptions and modeling choices based on the best available, but often incomplete, knowledge. Groundwater modeling is further complicated by the fact that calibrating groundwater models is an “ill-posed” problem, with more degrees of freedom than data available. This leads to the potential for several different combinations of (correlated) parameters giving the same calibration results. The modeler has to be judicious in selecting the most critical group of parameters and establishing physical/geologic constraints on the parameters to resolve non-uniqueness. Nevertheless, due to the non-unique property of the model calibration process, final parameter distributions depend on the trajectory taken to reach to a given set of calibrated parameters.

The ELPMA Model is a numerical representation of a groundwater basin characterized by complicated fold- and fault-ridden geology. A key aspect of the basin's water budget is recharge driven by the dynamic interplay of surface water in the Arroyo Las Posas/Somis with the underlying groundwater system. The model was built and calibrated based on basin-specific geologic and groundwater data collected over the span of several decades. Calibration results indicate that the model is a robust tool for predicting regional and local hydraulic response to groundwater injection/extractions as well as recharge from the Arroyo. Model results also compare favorably with streamflow gage records, and dry-weather estimates of surface-water infiltration. Nevertheless, key uncertainties remain and are summarized below:

- Arguably, the greatest sources of uncertainty in the model are historical (pre-1985) groundwater extractions and groundwater levels. Few groundwater-level or extraction records are available prior to the 1980s. This leads to uncertainty in (1) the initial conditions for much of the basin, and (2) historical pumping and water level estimates during the simulation period, both of which impact predictions in more recent periods.
- While reasonable data was available to characterize, model, and calibrate the Shallow Aquifer and FCA, very little data was available in the Upper San Pedro/Saugus Formation or the GCA. Currently, hydraulic properties of the Upper San Pedro/Saugus Formation and GCA were calibrated primarily to match water level responses in the FCA, Shallow Aquifer. Having more direct measurements of water levels and geology in both these units would reduce uncertainty in the model.
- In addition to recharge from the Arroyo, the basin also receives areal recharge from outcrops to the north and east. Historical groundwater levels indicate an east-west flow direction, presumably driven by recharge from the east. To calibrate the ELPMA model, focused recharge from Happy Camp Canyon Creek was included in the model. Independent estimates of recharge from the north and east are not available and remain uncertain. Further investigation of recharge mechanisms in the north and east would improve the reliability of model parameters and predictions.
- The model was calibrated assuming that agricultural return flows do not really reach the deep (semi-confined) groundwater system over time-spans commensurate with this model. Recharge estimates were based on the BCM (Flint and Flint, 2014), which is a shallow root zone water-budget model. Additional recharge in the form of tributary recharge (from seasonal tributaries as well as Happy Camp Canyon Creek) was included in the model to calibrate heads. The magnitude and spatial distribution of deep recharge and its relationship with return flows remain key uncertainties in the model.

- As discussed earlier, the model responds to aggregate recharge from all sources and is not able to distinguish between different sources of water. Given the uncertainty in different recharge terms, it is possible that smaller recharge terms (such as M&I and septic returns) are ‘compounded’ within the larger terms.
- The Moorpark Anticline is seen to exert a structural control on groundwater flow in the basin. Water level and water quality trends indicate that the Anticline (especially to the east) impedes flow from the south to the north. Model results indicate that portions of the Anticline become unsaturated under low water level conditions. However, the structure of this important geologic feature and its full influence on the overlying units remains uncertain. Few well logs were available that could help define the stratigraphy, dip and orientation of the Anticline. Additional investigations on the geologic structure and water level trends in this area would greatly enhance the predictive capabilities of the model.
- In general, very little data were available for areas to the east and northeast of the ASR well fields. Given that these areas are potential sources of recharge, additional information on the geology and the lithology in the east and northeast would be useful in further refining and calibrating the model in these areas.
- Several faults were included in the model to best capture regional groundwater trends. However, the extent, orientation, and hydraulic properties of the faults remain uncertain. The model also includes some unnamed faults to the north and east where water levels seem to be impounded (as evident from sharp lateral gradients in hydraulic heads). Ground-truthing the presence (or absence) of these faults would improve the confidence in the model.
- Uncertainty also exists in the flow-width and flow-depth relationships used in the SFR package for streamflow routing. These relationships were scaled to achieve calibration of streamflow contributions during high and low flows. While, estimates of losses during dry-weather flows were available (Engle 2012; 2013), no direct measurement of stream losses during wet periods or high-flow conditions were available. Direct comparison with flows at downstream gages was challenging due to the fact that overland flow contributions can be significant under such conditions, making it difficult to estimate net losses across different reaches of the Arroyo. Overall, streamflow contributions during high flows were indirectly calibrated by matching long term heads at wells near the Arroyo, while constraining low-flow stream losses to estimates from the Larry Walker Study. Another challenge with calibrating to high flow is that the model has a stress-period of one month, which is longer than the scale of storm systems in the basin, which often last less than an hour depositing a lot of water in short durations. Areal imagery was used as the basis for

defining the flow-width relationship in the Arroyo. However, areal images are snapshots in time and may not be indicative of the ‘effective’ scale at which the channel interacts with the groundwater system. In the future, it may be useful to develop modeling tools that could be used to scale short duration high-flow events and estimate effective properties applicable to the groundwater model during such events.

- Another uncertainty that impacts the streamflow package is related to errors or incomplete knowledge of riverbed elevations, geometry, and permeabilities. The Arroyo passes over several drop structures and riverbed elevations show steep changes in topography at some locations. These locations are where the gradient between the stage in the stream and groundwater may change causing flow direction to reverse (losing streams can become gaining). Results from the SFR package can be further improved by incorporating high-resolution data for riverbed elevations and channel geometry.
- Finally, model results indicate that the streamflow package is not able to fully simulate gaining streamflow conditions downgradient of the Moorpark percolation ponds. An improved understanding of the local flow system at and around the Moorpark WWTP percolation ponds would enhance the predictive capacity of the model to simulate local surface water dynamics.

9.0 SENSITIVITY ANALYSIS

This section will be developed based on additional comments from CMWD, FCGMA, and other stakeholders.

10.0 PREDICTIVE SCENARIOS

This section will be developed based on additional comments from CMWD, FCGMA, and other stakeholders.

11.0 SUMMARY AND CONCLUSIONS

This report presents work done by INTERA on conceptualizing, constructing, and calibrating a numerical groundwater model for the East and South Las Posas Basins (Las Posas Basins). The groundwater modeling process was broken into two phases. The first phase consisted of refining an existing geologic model of the ELPMA developed by CH2M (2017) and developing conceptual estimates of key water budget components, such as diffuse recharge from precipitation, focused recharge from the Arroyo, recharge from agricultural/municipal return flows, groundwater losses to evapotranspiration (ET), groundwater losses to pumping, and any underflow to or from the

Basins. This phase relied on the existing body of knowledge and literature to estimate the various components of the water budget, in addition to the uncertainty associated with each term.

Key water budget processes were then translated into a numerical framework using MODFLOW-NWT (Niswonger et al., 2000), an industry standard groundwater simulation code developed by the USGS, which is ideal for systems with partially saturated and unconfined groundwater conditions as are typical of the Basins. Since surface-water/groundwater interactions were key to the basin, the updated streamflow routing (SFR2) package was used to model the complex interactions between the groundwater and surface flows. Considerable time and effort was spent on calibrating the model. Calibration objectives included capturing historical spatial and temporal trends in water levels, calibrating to observed vertical and lateral hydraulic gradients across and between the individual hydrostratigraphic units, simulating known periods and quantities of groundwater gains from and losses to the Arroyo, and replicating groundwater velocities and gradients consistent with water quality trends in the Basin. Significant effort was also spent in characterizing and modeling structural controls on the groundwater flow in the basin and this model represents INTERA's current understanding and interpretation of many of the key structural features, such as the various faults and the Moorpark Anticline, in the LPVB. Throughout this process close communication was maintained with CMWD's groundwater manager, to ensure that the model incorporated institutional knowledge of the basin and CMWD and other entities' operations in the basin.

Based on all the data reviewed and incorporated into the calibration dataset, the model is well calibrated. Calibration residual metrics are well within the industry standard of the mean absolute error (or RMSE) being less than 10% of the observed range in target values. Moreover, the model does well in capturing surface-water/groundwater interactions and simulates net gains and losses from the Arroyo with reasonable accuracy. Results on net stream loss/groundwater recharge compare favorably with field-data collected as part of the Larry Walker Study (Engle 2012; 2013). The model is also able to capture the transience in dry-weather flows reaching the Pleasant Valley Basin. All this builds confidence in the robustness of the calibrated groundwater model and paves the way for its future use in evaluating various water management/operational alternatives.

12.0 DATA GAPS AND FUTURE WORK

This section will be developed based on additional comments from CMWD, FCGMA, and other stakeholders.

13.0 REFERENCES

- Anderson, M.P., and Woessner., W.W., 1992, Applied groundwater modeling: Simulation of flow and advective transport: Academic Press, Inc., San Diego, 381 p.
- Bachman, S., 2012. Las Posas Basin ASR Project Annual Report 2007-2010, prepared for Calleguas Municipal Water District.
- Bachman, S., 2016. Moorpark Desalter Groundwater Modeling, prepared for Ventura County Water Works District #1, February 2016.
- Batu, V., 1998, Aquifer Hydraulics: A Comprehensive Guide to Hydrogeologic Data Analysis, John Wiley & Sons, New York, 727p.
- Bondy Groundwater Consulting, 2016, Las Posas Valley Basin ASR Project Annual Report 2015, prepared for Calleguas Municipal Water District, October 25, 2016.
- California Department of Water Resources, 2003. California's Groundwater. Sacramento, CA: California Department of Water Resources, Bulletin 118, Updated 2003.
- California Invasive Plant Council, 2011. *Arundo donax (giant reed)*: Distribution and Impact Report, prepared for the State Water Resources Control Board.
- Calleguas Municipal Water District and Metropolitan Water District of Southern California, 1989. North Las Posas Basin Hydrogeologic Investigation.
- CH2M, 2017. Development of a Conceptual Model for the Las Posas Valley Basin – East and South Sub-Basins, prepared for Calleguas Municipal Water District, January 2017.
- CH2MHILL, 2001. Wellfield No. 2 Well Completion Report (ASR-5 through ASR-18), prepared for Calleguas Municipal Water District, October 2001.
- CH2MHILL, 1993. Technical Memorandum, Hydrogeology and Three-Dimensional Groundwater Flow Model of the Las Posas Basin, Ventura County, California, January 5, 1993.
- Cey E.E, Rudolph, D.L, Parkin, G.W, and Aravena, R. 1998. Quantifying groundwater discharge to a small perennial stream in southern Ontario, Canada. *Journal of Hydrology*, 210:21-37.
- Cooper, H.H., and Jacob, C.E., 1946. A generalized graphical method for evaluating formation constants and summarizing well field history, Am. Geophys. Union Trans., vol. 27, pp. 526-534.
- Daly, C. et.al, 2008. Physiographically sensitive mapping of climatological temperature and precipitation across the conterminous United States. *Int. J. Climatol.*, 28: 2031–2064.
- DeOreo and Mayer, 2012. Insights into Declining Single Family Residential Water Demands. *American Water Works Association Journal*, Vol 104 p. E383 – E394.
- Dibblee, T.W., 1992. Geologic Map of the Moorpark Quadrangle Ventura County, California, Scale 1:24,000.
- Dibblee, T.W. 1990. Geologic Map of the Camarillo & Newbury Park Quadrangle Ventura County, California, Scale 1:24,000.
- DeVecchio, D.E., Keller, E.A., Fuchs, M., and Owen L.A., 2012. “Late Pleistocene Structural Evolution of the Camarillo Fold Belt: Implications for Lateral Fault Growth and Seismic Hazard in Southern California.” *Lithosphere* 4(2):91–109. doi: 10.1130/L136.1.

- Doherty, J., 2004, PEST Model Independent Parameter Estimation, User Manual: 5th Edition: Brisbane, Australia, Watermark Numerical Computing.
- Dudek, 2017, Preliminary Draft Groundwater Sustainability Plan for the Las Posas Valley Basin, prepared for the Fox Canyon Groundwater Management Agency, November 2017. Accessed January 2018. <http://www.fcgma.org/component/content/article/8-main/115-groundwater-sustainability-plans>.
- DWR (California Department of Water Resources), 1975. California's Groundwater Bulletin 118: Las Posas Valley Groundwater Basin. Accessed January 2018. http://www.water.ca.gov/pubs/groundwater/bulletin_118/california's_ground_water_bulletin_118-75_/b118-1975.pdf
- DWR (California Department of Water Resources), 2003. California's Groundwater Bulletin 118: Las Posas Valley Groundwater Basin. Last updated January 20, 2006. Accessed October 2016. http://www.water.ca.gov/pubs/groundwater/bulletin_118/basindescriptions/4-8.pdf.
- DWR (California Department of Water Resources), 2016. 2016 Bulletin 118 Interim Update. Accessed November 2017. <http://www.water.ca.gov/groundwater/bulletin118/update.cfm>
- Engle, D., 2012. Larry Walker Associates, Memorandum dated January 15, 2012 from Diana Engle to Susan Mulligan, General Manager at Calleguas Municipal Water District, *Phase I Study: Surface Flow and Groundwater Recharge in Arroyo Las Posas*
- Engle, D., 2013. Larry Walker Associates, Memorandum dated August 12, 2013 from Diana Engle to Bryan Bondy at Calleguas Municipal Water District, *Draft data report for the Phase II Program for Long-Term Monitoring of Flow and Recharge in Arroyo Las Posas*.
- FGMA, 2015, Calendar Year 2014 Annual Report.
- Flint, L.E., and Flint A.L., 2014. California Basin Characterization Model: A Dataset of Historical and Future Hydrologic Response to Climate Change, U.S. Geological Survey Data Release, [doi:10.5066/F76T0JPB](https://doi.org/10.5066/F76T0JPB)
- Flint, L.E., Flint, A.L., Thorne, J.H. & Boynton, R., 2013. Fine-scale hydrologic modeling for regional landscape applications: the California Basin Characterization Model development and performance. *Ecol. Process.* 2, 1–21 (2013).
- Fugro Consultants, Inc., 2014, Report of Monitoring Well Pumping Tests and Analysis: Shallow Monitoring Well Network Installation Program, Phase I Ventura County, California, prepared for Calleguas Municipal Water District, May 2014.
- Hanson, R.T., Martin, P., Koczot, K.M., 2003. Simulation of Ground-Water/Surface-Water Flow in the Santa Clara-Calleguas Ground-Water Basin, Ventura County, California, U.S. Geological Survey Water Resources Investigations Report 02-4136.

- Harbaugh, A.W., Banta, E.R., Hill, M.C., and McDonald, M.G., 2000, MODFLOW-2000, the U.S. Geological Survey modular groundwater model—User guide to modularization concepts and the groundwater flow process: U.S. Geological Survey Open-File Report 00–92, 121 p.
- Harbaugh, A.W., 2005, MODFLOW-2005, the U.S. Geological Survey modular ground-water model -- the Ground-Water Flow Process: U.S. Geological Survey Techniques and Methods 6-A16.
- Harden, D., 2003. California geology: Englewood Cliffs, New Jersey, Prentice Hall, 576 p.
- Hazen, A., 1911. Discussion—dams of sand foundations: Transactions, American Society of Civil Engineers, v. 73, 1999.
- Hopkins Groundwater Consultants, Inc., 2008. Preliminary Hydrogeological Study Northeast Pleasant Valley Basin Surface Water and Groundwater Study Somis, California, prepared for Calleguas Municipal Water District, November 2008.
- Hopkins Groundwater Consultants, Inc., 2013. Summary of Operations Report and Preliminary Hydrogeological Study: Moorpark Desalter Pilot Well Test Project Moorpark, California, prepared for Ventura County Waterworks District No. 1, February 2013.
- Huber, A.M., 2006. The Proliferation of *Arundo donax* in Arroyo Las Posas. Poster session presented at the California Invasive Plant Council Symposia, October 5-7, 2006 Rohnert Park, California
- Hydrometrics Water Resources and GSI Water Solutions, 2016. Las Posas Valley Basin Groundwater Sustainability Plan, prepared for the Fox Canyon Groundwater Management Agency, preliminary draft May 2016.
- Izbicki, J.A., and Martin, P., 1997. Use of Isotopic Data to Evaluate Recharge and Geologic Controls on the Movement of Ground Water in Las Posas Valley, Ventura County, California, U.S. Geological Survey Water-Resources Investigations Report 97-4035, Prepared in cooperation with the Calleguas Municipal Water District.
- Kamerling, M.J. and Luyendyk, B.P., 1985, Paleomagnetism and Neogene tectonics of the northern Channel Islands, California, *Journal of Geophysical Research*, v. 95, p 4995-5015.
- Langhoff J.H, Rasmussen K.R., and Christensen S, 2006. Quantification and regionalization of groundwater-surface water interaction along an alluvial stream. *Journal of Hydrology*, 320:342-358.
- Las Posas Users Group (LPUG), 2012, Final Draft V.1 Las Posas Basin-Specific Groundwater Management Plan.
- Niswonger, R.G., Panday, Sorab, and Motomu, I., 2011, MODFLOW-NWT, A Newton formulation for MODFLOW-2005: U.S. Geological Survey Techniques and Methods 6-A37, 44 p.
- Niswonger, R.G. and Prudic, D.E., 2005, Documentation of the Streamflow-Routing (SFR2) Package to include unsaturated flow beneath streams--A modification to SFR1: U.S. Geological Survey Techniques and Methods, Book 6, Chap. A13, 47 p.
- Padre Associates, Inc., 2013. Final Mitigated Negative Declaration for the Ventura County Waterworks District No. 1 Moorpark Wastewater Treatment Plant Reclaimed Water Distribution System Phase IV, June 2013.

- Pollock, D.W., 1994, User's Guide for MODPATH/MODPATH-PLOT, Version 3, A particle tracking post-processing package for MODFLOW, the U.S. Geological Survey finite-difference ground-water flow model: Reston, VA: U.S. Geological Survey, Open-File Report 94-464.
- Priestley, C.H.B., and R.J. Taylor. 1972. On the assessment of surface heat flux and evaporation using large-scale parameters. *Mon. Weather Rev.*, 100:81-82.
- Psomas, 2014, 2010. Urban Water Management Plan, Ventura County Waterworks District No. 1, revised June 20, 2014.
- Ritchey, J.D., and Rumbaugh, eds., J.O., 1996, Subsurface fluid-flow (ground-water and vadose zone) modeling, ASTM STP 1288: West Conshohocken, PA., American Society for Testing and Materials, pp. 61 - 80.
- Rumbaugh, J.O. and D. Rumbaugh, 2005. Groundwater Vistas. User's Guide, Version 4, Environmental Simulations, Inc.
- Soil Survey Staff, Natural Resources Conservation Service, United States Department of Agriculture. Web Soil Survey. Available online at <https://websoilsurvey.nrcs.usda.gov/>. Accessed [May 26, 2016].
- Staal, Gardner, and Dunne, Inc. 1990. Hydrogeologic Assessment North Las Posas Basin ASR Demonstration Project – Task 1 Background Review Ventura County, California, 10 Plates.
- State Water Resources Control Board (SWRCB), 1956. Ventura County Investigation, Bulletin 118, October and revised April 1956. Accessed at: http://www.water.ca.gov/waterdatalibrary/docs/historic/Bulletins/Bulletin_12/Bulletin_12_1956.pdf
- Tan S. S., Clahan K. B., et al. 2004. Geological Map of the Santa Paula 7.5' Quadrangle Ventura County, California: A Digital Database: California Geological Survey, v. 1.0, Scale 1:24,000, 1 Plate.
- Theis, C.V., 1935. The relation between the lowering of the piezometric surface and the rate and duration of discharge of a well using groundwater storage, *American Geophysical Union Trans.*, vol. 16, pp. 519-524.
- Todd Groundwater, 2016. Characterization and Groundwater Supply Assessment for Simi Valley Basin, prepared for County Waterworks District No. 8, City of Simi Valley.
- Triana, F., Nassi o Di Nasso, N., Ragolini, G., Roncucci, N. and Bonari, E., 2015. Evapotranspiration, crop coefficient and water use efficiency of giant reed (*Arundo donax L.*) and miscanthus (*Miscanthus × giganteus Greef et Deu.*) in a Mediterranean environment. *GCB Bioenergy*, 7(4), pp.811-819. <http://onlinelibrary.wiley.com/doi/10.1111/gcbb.12172/full>

- Turner, J.M. 1975. "Aquifer Delineation in the Oxnard-Calleguas Area, Ventura County." In Compilation of Technical Information Records for the Ventura County Cooperative Investigation: Volume I. Prepared by the Ventura County Public Works Agency Flood Control and Drainage Department for the California Department of Water Resources. 1-45.
- United States Census, 2015. Quickfacts, Accessed at:
<http://www.census.gov/quickfacts/table/PST045215/0649138>.
- Ventura County Environmental Health Division, 2017. Onsite Wastewater Treatment System Applications/Permits Database. Available at
http://vcrma.org/envhealth/EHD_FACILITY_LISTS/liquid_waste_sites.pdf.
- Ventura County Public Works Agency. 1975. Compilation of Technical Information Records for the Ventura County Cooperative Investigation, State of California Department of Water Resources, v. 1, 102 p., 11 Plates (includes three technical papers by M. Mukae and J. Turner). (Plates 1-1b, I-2b, II-6)
- Wildscape Restoration, Inc., 2015. Arroyo Las Posas and Arroyo Simi Arundo Removal Feasibility and Water Savings, prepared for Ventura County Water and Sanitation Department, January 2015.
- Wood, B.D., 1913. Gazetteer of Surface Waters of California; Part III, Pacific Coast and Great Basin Streams: U.S. Geological Survey Water-Supply Paper 297, 244 p.

FIGURES